Cell Polarity Establishment in the Budding Yeast *Saccharomyces cerevisiae*

by

Audrey Sinclair Howell

Program in Genetics and Genomics
Duke University

Date:_____

Approved:

_____
Daniel Lew, Supervisor

_____
Vann Bennett

_____
Kerry Bloom

_____
Steve Haase

_____
Daniel Kiehart

Dissertation submitted in partial fulfillment of
the requirements for the degree of Doctor
of Philosophy in the Program in
Genetics and Genomics
of Duke University

2009

ABSTRACT

Cell Polarity Establishment in the Budding Yeast *Saccharomyces cerevisiae*

by

Audrey Sinclair Howell

Program in Genetics and Genomics
Duke University

Date:_____

Approved:

_____
Daniel Lew, Supervisor

_____
Vann Bennett

_____
Kerry Bloom

_____
Steve Haase

_____
Daniel Kiehart

An abstract of a dissertation submitted in partial
fulfillment of the requirements for the degree
of Doctor of Philosophy in the Program in
Genetics and Genomics Duke University

2009

Abstract

Establishing an axis of cell polarity is central to cell motility, tissue morphogenesis, and cell proliferation. A highly conserved group of polarity regulators is responsible for organizing a wide variety of polarized morphologies. One of the most widely expressed polarity regulators is the Rho-type GTPase Cdc42. In response to cell cycle cues the budding yeast *Saccharomyces cerevisiae* polarizes Cdc42p to a discrete site on the cell periphery. GTP-Cdc42p recruits a number of effectors that aid in the organization of a polarized actin cytoskeleton. The polarized actin cytoskeleton acts as tracks to facilitate the delivery of the secretory vesicles that will grow the bud, an essential process for an organism that proliferates by budding. We have employed treatment with the actin depolymerizing drugs Latrunculin A and B as well as high-speed timelapse microscopy of fluorescently labeled polarity proteins to characterize the assembly of the incipient bud site.

Often, ensuring that only a single axis of polarity is established is as important as generating asymmetry in the cell. Even in the absence of positional cues dictating the direction of polarization, many cells are still able to self-organize and establish one, and only one, polarity axis through a process termed symmetry breaking. Symmetry breaking is thought to employ positive feedback to amplify stochastic fluctuations in protein concentration into a larger asymmetry. To test whether singularity could be guaranteed by the amplification mechanism we re-wired yeast to employ a synthetic positive feedback mechanism. The re-wired cells could establish polarity, however they occasionally made two buds simultaneously, suggesting that singularity is guaranteed by the amplification mechanism.

Contents

List of Tables

List of Figures

1. Introduction

Many cell types have a clearly defined axis of polarity. The type of cell and polarized morphology can vary greatly, from chemotaxing neutrophils to epithelial cells to budding yeast. However, in all cases properly establishing a "front" of the cell as distinct from the "back" of the cell is essential for the cell's function. Additionally, in order for the "front" of the cell to be functional, it often needs to be the only one. That is, when establishing an axis of polarity, the cell must ensure that it only establishes a single axis (referred to here as singularity). Usually, there are cues in place to determine where the "front" of the cell will be. These cues can be extrinsic, such as in the case of chemotaxing cells or intrinsic, such as in budding yeast. However, in the absence of all apparent spatial cues, many cells still establish a single axis of polarity (Wedlich-Soldner and Li, 2003) through a process termed symmetry breaking. The ability of cells to break symmetry and maintain singularity suggests that there is a core internal polarity mechanism at work in many cells whose activity can be biased by polarity establishment cues.

1.1 Establishing cell polarity

1.1.1 Theoretical models of polarity establishment

How do cells transition from a depolarized state with a homogenous distribution of polarity factors to the highly asymmetric protein distribution necessary to create polarized cell morphologies? The process of cell polarization has been extensively

studied in chemotaxing cells such as neutrophils and the free-living soil amoeba *Dictyostelium discoideum*. Chemotaxing cells are able to detect gradients of chemoattractants, and polarize to migrate towards the source. Several models have been proposed to explain how the cells are able to accomplish this polarization (Iglesias and Devreotes, 2008). The first step in polarizing towards and extrinsic cue is detecting the presence of the cue and the positional information it includes. Models based on the principle of local excitation, global inhibition (LEGI) couple fast response to detection of the chemoattractant by the receptor to a global inhibitory signal (Levchenko and Iglesias, 2002; Parent and Devreotes, 1999). In these models, receptor-ligand binding results in a local activation of polarity factors in proportion to the number of ligand-bound receptors in close proximity (Iglesias and Devreotes, 2008). In addition, receptor-ligand binding results in the production of a global inhibitor that can rapidly diffuse around the cell and block activation of polarity factors in other parts of the cell, creating an asymmetric distribution of activated polarity factors.

Positive feedback of local activating events has been proposed to aid in the amplification of chemoattractant signaling. Chemotaxing cells are able to polarize in very shallow gradients of chemoattractant (1-2% difference in concentration between the front and rear of the cell) (Iglesias and Devreotes, 2008). Positive feedback could be used to amplify the activation of polarity factors so that the activating events are not proportional to local receptor-ligand binding. Such positive feedback would create a larger gradient of activated polarity factors inside the cell than the actual gradient of chemoattractant outside of the cell. If positive feedback plays a role in polarization in response to a

chemoattractant gradient, then that could potentially help explain how chemotaxing cells polarize in the absence of a gradient. In a uniform field of chemoattractant, neutrophils polarize and migrate in a random orientation (Devreotes and Zigmond, 1988) through a process termed symmetry breaking.

A model utilizing positive feedback initiated by stochastic events to generate asymmetry in a biological system was first proposed by Alan Turing in 1952 (Turing, 1952) and later elaborated to include polarization of single cells by Gierer and Meinhardt (Gierer and Meinhardt, 1972). In these models, clusters of some polarity factor can arise from an initially symmetric distribution through amplification of stochastic noise (such as fluctuations in protein concentrations, or stochastic receptor occupancy fluctuations). If there is a self-enhancing amplification mechanism present in the cell, then a stochastic fluctuation can be amplified into a larger asymmetry.

Although amplification of stochastic clusters of polarity factors can explain how large asymmetries can develop in initially symmetric cells, positive feedback alone does not explain why many cells display singularity, with only one dominating asymmetry. Theoretically, positive feedback could amplify multiple clusters in a cell at once, so how do cells ensure singularity? The original model from Gierer and Meinhardt included a freely diffusing global inhibitor coupled to the positive feedback mechanism (Gierer and Meinhardt, 1972). In the same manner as the global inhibitor in the LEGI model, by rapidly diffusing around the cell, a global inhibitor could block the amplification of any additional polarization sites, leaving a single axis of polarity. Competition between multiple amplifying clusters for some limiting polarity factor could also, in theory,

guarantee singularity without the need for an additional inhibitor (Goryachev and Pokhilko, 2008; Onsum and Rao, 2009).

1.1.2 Identification of polarity regulators

What are the molecular regulators of polarity establishment? Although the models presented above offer possible mechanisms for generating cell polarity, in many cases, such as the putative global inhibitor, molecular components predicted by the models have yet to be discovered (Onsum and Rao, 2009). Geneticists have attempted to identify regulators of polarity establishment through genetic screens for mutants with polarity defects.

The conserved Par6 polarity complex was identified through screens of *Caenorhabditis elegans* for mutants defective in anterior-posterior patterning. Establishing an axis of polarity in the *C. elegans* zygote is the first step in patterning the anterior-posterior axis of the animal. Following reorganization of the cytoplasm, the cell undergoes 5 asymmetric cell divisions. These divisions result in the partitioning of maternal transcription factors that establish the fates of the 6 founder cells in the embryo (Kemphues, 2000). Genetic screens for partitioning-defective (Par) mutants identified 7 genes responsible for generating cell polarity. Two of these proteins, Par6 and Par3, localized to the anterior pole of the cell following fertilization (Hung and Kemphues, 1999). Par6 and Par3 formed a complex with the atypical protein kinase C, PKC3, and localization of both Par3 and PKC3 to the apical pole was dependent on Par6 (Hung and Kemphues, 1999). Formation and activation of this complex are required for positioning the microtubule spindle for the asymmetric cell divisions following fertilization (Grill et

al., 2001) The Par6-Par3-PKC3 complex is found in many other eukaryotes (although not in yeast) and is involved in polarizing the microtubule cytoskeleton in epithelial cells and migrating astrocytes as well as in embryos (Etienne-Manneville and Hall, 2003). Although they will not be discussed here, additional complexes that regulate cell polarity (Scribble, Crumbs) have been identified through genetic screens in *Drosophila melanogaster* (Assemat et al., 2008).

The Rho-type GTPase Cdc42p and its guanine nucleotide exchange factor, Cdc24p, were both isolated as mutants of *Saccharomyces cerevisiae* that failed to establish an axis of polarized growth and bud (Adams et al., 1990; Sloat et al., 1981; Zheng et al., 1994). In the absence of Cdc42p, the actin cytoskeleton does not become polarized (Adams et al., 1990). Yeast proliferates by budding, which requires a polarized actin cytoskeleton. Blocking actin cytoskeleton polarization leads to a failure in bud emergence and cells grow isotropically, becoming large, round and multinucleate before eventually lysing (Pruyne and Bretscher, 2000b). Although at first glance polarity establishment in budding yeast and *C elegans* would appear to be very different, they are both regulated by Cdc42. Further investigation of Par6 showed that it is an effector of CDC-42. Binding of GTP-CDC-42 to Par6-Par3-PKC3 complexes through Par6, resulted in activation of PKC3 (Garrard et al., 2003) and knockdown of CDC-42 expression through RNA interference resulted in partitioning defects in *C. elegans* (Gotta et al., 2001). Cdc42 is highly conserved with yeast and human *CDC42* sharing 80% sequence identity (Munemitsu et al., 1990; Shinjo et al., 1990) and present in a wide variety of

eukaryotes (Etienne-Manneville, 2004). The balance of this thesis will focus on Cdc42p-mediated polarity establishment in the budding yeast *Saccharomyces cerevisiae.*

1.2 Yeast polarity

1.2.1 Polarized growth during the yeast life cycle

Cdc42p is responsible for polarizing both the actin and septin cytoskeletons in yeast. The septins are a set of cytoskeletal filaments that are initially organized as a ring around the incipient bud site (Kim et al., 1991). Upon bud emergence they are rearranged into a collar at the mother-bud neck (Gladfelter et al., 2001). Although not required for bud emergence, the septins act as a scaffold to concentrate a variety of signaling molecules, aid in shaping the bud and strengthening the cell wall at the division site through localization of chitin synthases, and may be a diffusion barrier partitioning the mother and bud plasma membranes (Gladfelter et al., 2001). Cdc42p is necessary for actin-mediated polarized growth (Adams et al., 1990). The actin cytoskeleton mediates polarized growth in yeast and there are two actin structures responsible for bud growth: patches and cables. Actin patches form along the cortex of the cell and facilitate endocytosis (Kaksonen et al., 2003). Actin cables consist of bundles of actin filaments and act as tracks for myosin-mediated trafficking (Pruyne and Bretscher, 2000a). Secretory vesicles containing the material needed to reorganize the cell wall and grow the bud are trafficked along actin cables towards sites of localized Cdc42p to facilitate polarized growth. Once at the polarization site, Cdc42p helps facilitate vesicle docking and fusion (Adamo et al., 2001) during exocytosis to grow the bud (Pruyne and

Bretscher, 2000a). In addition to transporting secretory vesicles for bud growth, such diverse cargo as: vacuolar membranes; protein-mRNA complexes; and the ends of microtubules during mitotic spindle alignment, are all trafficked towards the growing bud by two type V myosins, Myo2p and Myo4p (Irazoqui and Lew, 2004; Segal and Bloom, 2001). Mitochondria are also segregated into the bud along actin cables, although whether or not myosins are involved has been controversial (Boldogh et al., 2004). Therefore given the sheer amount of material trafficked along actin cables, polarization of actin cables in any one direction results in polarized growth. Actin is not required for vesicle fusion and consequently, growth *per se*. However, in the absence of a polymerized actin cytoskeleton yeast cells grow isotropically, becoming large and round (Ayscough et al., 1997). By polarizing the actin and septin cytoskeletons, Cdc42p regulates the two predominant forms of polarized growth: shmooing and budding.

Polarized growth is central to the life cycle of *Saccharomyces cerevisiae* (Herskowitz, 1988). Yeast can stably proliferate through budding as either haploid or diploid cells. However, there are two mating types of haploid yeast, **a** and α, and when two haploids of opposite mating type are in close proximity, they can mate to form an **a**/α diploid cell. Polarized growth is integral to both budding and mating

Polarized growth in the form of a mating projection, or shmoo, facilitates mating between yeast (Fig. 1.1A). As a non-motile organism, yeast can only grow towards a mating partner. Haploid yeast secrete mating-type specific pheromones that signal their presence to cells of the opposite mating type. For example, α cells emit α-factor, a freely

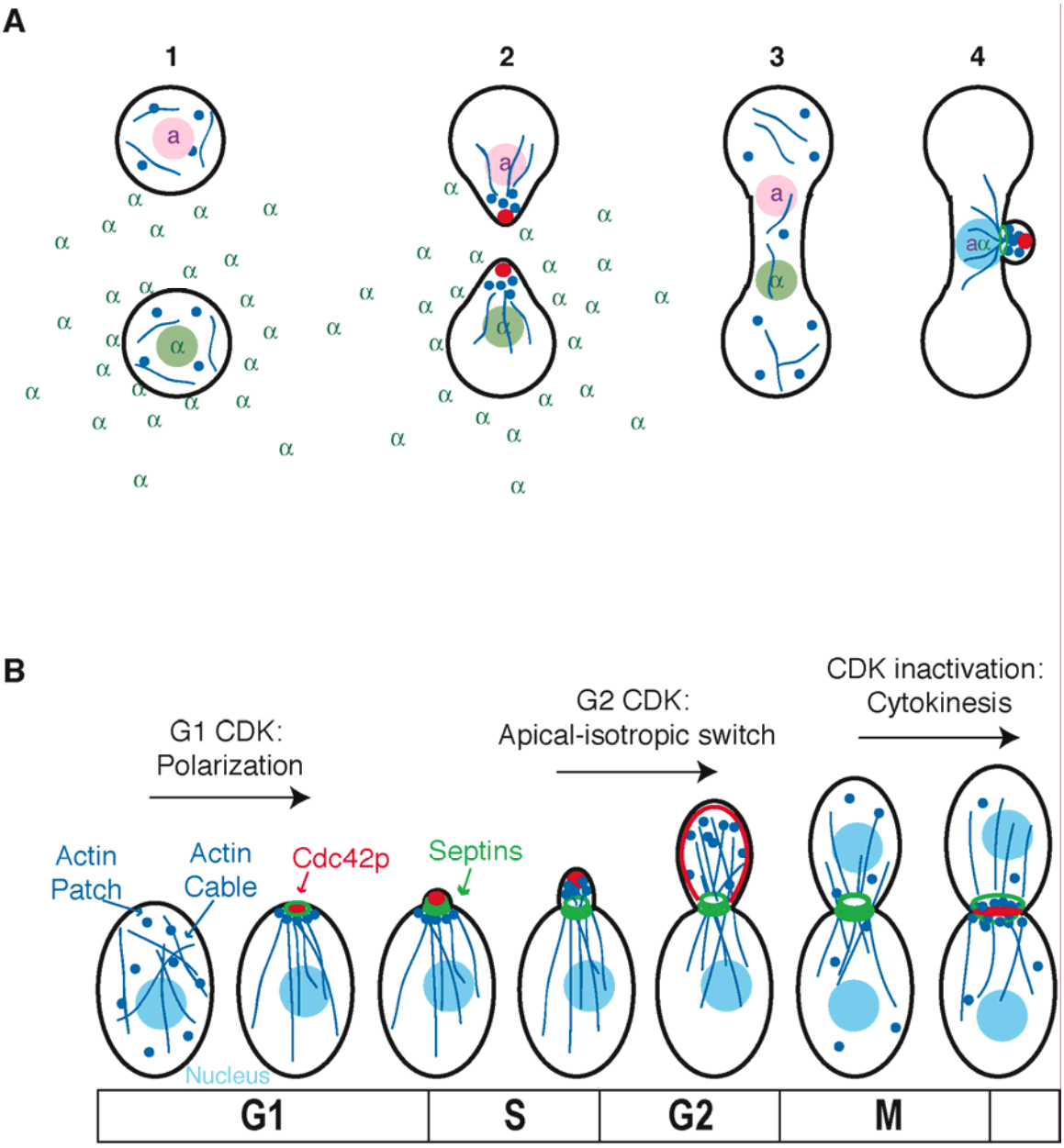

Figure 1.1 Yeast polarized growth

(A) Haploid yeast cells secrete mating pheromone (1). **a** cells also express **a** factor, but for clarity it is not shown. In response to pheromone haploid yeast form a mating projection, or shmoo, in the diection of the highest pheromone concentration (2). Once the cells meet they will fuse (3) to form a stable diploid cell (4). **(B)** In response to cyclin/CDK activity, yeast will reorient Cdc42p and the actin cytoskeleton.

diffusible peptide. As the α-factor diffuses away from the cell, it creates a gradient of α-factor concentration that can be utilized by **a** cells to orient polarized growth. Upon detecting the presence of α-factor, an **a** cell arrests the cell cycle in early G1 (so that the nuclei of eventual mating partners can fuse at the same point in the cell cycle), and polarizes Cdc42p, actin cables and actin patches to a discrete site on the cell periphery to orient polarized growth in the direction of the highest concentration of pheromone (Fig. 1.1A 2). The α cell also responds to **a** factor in the same manner. Eventually, the shmoos of the two cells grow close enough together for the cell walls (and subsequently the plasma membranes and nuclei) to fuse, forming a diploid **a**/α cell (Herskowitz, 1988).

Establishing an axis of polarized growth is essential to form a bud (Fig. 1.1B). As in shmooing cells, polarized growth during budding begins by polarizing Cdc42p to a discrete site on the cell periphery. In response to increases in cyclin dependent kinase/cyclin activity at START, yeast cells polarize Cdc42p, both actin patches and actin cables, and septins to a discrete site on the cell periphery (Lew and Reed, 1993; Pruyne and Bretscher, 2000b). Cdc42p and the actin cytoskeleton stay polarized to the tip of the growing bud until G2, when cells are ready to enter mitosis. At that point, cells switch from apical growth, in which the cell mainly continues growing at the tip of the bud, to isotropic growth, where the actin cytoskeleton is less polarized and the bud generally increases in size (Lew and Reed, 1993). Following mitotic exit, an actomyosin ring forms at the bud neck to aid cytokinesis, and Cdc42p, actin cables and actin patches also repolarize to the bud neck to aid in septum formation (Fig 1.1B) (Lew and Reed, 1993;

Moseley and Goode, 2006). The cytoskeletal reorganizations that occur during shmooing and budding are mediated by effectors recruited to locations of GTP-Cdc42p polarization.

1.2.2 Cdc42p regulators and effectors

Like other GTPases, Cdc42p exists in both GTP- and GDP-bound states. Three classes of proteins regulate Cdc42p nucleotide status: guanine nucleotide exchange factors (GEFs), GTPase-activating proteins (GAPs) and guanine dissociation inhibitors (GDIs). Through these regulators, the concentration and localization of GTP-Cdc42p available to interact with effectors (Fig. 1.2) can be precisely controlled.

GEF: Budding yeast has a single essential Cdc42p GEF, Cdc24p, responsible for exchanging GDP for GTP and thereby activating Cdc42p (Sloat et al., 1981; Zheng et al., 1994). Loss of Cdc24p resembles loss of Cdc42p in cells. Without Cdc24p, cells fail to polarize the actin cytoskeleton or bud (Sloat et al., 1981; Snyder et al., 1991).

GAPs: Cdc42p has five putative GAPs: Bem2p (Marquitz et al., 2002), Bem3p (Zheng et al., 1994), Rga1p (Chen et al., 1996; Stevenson et al., 1995), Rga2p (Smith et al., 2002) and Rgd2p (Roumanie et al., 2001). GAPs increase Cdc42p's GTPase activity and deactivate Cdc42p by turning GTP-Cdc42p into GDP-Cdc42p. Careful examination of budding patterns revealed that Rga1p appears to block formation of a bud within the previous division site by creating an exclusion zone for GTP-Cdc42p within the division site (Tong et al., 2007). Unlike Cdc24p, no single Cdc42p GAPs is essential, and what, if any, role they may be playing in polarity establishment is unclear.

GDI: Cdc42p is a peripheral membrane protein that associates with membranes through a C-terminal polybasic motif followed by a geranylgeranyl isoprene group added

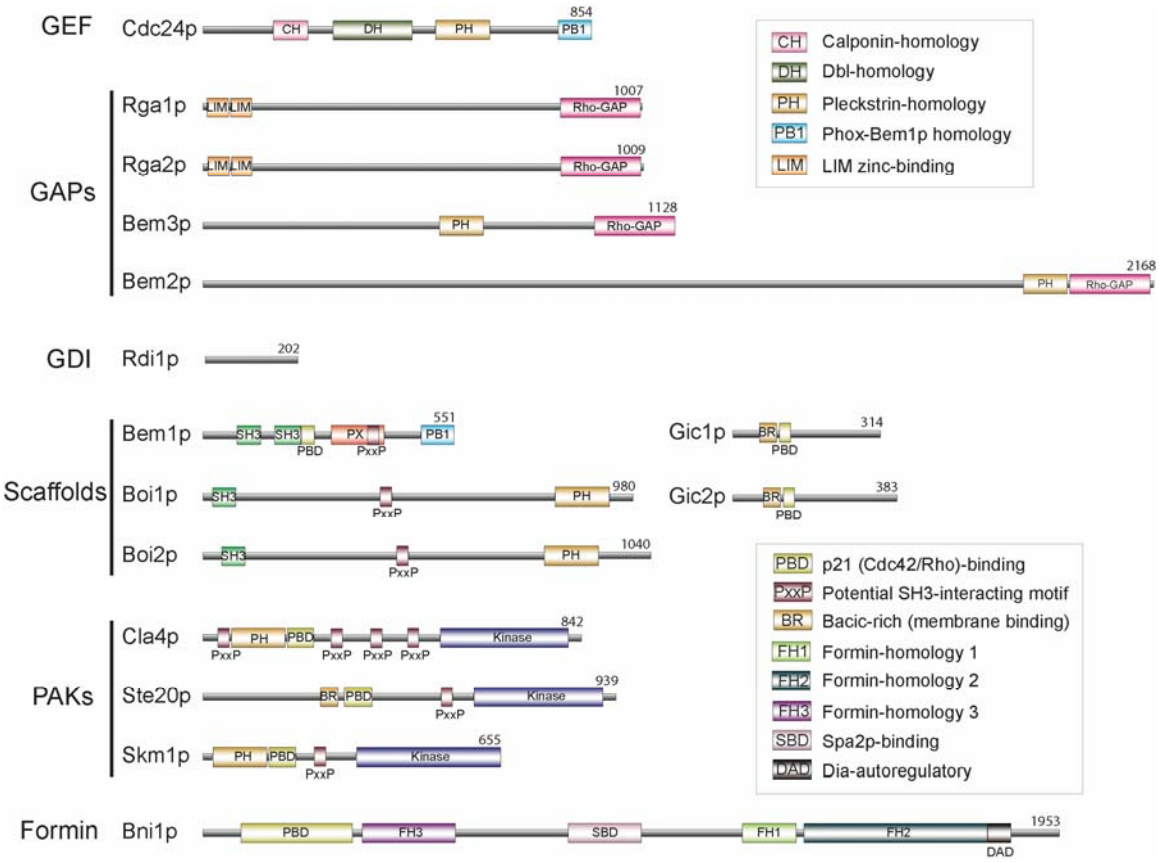

Figure 1.2 Regulators and effectors of Cdc42p

Schematic of the regulators and effectors of Cdc42p that will be further discussed in this thesis.

at the C*AA*X box (Park and Bi, 2007). Cdc42p can be pulled off the membranes by its sole GDI, Rdi1p (Masuda et al., 1994). By allowing Rdi1p-Cdc42p to diffuse in the cytoplasm and potentially be reinserted in a membrane at a different location in the cell, Rdi1p binding increases the intracellular mobility of Cdc42p. Binding of Rdi1p also blocks both exchange of GDP for GTP on Cdc42p and GTPase activity. However, deletion of *RDI1* has no apparent effect on polarized growth, suggesting that either its role is minor or that redundant mechanisms can contribute to the polarization process (Masuda et al., 1994).

Local concentrations of GTP-Cdc42p generated by the GAPs and GEF recruit effectors that help reorganize the actin cytoskeleton.

PAKs: There are three p-21 Activated Kinases (PAKs), Ste20p, Cla4p and Skm1p, in yeast. The PAKs each contain a CRIB (for "Cdc42/Rac Interactive Binding") domain (also known as the "p21-Binding Domain", or PBD) that specifically interacts with GTP-Cdc42p. Ste20p and Cla4p localize to sites of polarized growth and have proposed roles in both actin and septin organization (Cvrckova et al., 1995; Holly and Blumer, 1999; Peter et al., 1996; Weiss et al., 2000), however, the role of Skm1p remains unclear. Ste20p was first identified based on it role in activating the mitogen activated protein kinase (MAP kinse) pathway downstream of the pheromone receptor (Leberer et al., 1992). In addition to regulating actin cytoskeleton organization through MAP kinase signaling, Ste20p may also phosphorylate the formin Bni1p (Goehring et al., 2003). Cla4p plays a role in septin ring assembly (Dobbelaere et al., 2003; Versele and Thorner, 2004) and also phosphorylates Cdc24p (Bose et al., 2001). Ste20p and Cla4p appear to be

partially redundant. *ste20Δ* and *cla4Δ* single deletions are viable (although Cla4p cannot substitute for Ste20p in the pheromone response pathway) but the *ste20Δcla4Δ* mutant is dead, presumably due to cytokinesis defects associated with poorly organized septins (Cvrckova et al., 1995).

Scaffolds: Although Bem1p is not essential in otherwise wildtype cells, *bem1Δ* cells have severe defects in polarity establishment, becoming large, round and multinucleate (Bender and Pringle, 1991). Bem1p binds to GTP-Cdc42p through a CI (Cdc42p interacting) domain (Yamaguchi et al., 2007) distinct from the CRIB domain described above. In addition to GTP-Cdc42p, Bem1p binds to several other proteins involved in polarity establishment, signal transduction and exocytosis. Bem1p binds to Cdc24p through its C-terminal PB1 domain (Ito et al., 2001; Peterson et al., 1994), and to the PAKs Cla4p and Ste20p through its second Src homology3 (SH3-2) domain (Bose et al., 2001; Winters and Pryciak, 2005). Based on analysis of point mutations and protein fusions, the role of Bem1p in polarity establishment appears to be to bring Cdc24p in association with a PAK (Kozubowski et al., 2008) to help generate more localized GTP-Cdc42p.

Two putative Cdc42p effectors, Boi1p and Boi2p, were identified based on their ability to bind Bem1p. Like the PAKs, Boi1p and Boi2p bind to the second SH3-2 domain in Bem1p and although they do not have a CRIB domain, they appear to be able to bind GTP-Cdc42p via their PH domains (Bender et al., 1996; Matsui et al., 1996). *boi1Δ boi2Δ* cells display polarity defects, becoming large and round, but their function in polarity establishment is unclear (Bender et al., 1996; Matsui et al., 1996).

Gic1p and Gic2p were identified as Cdc42p effectors based on the presence of CRIB domains. Gic1p and Gic2p localized to sites of polarized growth, and deletion of both genes results in actin cytoskeleton defects, leading to the hypothesis that they play a role in actin cytoskeleton organization (Brown et al., 1997; Chen et al., 1997). Consistent with this view, Gic2p interacts physically and genetically with components of the polarisome (see below) (Jaquenoud and Peter, 2000), although the functional significance of this interaction is unclear. Gic1p and Gic2p also appear to help recruit septins to the incipient bud site and display septin defects at high temperatures (Iwase et al., 2006), suggesting that they may function downstream of Cdc42p polarization.

Formins: Cdc42p can most directly affect organization of the actin cytoskeleton through regulation of the formin Bni1p. Actin cables in yeast are nucleated by the Diaphanous-related formins, Bni1p and Bnr1p (Moseley and Goode, 2006). Members of the Diaphanous-related formin family have a characteristic set of domains responsible for their activity and regulation: formin homology 2 (FH2) domain, FH1 domain, GBD (CRIB), Diaphanous inhibitory domain (DID), and Diaphanous autoregulatory domain (DAD). The FH2 domain nucleates actin assembly (Evangelista et al., 2002). Regulation of actin nucleating activity by Rho GTPases is best understood in the mammalian formins mDia1 and mDia2. Work on these proteins has shown that they are regulated through autoinhibition. The amino-terminal DID domain binds to the carboxy-terminal DAD domain, blocking the nucleating ability of the FH2 domain (Alberts, 2001; Li and Higgs, 2003; Watanabe et al., 1999). This autoinhibition is relieved by Rho binding to the GBD domain (Alberts, 2001; Watanabe et al., 1999). Binding between the DID and DAD

domains has not been reported in Bni1p or Bnr1p, and the relevant residues do not appear to be conserved, suggesting that formin activity may be regulated differently in yeast (Moseley and Goode, 2006).

Although regulation of formin activity by Cdc42p in yeast remains poorly understood, a group of proteins referred to as the polarisome appear to help regulate Bni1p localization and activity. The Bud6p, Spa2p, and Pea2p proteins localize to sites of polarized growth and physically interact with Bni1p (Moseley and Goode, 2006). Bud6p was first identified based on its physical interaction with actin and in a genetic screen for mutants defective in diploid bud site selection (Amberg et al., 1995; Zahner et al., 1996). Bud6p, like profilin, binds to actin monomers, and may promote Bni1p nucleating activity by increasing the local ATP-actin available or positioning the actin to assemble nuclei (Moseley et al., 2004). Spa2p and Pea2p may help to localize Bni1p to site of polarized growth (Ozaki-Kuroda et al., 2001).

Bnr1p can partially compensate for loss of Bni1p even though they nucleate distinct populations of cables. Bni1p is responsible for nucleating actin filaments at sites of polarized growth (Pruyne et al., 2004). In contrast, Bnr1p is stably localized to the septin ring and nucleates actin cables that extend back into the mother cell (Buttery et al., 2007; Pruyne et al., 2004). Deletion of *BNI1* does not block polarized growth, however, suggesting that Bnr1p can partially compensate for the loss of formin at sites of polarized growth (Imamura et al., 1997). *BNI1* was originally isolated based on its synthetic lethality with a septin mutation (Zahner et al., 1996), a genetic interaction that had been difficult to explain given Bni1p's role as an actin nucleator. If cells must rely on septin-

associated Bnr1p in the absence of Bni1p, then that may explain why *BNI1* genetically interacts with mutations affecting septin organization. Bnr1p requires septins in order to localize to the bud neck (Pruyne et al., 2004). Cells with septin defects and no Bni1p would have no polarized source of actin filaments.

Although we are beginning to assign roles for the Cdc42p effectors at the incipient bud site downstream of Cdc42p polarization, it is still unclear how much of a role feedback is playing in the phenotypes we observe. For example, Cla4p appears to have a role in organizing the septin ring downstream of Cdc42p polarization, however in association with Bem1p and Cdc24p it is also able to influence Cdc42p polarization. It is possible that the Gic proteins have a similar feedback role affecting Cdc42p polarization, but that we simply have not yet identified the mechanism.

1.2.3 Polarization of Cdc42p in response to extrinsic cues (mating)

In the presence of pheromone from cells of the opposite mating type, yeast cells polarize the actin cytoskeleton and shmoo towards the direction of the highest concentration of pheromone (Segall, 1993). Binding of pheromone to a serpentine G-protein coupled receptor on the plasma membrane results in dissociation of Gα from the Gβγ subunits (Fig. 1.3) (Dohlman and Thorner, 2001). Free Gβγ is then available to signal cell cycle arrest as well as Cdc42p polarization. Gβγ promotes polarization of GTP-Cdc42p in the vicinity of activated receptor by recruiting the GEF, Cdc24p, through binding to the adaptor protein Far1p (Butty et al., 1998; Nern and Arkowitz, 1999). By bringing Cdc24p to the site of high receptor activation, liganded receptor creates a local increase in GTP-Cdc42p in its vicinity.

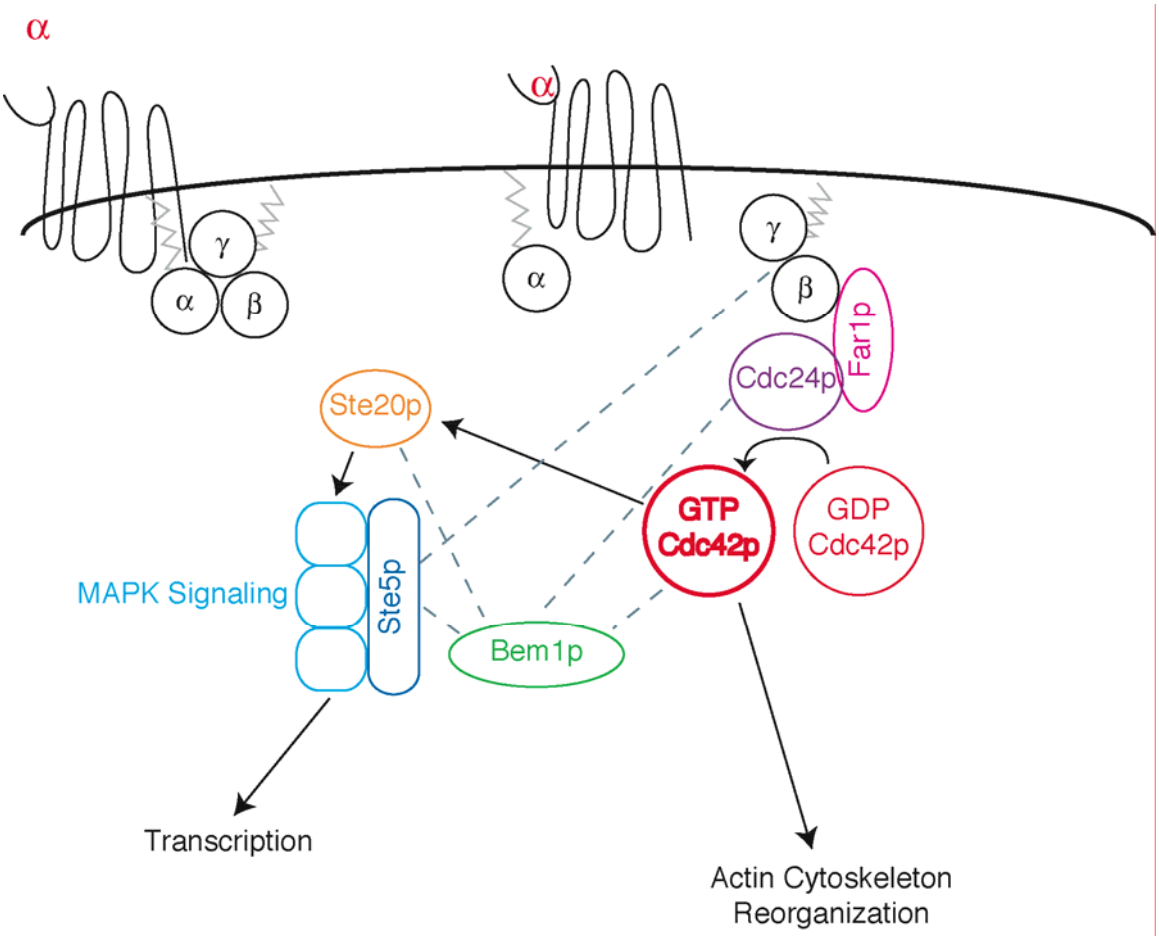

Figure 1.3 Polarization of Cdc42p in response to mating pheromone

Binding of pheromone to the receptor results in the reorganization of the actin cytoskeleton for mating projection formation as well as activation of the MAP kinase signaling cascade. The grey zigzag lines indicate lipid modification. Dotted grey lines indicate physical interactions.

Gβγ-mediated activation of the MAP kinase pathway cooperates with GTP-Cdc42p polarization to promote pheromone response. Gβγ activates the MAP kinase pathway to signal cell cycle arrest and mating specific transcription by recruiting the PAK Ste20p and Ste5p (a scaffold for the MAP kinase cascade) to its location at the plasma membrane (Dohlman and Thorner, 2001). In the absence of pheromone, haploid cells sequester Cdc24p and Far1p in the nucleus before START. One of the results of MAP kinase signaling is release of Cdc24p and Far1p from the nucleus, enabling them to be recruited to the polarization site (Dohlman and Thorner, 2001). In addition to acting as the MAPK kinase kinase kinase, Ste20p is an effector of Cdc42p (Leberer et al., 1997; Peter et al., 1996) and binding to GTP-Cdc42p at the shmoo tip may help to activate Ste20p's role in MAP kinase signaling. The scaffold protein Bem1p, which binds to both Ste20p and GTP-Cdc42p, is also found in complexes with the scaffold Ste5p (Leeuw et al., 1995), further linking the polarity establishment machinery with MAP kinase signaling. In fact, Cdc42p and Cdc24p are required for MAP kinase activation (Simon et al., 1995; Zhao et al., 1995). These findings support the model that polarized GTP-Cdc42p recruits more scaffolds and effectors to reinforce the concentration of GTP-Cdc42p and MAP kinase signaling as well as recruiting effectors to reorganize the actin cytoskeleton to facilitate shmoo formation.

1.2.4 Polarization of Cdc42p in response to intrinsic cues (budding)

Yeast cells normally bud in highly regular patterns (Fig. 1.4A). These patterns of bud formation leave scars in the cell wall. Due to asymmetric digestion of the septum that forms between mother and daughter cells during cytokinesis, mother cells are left with a

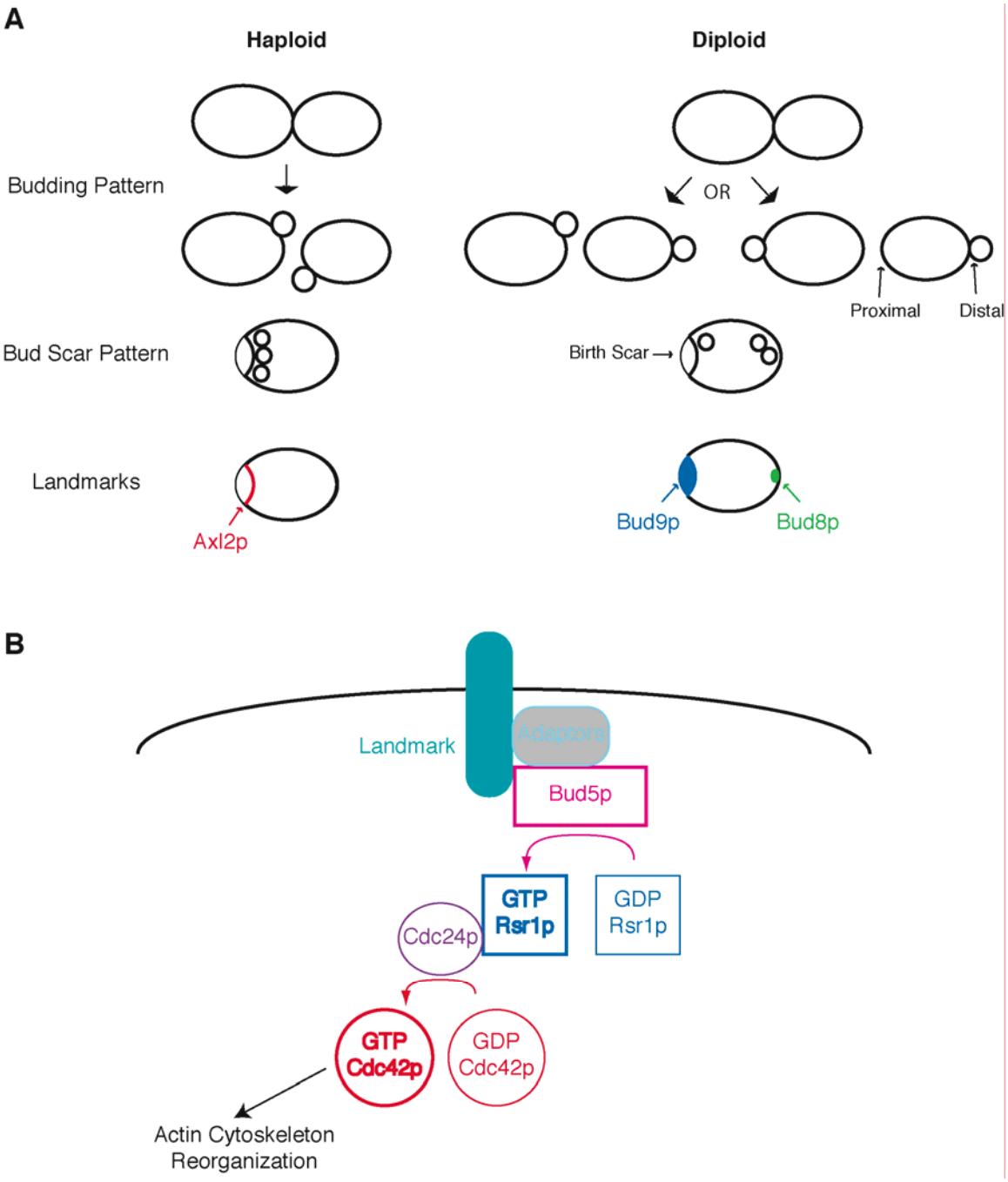

Figure 1.4 Polarization of Cdc42p in response to bud site selection cues

(A) Yeast cells bud in a highly regular pattern that is dictated by the landmark proteins. **(B)** The landmark proteins recruit the Rsr1p-GTPase module to in turn recruit the Cdc42p GEF Cdc24p.

chitin-rich ring, or bud scar, on the cell surface, while daughter cells are left with a broader scar that is enriched in mannan and lacks chitin, called a birth scar (Lew and Reed, 1993; Tkacz and Lampen, 1972). Staining the cell wall with the fluorescent dye calcofluor, which binds to chitin (Cabib and Bowers, 1975; Pringle, 1991), or with fluorescently labeled Concanavalin A, which binds to α-mannan, clearly labels the bud scars and birth scar respectively in cells. Haploid yeast display an "axial" budding pattern, and always position the next bud adjacent to the previous cell division site (Chant and Pringle, 1995). Staining haploid cells with calcofluor yields a characteristic chain of bud scars. In contrast, diploid cells display a "bipolar" budding pattern. A first-time diploid mother cell will always place its first bud at the distal end of the cell opposite the birth scar (Chant and Pringle, 1995). A multiple-time mother cell will place a bud at either pole of the cell, but adjacent to a previous division site (Chant and Pringle, 1995). Genetic screens for mutants that failed to bud according to these patterns identified a set of proteins, the bud site selection machinery, responsible for regulating the position of bud emergence. The bud site selection machinery broadly consists of landmark proteins that mark the site sites of bud emergence, and the Rsr1p GTPase module that interprets the landmarks to help generate GTP-Cdc42p (Park and Bi, 2007).

The landmark proteins are a set of integral-membrane proteins deposited at specific sites during bud growth (Fig. 1.4A). Haploid cells utilize the Axl2p landmark (Roemer et al., 1996). Axl2p localizes to the bud neck in medium and large budded cells and following cytokinesis, remains as a ring marking the division site (Halme et al., 1996). Diploid cells utilize several landmark proteins that mark both poles of the cell.

Bud8p localizes to the tips of growing buds and marks the distal pole on diploid daughter cells (Harkins et al., 2001). *bud8* mutants exhibit a unipolar budding pattern in which the buds emerge at the proximal pole of the cell (marked by the birth scar) (Zahner et al., 1996). In contrast, Bud9p appears to have the complementary function to Bud8p. Bud9p is localized to the proximal pole as a ring around the previous division site (Harkins et al., 2001), and *bud9* mutants exhibit a unipolar budding pattern in which the buds emerge at the distal pole of the cell (Zahner et al., 1996). Diploid cells contain two other integral-membrane landmark proteins, Rax1p and Rax2p, both of which localize to both poles of the cell and appear to function as long-term markers of previous division sites in diploids (Kang et al., 2004a).

The Ras-like GTPase Rsr1p is at the heart of the bud site selection machinery in both haploid and diploid cells (Fig. 1.4B) (Bender and Pringle, 1989; Chant and Herskowitz, 1991). Along with its GEF, Bud5p (Bender, 1993; Chant et al., 1991), and its GAP, Bud2p (Bender, 1993; Park et al., 1993), Rsr1p connects the landmark proteins listed above to Cdc24p, Cdc42p and Bem1p (Park and Bi, 2007). The current model of the bud site selection machinery hypothesizes that the landmark proteins, in both haploids and diploids, recruit Bud5p to their location causing a local increase in GTP-Rsr1p (Kang et al., 2004b; Kang et al., 2001). GTP-Rsr1p specifically interacts with Cdc24p (Park et al., 1997) thereby helping to recruit it to the site marked by the landmarks. Localized Cdc24p could then help generate local increases in GTP-Cdc42p. GTP-Cdc42p could then recruit the effectors necessary to create a polarized cytoskeleton and facilitate bud emergence at that site.

Our current model of bud site selection appears to provide a clear hierarchy to recruit Cdc42p to the incipient bud site, but unlike the pheromone response pathway, the landmark proteins do not dictate a discrete site on the cell periphery. Axl2p is present in a ring around the previous division site, and the next bud in a haploid cell could potentially emerge at any point along that ring. The cues dictating the diploid bipolar budding pattern are even more ambiguous. A diploid mother cell that has already gone through multiple rounds of cell division could have many, many possible locations to place the bud. Yet somehow when confronted with multiple polarization cues, Cdc42p still polarizes to one, and only one, site on the cell periphery.

1.2.5 Polarity establishment in the absence of positional cues

What happens to polarity establishment when positional cues are removed? In the absence of Rsr1p, Bud5p, or Bud2p, the position of bud emergence is randomized, but budding efficiency is unaffected (Bender, 1993; Bender and Pringle, 1989; Chant et al., 1991; Park et al., 1993). Without any positional cues from either a pheromone gradient or Rsr1p, **a** cells are still able to respond to α-factor and shmoo, they simply shmoo in a random direction (Madden and Snyder, 1992). Therefore yeast cells must contain some core polarity establishment mechanism that can polarize the cell independent of positional cues. In general, polarity establishment in the absence of all positional cues is referred to as symmetry breaking.

1.3 Symmetry breaking

1.3.1 GEF-PAK-mediated symmetry breaking

The Turing-type models of symmetry breaking polarization require a positive feedback loop to amplify stochastic fluctuations of polarity factors. What is the molecular basis for the positive feedback loop in yeast? A possible mechanism for the positive feedback loop required for symmetry breaking relies on the formation of a complex between GTP-Cdc42p, Bem1p, Cdc24p and a PAK kinase (Kozubowski et al., 2008). Bem1p is required for symmetry breaking (Irazoqui et al., 2003). Specifically, the protein-protein interactions mediated by the PB1 domain and the SH3-2 domain of Bem1p are required for symmetry breaking (Irazoqui et al., 2003). The PB1 domain mediates interaction with Cdc24p (Ito et al., 2001; Peterson et al., 1994). The SH3-2 domain of Bem1p binds many proteins, however only the PAKs are required for symmetry breaking (Kozubowski et al., 2008). By combining point mutations with fusions between Bem1p and either Cla4p or Cdc24p, and between Cla4p and Cdc24p, Kozubowski determined that a complex between Bem1p, Cdc24p and a PAK kinase is required for symmetry breaking (Kozubowski et al., 2008). Positive feedback could result from GEF-PAK complex formation if a Bem1p-Cdc24p-PAK complex could be recruited to a stochastic cluster of GTP-Cdc42p through interaction with the PAK CRIB domain. Binding to GTP-Cdc42p would activate the PAK, allowing it to phosphorylate and possibly activate the associated Cdc24p (Bose et al., 2001). Activated Cdc24p could convert neighboring GDP-Cdc42p to GTP-Cdc42p, which could then recruit more GEF-

PAK complex, thereby amplifying the original cluster of GTP-Cdc42p (Kozubowski et al., 2008).

1.3.2 The role of actin in symmetry breaking

An alternative positive feedback mechanism to the GEF-PAK amplification loop described above that relies on actin-mediated trafficking and recycling has been proposed to be functioning in yeast. Overexpression of GTP-locked Cdc42p^{Q61L} could promote polarization at random sites in G1-arrested cells (Wedlich-Soldner et al., 2003), although the levels of protein needed to induce spontaneous polarization also resulted in cell death (Irazoqui et al., 2003). Symmetry breaking by Cdc42p^{Q61L} required a polymerized actin cytoskeleton and myosin-mediated vesicular trafficking (Wedlich-Soldner et al., 2003). The authors proposed that clusters of Cdc42p^{Q61L} grew via a feedback loop in which Cdc42p^{Q61L} nucleated actin cables, which then delivered more Cdc42p^{Q61L} on secretory vesicles (Wedlich-Soldner et al., 2003). Sustained polarization required retrieval of Cdc42p^{Q61L} by endocytosis before it diffused too far from the cluster (Marco et al., 2007).

Although the actin-mediated positive feedback loop was first described in a highly artificial system, Wedlich-Soldner and colleagues proposed that an actin-mediated positive feedback mechanism polarizes wild type Cdc42p as well (Wedlich-Soldner et al., 2004). Cells containing Cdc24p-GFP and Cdc42p-GFP were arrested in early G1 by cyclin depletion. Upon release in the presence of the actin depolymerizing drug Latrunculin A (Lat A), polarization of Cdc24p-GFP and Cdc42p-GFP was delayed compared to untreated cells (Wedlich-Soldner et al., 2004). A similar delay in Cdc24p-GFP and Cdc42p-GFP polarization was observed in *bem1Δ* cells following release from

arrest. Additionally, the Cdc24p-GFP signal sometimes disappearined in *bem1Δ* cells (Wedlich-Soldner et al., 2004). When both the putative actin-mediated feedback loop and GEF-PAK feed back loop were disrupted (through addition of Lat A to *bem1Δ* cells), the cells failed to polarize Cdc24p-GFP or Cdc42p-GFP following release from cell cycle arrest (Wedlich-Soldner et al., 2004). These observations lead the authors to conclude that an actin-mediated positive feedback loop normally functions in parallel to the GEF-PAK feedback loop.

There are several reasons to think that the actin-mediated positive feedback mechanism proposed for $Cdc42p^{Q61L}$ is not normally central to symmetry breaking by wild-type Cdc42p. First, Cdc42p polarization does not require polymerized actin either during wild type polarization in response to bud site selection cues (Ayscough et al., 1997) or during symmetry breaking (Irazoqui et al., 2003). Second, it seems implausible that endogenous molecules of GTP-Cdc42p (that are not locked in the GTP-bound state by mutation) would have a long enough lifetime to persist through a full round of endocytosis, membrane trafficking, and exocytosis, as required by the model. Finally, inactivation of the GEF-PAK diffusional amplification mechanism by deleting the *BEM1* scaffold completely abolishes symmetry-breaking polarization (Irazoqui et al., 2003) and severely impairs polarization even in the presence of the bud site selection system (Bender and Pringle, 1991). Thus, an actin-based mechanism is neither necessary (in the presence of Bem1p) nor sufficient (in the absence of Bem1p) to promote symmetry-breaking polarization.

The actin cytoskeleton has been proposed to have a negative impact on polarity establishment during symmetry breaking in addition to a possible positive feedback role. When Ozbudak and colleagues attempted to film symmetry breaking polarization of GTP-Cdc42p (through a construct containing the PBD domain of the Cdc42p effector Gic2p fused to GFP) or Bem1p-CFP, they surprisingly found that the cells were able to polarize both proteins, but that the polarization was unstable (Ozbudak et al., 2005). PBD-GFP and Bem1p-CFP both polarized to large crescents on the cell periphery that then appeared to randomly wander the cortex of the cell before stopping and budding (Ozbudak et al., 2005). They did not observe this motile polarization site in the presence of Rsr1p (where symmetry breaking is not required) or when the actin cytoskeleton was depolymerized through treatment with Lat A (Ozbudak et al., 2005). These observations lead the authors to conclude that there is a delayed actin-mediated negative feedback loop that works to destabilize the polarization site, possibly through endocytic dispersal of polarity factor by actin patches, or delivery of Cdc42p GAPs on secretory vesicles along the polarized actin cables. The presence of an actin-mediated negative feedback loop remains uncertain, however. Although this study did observe traveling crescents of polarized proteins, the period between polarization and budding in their experiments was 60 minutes (Ozbudak et al., 2005), significantly longer than the approximately 10 minute period between polarization and budding that has been reported in fixed cells (Lew and Reed, 1993). Therefore it remains unclear whether the motile polarization site was an experimental artifact, or a characteristic of symmetry breaking polarization.

1.4 Singularity in polarity establishment

Is singularity in budding an intrinsic characteristic of the amplification mechanism, or is there a global inhibitor that acts to prevent multiple polarization sites from forming? Yeast geneticists have attempted to identify mutations that result in cells making more than one bud simultaneously, but to date only a single convincing mutation, *cdc42-22*, has been identified (Caviston et al., 2002). *cdc42-22* cells could grow two buds simultaneously and were able to polarize and bud in a random orientation in the absence of cell cycle cues or the GEF Cdc24p (Caviston et al., 2002). The fact that a mutation in *CDC42* perturbs singularity and that the endogenous GEF-PAK mechanism appears to be non-functional in *cdc42-22* cells suggests that singularity is intrinsic to the Cdc42p amplification mechanism. Consistent with this hypothesis, a recent mathematical model of polarity establishment in yeast hypothesized that singularity is guaranteed by competition between bud sites for a limiting amount of Bem1p-Cdc24p complex eventually leaving only a single incipient bud site (Goryachev and Pokhilko, 2008). However, there has been no experimental evidence supporting competition between multiple polarity sites so it is unknown whether competition is functioning in yeast cells. Additionally, due to the many pleiotropic defects in *cdc42-22* cells (such as a failure to follow cell cycle or bud site selection cues) the effect Cdc42-22p has on cells has been unclear. Therefore the mechanisms guaranteeing singularity in yeast remain elusive.

1.5 Thesis objectives

Genetic and biochemical studies have provided insight into the composition of the polarized patch of proteins that forms with Cdc42p at the polarization site (Irazoqui and Lew, 2004), however, much about the fundamental nature of the incipient bud site remains unknown. Are there distinct stages of incipient bud site assembly? Cdc42p and its effectors responsible for reorganizing the actin cytoskeleton are all peripheral membrane proteins. Where they have been investigated by fluorescence recovery after photobleaching (FRAP) analysis, the polarized proteins appear to be highly dynamic at the polarization site, turning over the polarized protein within a matter of seconds (Wedlich-Soldner et al., 2004). Is the entire complement of proteins at the incipient bud site as unstable as these proteins and constantly in flux? If not, then is there an "anchor" or group of proteins that remain relatively stable to facilitate bud growth? Through the use of live-cell microscopy we wished to characterize the assembly of the incipient bud site.

What is the relationship between the actin cytoskeleton and polarity establishment? A polymerized actin cytoskeleton is not necessary to polarize Cdc42p and a number of other incipient bud site proteins (Ayscough et al., 1997; Irazoqui et al., 2003). However, a polarized actin cytoskeleton is necessary to grow a bud. Therefore, under most circumstances Cdc42p will be polarizing its effectors, and potentially itself, in the presence of actin cables and patches. There are conflicting models as to whether actin predominantly aids polarization (Wedlich-Soldner et al., 2003) or can be a destabilizing force (Ozbudak et al., 2005). Does the actin cytoskeleton have the same effect on polarity

establishment in the presence and absence of polarization cues? We were interested in better understanding the roles that actin patches and actin cables play in Cdc42p polarization.

How do yeast cells guarantee singularity in budding? The loss of singularity in *cdc42-22* cells suggests that singularity in budding may be an inherent property of the Cdc42p amplification mechanism in yeast. We wanted to test whether singularity in budding is inherent to the amplification mechanism, or imposed by an external "singularity guaranteeing" process.

2. Opposing Roles For Actin in Cdc42p Polarization

Published as Irazoqui et al. 2005. *Molecular Biology of the Cell*. 16:1296-304.

2.1 Introduction

The Rho-family GTPase Cdc42p is critical for cell polarity in both yeast and mammalian cells (Etienne-Manneville, 2004; Pringle et al., 1995). In *Saccharomyces cerevisiae*, cell cycle commitment in late G1 triggers cell polarization in preparation for bud formation (Lew and Reed, 1993). This process involves the concentration of Cdc42p together with many other proteins in a "cap" at the presumptive bud site, the polarization of actin cables toward that site, the clustering of cortical actin patches (thought to be sites of endocytosis (Kaksonen et al., 2003)) at that site, and the assembly of a ring of septin filaments surrounding the Cdc42p cap (Pruyne and Bretscher, 2000a). Cdc42p is essential for polarization of cytoskeletal filaments (Adams et al., 1990), and it is believed that the concentration of Cdc42p at the presumptive bud site is critical for effective cell polarization. Consistent with this view, experiments in mammalian cells demonstrated that whereas activated, membrane-targeted Cdc42p distributed throughout the cell cortex did not induce cytoskeletal changes, spatial clustering of that Cdc42p sufficed to induce dramatic actin polarization (Castellano et al., 1999). Thus, the molecular basis for Cdc42p polarization is of fundamental importance to polarity establishment.

Once a cell is polarized, many cortical proteins are asymmetrically distributed. Three general classes of models have been invoked to explain such polarization (Fig. 2.1). In the first model (Fig. 2.1A), a pre-existing stably polarized "anchor" interacts

(directly or indirectly) with the protein of interest, thereby increasing its local concentration. In yeast, a subset of "bud site selection" proteins are integral membrane proteins with large extracellular domains which are thought to interact with the rigid cell wall in a manner that renders them immobile in the plane of the membrane (Harkins et al., 2001). These proteins are deposited at the poles of the cell during bud formation, allowing them to serve as "landmarks" that can anchor proteins to those sites in the following cell cycle (Schenkman et al., 2002). In the second model (Fig. 2.1B), a "fence" of membrane-associated filaments forms a diffusion barrier such that proteins delivered to one compartment cannot cross the fence to another compartment. In yeast, the septin filament system is thought to act as a fence between the cortex of the bud and that of the mother, maintaining the asymmetric distributions of cortical proteins delivered to only one side (Barral et al., 2000; Takizawa et al., 2000). In the third model (Fig. 2.1C), asymmetric distribution arises through a dynamic process in which the polarized cytoskeleton delivers cortical proteins to the "front" of the cell, and endocytic retrieval of the proteins occurs before they can diffuse too far from that site. Recycling of the endocytosed proteins to the front of the cell maintains the polarized distribution. In yeast, endocytosis of integral membrane SNARE proteins was required for their asymmetric distribution, indicating that they are polarized by this mechanism (Valdez-Taubas and Pelham, 2003). In all cases, a polarized cytoskeleton is needed to set up the asymmetry: the anchors and fences must be deposited or assembled at the right location, and polarized delivery to right side of the fence or the front of the cell is key for the latter two models.

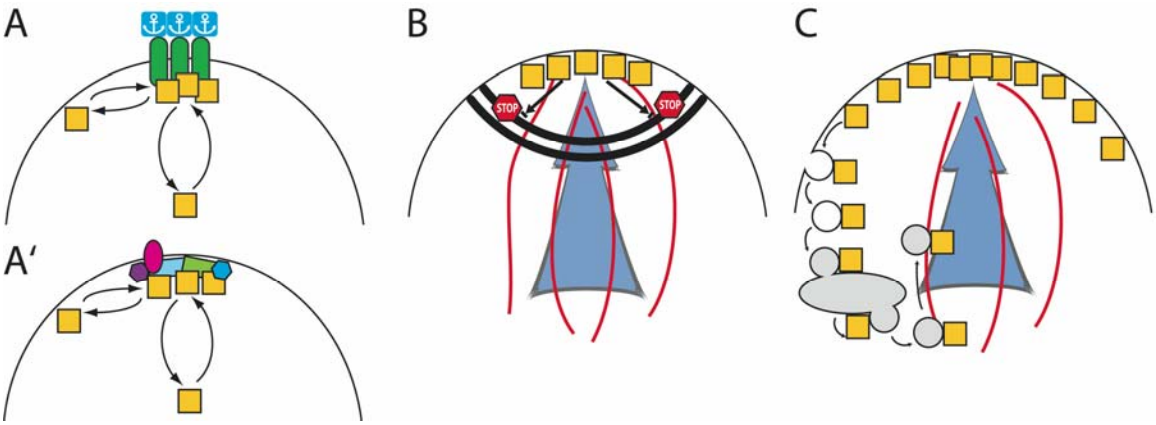

Figure 2.1 Mechanisms underlying polarized protein distribution.

A protein of interest (squares) displaying an asymmetric distribution at the cell cortex can attain that polarization via one or more of the indicated mechanisms. **(A)** A pre-existing asymmetric distribution of an anchored interacting factor can concentrate the protein of interest. Here, the interacting factor is shown connected to an extracellular anchor that might be a site of cell-cell contact, or an immobilizing extracellular matrix, or the yeast cell wall. A variant of the anchor model **(A')** is that a dynamic patch of interacting proteins is assembled by a symmetry-breaking process and serves to localize the protein of interest. Like the anchor model, this does not require input from the cytoskeleton. However, the anchor-like patch is not fixed but dynamic, and can assemble "de novo" at random locations. **(B)** A diffusion barrier (stop signs indicate blocked movement of the squares), such as the claudin-dependent tight junction, or the yeast septin-dependent neck cortex, can keep a cortical protein from crossing the fence (thick double black line). For this to produce a polarized distribution, the protein must be delivered to only one side of the fence (indicated by the blue arrow), along polarized cytoskeletal elements (red lines). **(C)** Polarized delivery (blue arrow and red lines as in **(B)** can yield a polarized distribution in the absence of a diffusion barrier if active recycling of the protein (here indicated by endocytic internalization, passage through a recycling endosome, and re-export along the polarized cytoskeleton) is fast enough to counter diffusion.

Which of these models accounts for Cdc42p polarization to the presumptive bud site? In a classic study, Ayscough et al. (1997) demonstrated that whereas F-actin was required for polarization of many proteins, depolymerization of all F-actin did not prevent Cdc42p polarization, suggesting that polarized delivery of Cdc42p or of other factors is not required for polarization of Cdc42p. The simplest explanation for that result is that Cdc42p is polarized via interactions with previously deposited anchors, and indeed the bud site selection landmarks are known to influence the location to which Cdc42p becomes polarized (Pringle et al., 1995). However, mutations that eliminate the landmarks themselves or other factors required for recognition of the landmarks do not prevent polarization, but only randomize the site at which polarization takes place (Chant, 1999). We recently showed that even in cells lacking effective landmarks to serve as anchors, Cdc42p could become polarized in the complete absence of F-actin or microtubules (Irazoqui et al., 2003). This result indicated that Cdc42p polarization could occur without pre-existing anchors and without the (actin-mediated) polarized delivery required by the fence and recycling models, indicating that this key regulator of polarity was itself polarized by a novel mechanism. Other data suggested that, together with interacting scaffolds and effectors including Bem1p, Cdc42p triggered the cooperative assembly of an anchor-like patch *de novo* (Irazoqui et al., 2003) (Fig. 2.1A').

A central finding supporting anchor models (Fig. 2.1A,A') for Cdc42p polarization was the ability of Cdc42p to polarize in the complete absence of F-actin. However, we now report that unlike loss of all F-actin, selective loss of actin cables causes the dispersal of Cdc42p from the pre-bud site in unbudded cells. Such dispersal is

reduced in an endocytosis mutant, suggesting that endocytic internalization of polarity factors by actin patches must be counteracted by polarized delivery along actin cables to maintain polarization of Cdc42p. Intriguingly, the polarized cap of Cdc42p in cells that have already formed a bud is much less sensitive to actin cable perturbation, suggesting that there are significant and previously unsuspected differences in the organization of the Cdc42p cap in budded and unbudded cells.

2.2 Results

2.2.1 Partial actin depolymerization results in loss of Cdc42p polarity

The role of F-actin in Cdc42p polarization has been addressed using Latrunculin A (Lat A), a G-actin binding compound isolated from the Red Sea sponge *Latrunculia magnifica* (Spector et al., 1983). Treatment of yeast cells with 100 μM (or more) Lat A results in the rapid disassembly of all detectable F-actin structures (Fig. 2.2A), blocking both polarized growth and endocytosis (Ayscough et al., 1997; Karpova et al., 2000). Because of the high cost of Lat A, we sought to extend our findings using its less expensive relative, Lat B. Lat B is not as potent as Lat A, and although detectable cables are lost following exposure to 100 μM Lat B, some F-actin patches remain (Fig. 2.2A) (McMillan et al., 1999). We were surprised to find that unlike Lat A, treatment of cells with Lat B led to a dispersal of Cdc42p from the pre-bud site (Fig. 2.2B), with most unbudded cells losing polarized Cdc42p staining within an hour of Lat B addition.

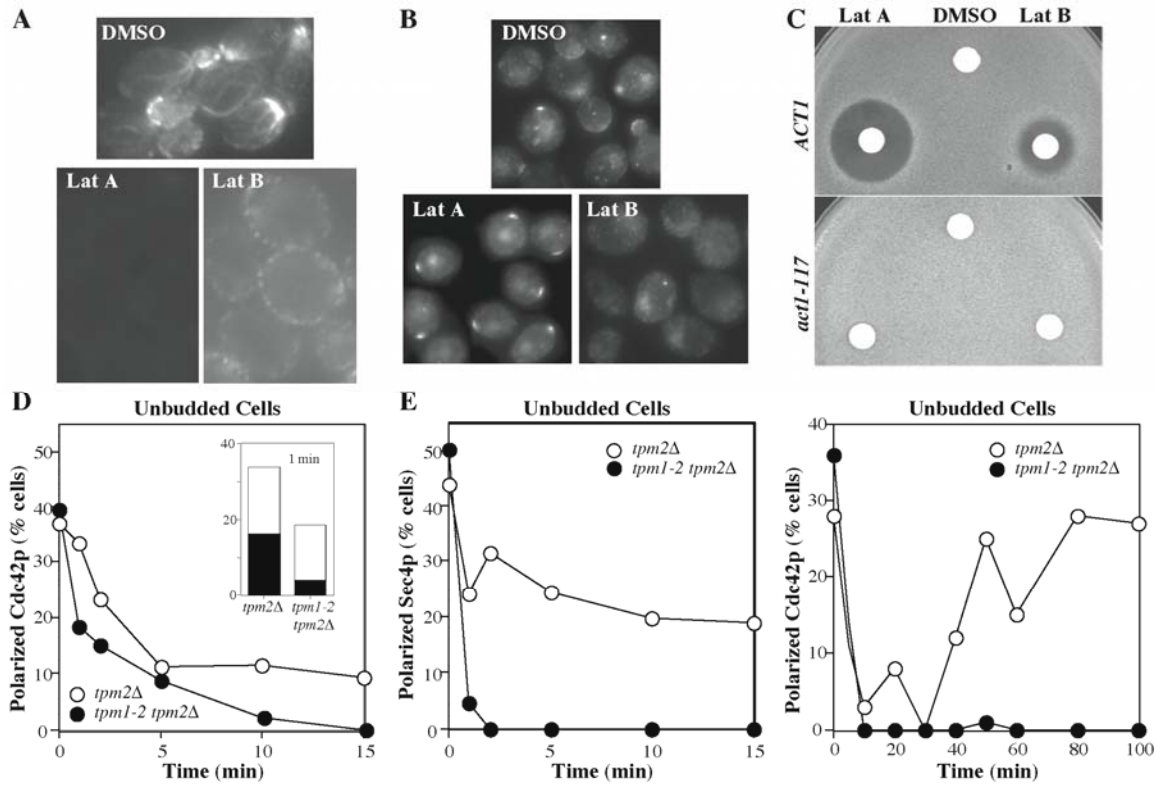

Figure 2.2 Loss of Cdc42p polarization upon partial actin depolymerization

(A) Wild-type cells (DLY5) were grown to exponential phase in YEPD at 30°C and treated with DMSO (control), Lat A (100 μM), or Lat B (100 μM) for 2 h. Cells were fixed and processed to visualize F-actin with alexafluor488-phalloidin. **(B)** Cells treated as above except in this case with 200 μM Lat B were processed to visualize Cdc42p by indirect immunofluorescence. **(C)** Lawns of wild-type (*ACT1*: DDY354) and latrunculin-resistant actin mutant (*act1-117*: DDY345) cells were spread on YEPD plates, sterile paper discs spotted with 10 μl DMSO (control), Lat A (2 mM), or Lat B (4 mM) were placed on the agar, and the plates were incubated for 2 days at 30°C. Growth inhibition by Lat A and (less potently) Lat B produced a clear zone or halo around the discs, but *act1-117* mutants were completely resistant to both Lat A and Lat B. Identical results were obtained with *act1-113* mutants (DDY342). **(D,E)** Tropomyosin mutant (*tpm1-2 tpm2*Δ: ABY971) and control (*tpm2*Δ: ABY973) cells were grown to exponential phase in YEPD at 24°C and shifted to 34.5°C at t=0. Rapid temperature shift was performed as described by Pruyne et al. (1998). Samples were fixed and double-stained to visualize Cdc42p **(D)** and Sec4p **(E)** by indirect immunofluorescence. >190 unbudded cells were scored for the presence of polarized signal at each time point. In the case of Cdc42p the polarized signal, though present, was diminished in the tropomyosin mutant after 1 min of shift: the inset in D indicates the proportion of cells with a bright polarized patch (black bar) versus a faint patch or extended crescent (white bar) at this time. **(F)** Cdc42p staining to a bright patch was quantitated in >100 unbudded cells from a separate experiment extending the temperature-shift to longer times.

One interpretation of these findings is that Lat B has another target in addition to actin, and that this second target causes dispersal of Cdc42p. However, we found that actin mutants previously shown to be resistant to Lat A (Ayscough et al., 1997) were also resistant to Lat B (Fig. 2.2C), suggesting that Lat B exerts its effects through actin. Consistent with this view, lower doses of Lat A also caused some Cdc42p dispersal (Fig. 2.3).

It is not clear from our data whether the dispersed Cdc42p remains at the cortex or redistributes to intracellular membranes, as immunofluorescence protocols do not reveal detectable unpolarized pools. Studies using GFP-Cdc42p, in contrast, detect abundant fluorescence throughout the cortex as well as on intracellular membranes (Richman et al., 2002; Wedlich-Soldner et al., 2004), but in that case the polarized signal is only a small fraction of the total, and redistribution would be hard to detect.

2.2.2 Selective loss of actin cables results in loss of Cdc42p polarity

Why would partial F-actin depolymerization disperse Cdc42p when full depolymerization does not? As actin cables appear to be more sensitive to Lat B than cortical patches, one possibility was that selective disruption of cables by Lat B was responsible for dispersing Cdc42p. To test this hypothesis we made use of temperature-sensitive tropomyosin mutants, which selectively lose actin cables but not patches upon shift to restrictive temperature, leading to the dispersal of polarized Sec4p (a secretory vesicle marker) within a minute after shift (Fig. 2.2E) (Pruyne et al., 1998). We found that polarized Cdc42p was dispersed from the pre-bud site within ten minutes upon shift of tropomyosin mutant cells to restrictive temperature (Fig. 2.2D). A complication with

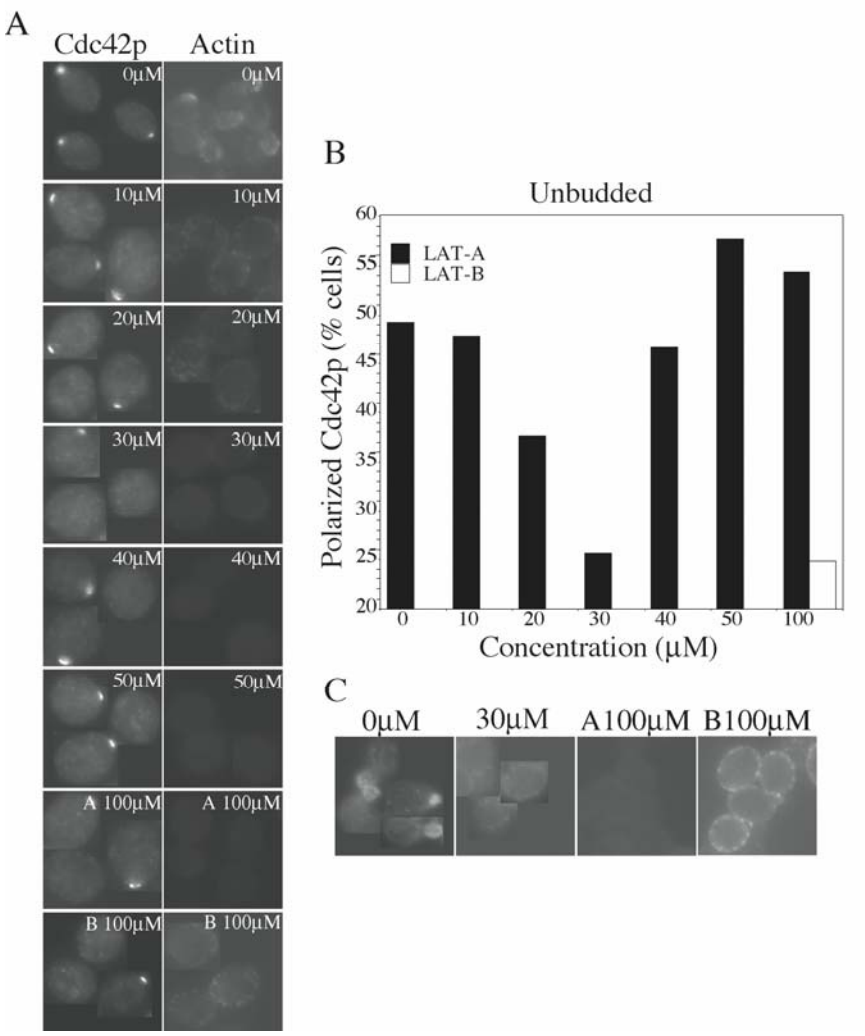

Figure 2.3 Treatment with low doses of Lat A resemble treatment with Lat B

Wild-type cells (DLY5) were grown to exponential phase in YEPD at 30°C and treated with the indicated doses of Lat A or Lat B for 2 h. Separate aliquots were processed to visualize F-actin or Cdc42p. **(A)** Representative cells from each sample, photographed using the same exposure times. **(B)** Quantitation of Cdc42p polarization, showing that in this experiment 100 μM Lat B and 30 μM Lat A promoted similar degrees of Cdc42p dispersal, while higher and lower doses of Lat A allowed greater maintenance of Cdc42p polarization. **(C)** Actin organization in cells treated with 100 μM Lat B and 30 μM or 100 μM Lat A (and untreated controls), photographed using different exposures optimized to detect the remaining actin structures. Only cortical patches (or their remnants) are detected in the treated cells. Surprisingly, there was reproducibly much less total F-actin in cells treated with 30 μM Lat A (the dose at which Cdc42p was most dispersed) than in cells treated with 100 μM Lat B (where Cdc42p was also dispersed). Both samples lacked detectable cables, but the remaining patches were much brighter in the Lat B-treated cells, suggesting that patch components can compete effectively with Lat B, but not with Lat A, for actin monomers.

this experiment is that even wild-type cells transiently disperse polarized Cdc42p upon temperature shift (Fig. 2.2D)(Ho and Bretscher, 2001). However, dispersal of Cdc42p from the pre-bud site was reproducibly more rapid in tropomyosin mutants than in wild-type cells. Indeed, considerable Cdc42p dispersal had occurred after only one minute at restrictive temperature in the tropomyosin mutant cells, and most of the cells still displaying polarized staining for Cdc42p had fainter or more diffuse staining compared to the bright Cdc42p spots in the wild-type cells (Fig. 2.2D, inset). Thus, selective loss of actin cables led to rapid dispersal of Cdc42p from the polarization site in unbudded cells. Moreover, unbudded wild-type cells recovered polarized Cdc42p staining by 50 min following temperature shift, but the unbudded tropomyosin mutant cells never recovered polarized Cdc42p (Fig. 2.2E), indicating that cables are required for regaining and/or maintaining polarity.

To ask whether loss of actin cables prevented the establishment as well as the maintenance of Cdc42p polarity, we isolated early G1 wild-type and tropomyosin mutant cells from asynchronous populations using centrifugal elutriation, incubated them at restrictive temperature, and examined Cdc42p localization as cells progressed through the cell cycle. The 50 min temperature shift recovery period in such cells occurs prior to cell cycle commitment and polarization. Wild-type and tropomyosin mutant cells both initially polarized Cdc42p at 80 min, but whereas wild-type cells retained polarized Cdc42p and went on to bud, the tropomyosin mutants lost polarized Cdc42p staining within 20 min and never formed a bud (Fig. 2.4A,B). Thus, Cdc42p polarization to the presumptive bud site can occur in the absence of actin cables, but it is not maintained.

Only 20% of tropomyosin-mutant cells showed a clear Cdc42p polarization at 80 min, as compared with 43% of control WT cells. Thus, the Cdc42p dispersal mechanism may be sufficiently effective to completely block Cdc42p polarization in many cells. Alternatively, all cells may be able to establish an initial Cdc42p polarity, which is then rapidly dispersed. As polarization of Cdc42p is triggered by a cell cycle cue and the population of cells was not perfectly synchronous with respect to cell cycle stage, we might only detect a robust Cdc42p cap in the 20% of cells that were in just the right cell cycle stage in this experiment.

One way that actin cables could contribute to Cdc42p polarity is by promoting polarized trafficking of cargo by myosin motors. The type V myosin Myo2p transports secretory vesicles and other cargo along actin cables (Schott et al., 1999; Schott et al., 2002). To test whether Myo2p-mediated trafficking was important for maintaining Cdc42p polarization at the pre-bud site, we repeated the synchrony experiment using temperature-sensitive *myo2-16* mutants. As shown in Fig. 2.4C,D, *myo2-16* cells initially polarized Cdc42p at the same time as wild-type controls, but then lost polarized Cdc42p staining and failed to form buds. A significantly higher fraction of cells were observed to polarize Cdc42p in the myosin mutants (Fig. 2.4C,D) as compared with the tropomyosin mutants (Fig. 2.4A,B). This observation may reflect the presence of residual Myo2p activity in the mutant, or perhaps a contribution from additional actin cable-mediated pathways (e.g. the related myosin Myo4p). Regardless, these experiments indicate that Myo2p-mediated polarized traffic along actin cables is required for maintainance (though not for initial establishment) of Cdc42p polarity at the pre-bud site.

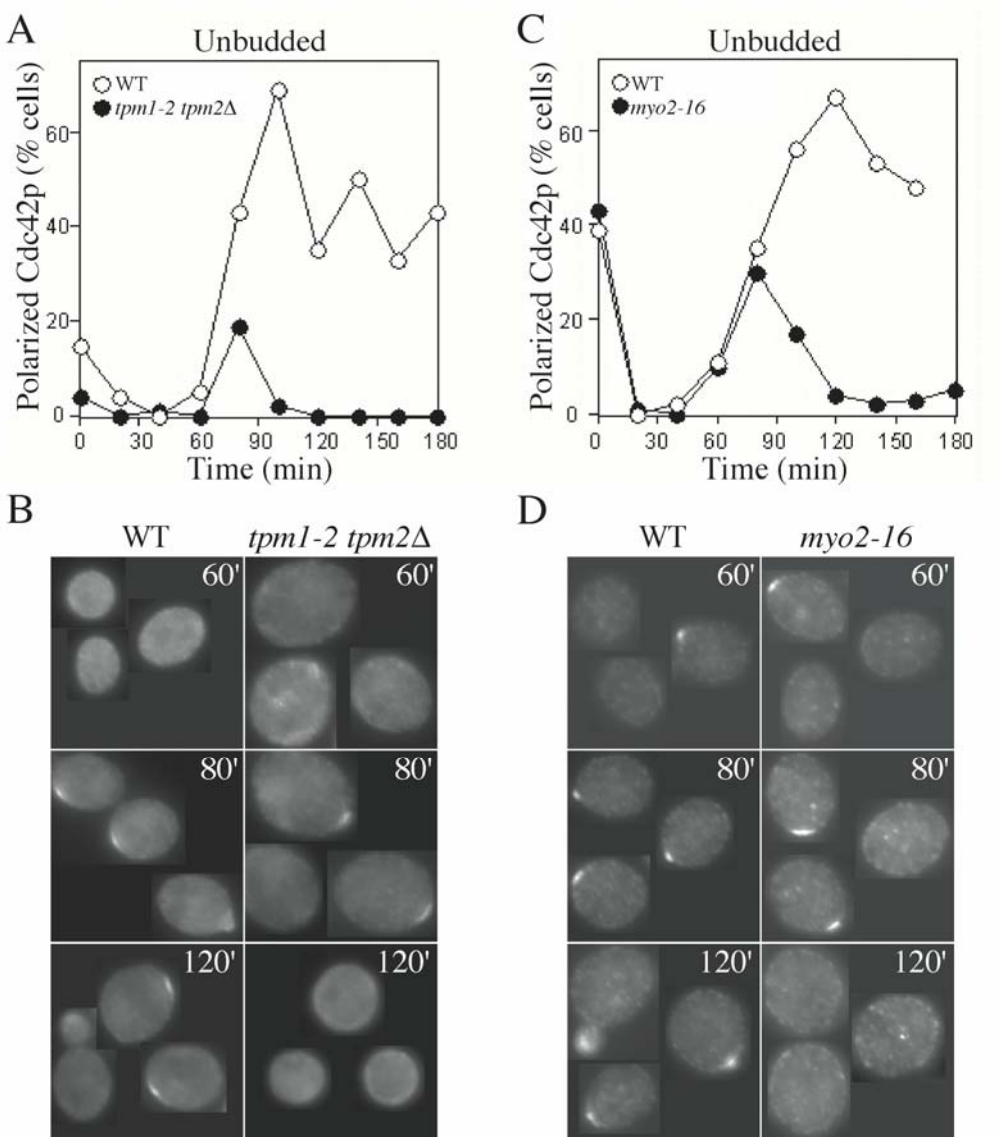

Figure 2.4 Selective loss of actin cables or Myo2p function impairs maintenance but not establishment of Cdc42p polarization.

(A,B) Tropomyosin mutant (*tpm1-2 tpm2*Δ: ABY971) and wild-type (ABY551) cells were grown to exponential phase in synthetic complete medium without histidine at 24°C, and small daughter cells were isolated by centrifugal elutriation, harvested by centrifugation, and resuspended in pre-warmed YEPD at 35°C (t=0). Samples were fixed at 20 min intervals and processed to visualize Cdc42p by indirect immunofluorescence. **(A)** Quantitation: >100 cells were scored for the presence or absence of Cdc42p polarization. **(B)** Representative cells from the indicated timepoints. **(C,D)** Myosin mutant (*myo2-16*: ABY553) and wild-type (ABY551) cells were treated as above except that the restrictive temperature was 37°C. **(C)** Quantitation: >100 cells were scored for the presence or absence of Cdc42p polarization. **(D)** Representative cells from the indicated timepoints.

2.2.3 Dispersal of Cdc42p involves endocytosis

Cdc42p is prenylated and peripherally associated with cellular membranes, but significant cytoplasmic pools also exist (Ziman et al., 1993). It is thought that the guanine nucleotide dissociation inhibitor (GDI) Rdi1p removes Cdc42p from the membrane to the cytosolic pool (Koch et al., 1997; Masuda et al., 1994). Thus, the Cdc42p dispersal following selective elimination of actin cables could occur via direct displacement of Cdc42p from the membrane by Rdi1p, or by endocytic uptake of Cdc42p (or of anchoring factors for Cdc42p) from the presumptive bud site. We found that dispersal of Cdc42p in response to Lat B was unaffected by deletion of *RDI1* (Fig. 2.5A,B). To test whether Cdc42p dispersal required endocytosis, we used temperature-sensitive *sla2* mutants (also called *end4*) that have a defect in the internalization step of endocytosis (Raths et al., 1993). Sla2p is a homolog of the mammalian huntingtin interacting protein (HIP1)(Henry et al., 2002) and is localized to actin patches (Yang et al., 1999). Sla2p binds to clathrin and is thought to be a conserved endocytic adaptor protein (Henry et al., 2002; Kaksonen et al., 2003). Wild-type and *sla2* mutant cells were shifted to restrictive temperature for 1 h to inactivate Sla2p (in the mutant) and allow recovery of Cdc42p polarity after the shift. Lat B was then added for 15 or 60 min and Cdc42p polarity was examined (Fig. 2.5C,D). Dispersal of Cdc42p from the pre-bud site was significantly reduced in *sla2* mutants compared to the controls, at both time points (Fig. 2.5C,D). Thus, Cdc42p dispersal occurs primarily by endocytosis, and F-actin cables are required to counteract this effect. As endocytosis is also dependent on F-actin (Ayscough et al., 1997), complete actin depolymerization by Lat A eliminates the

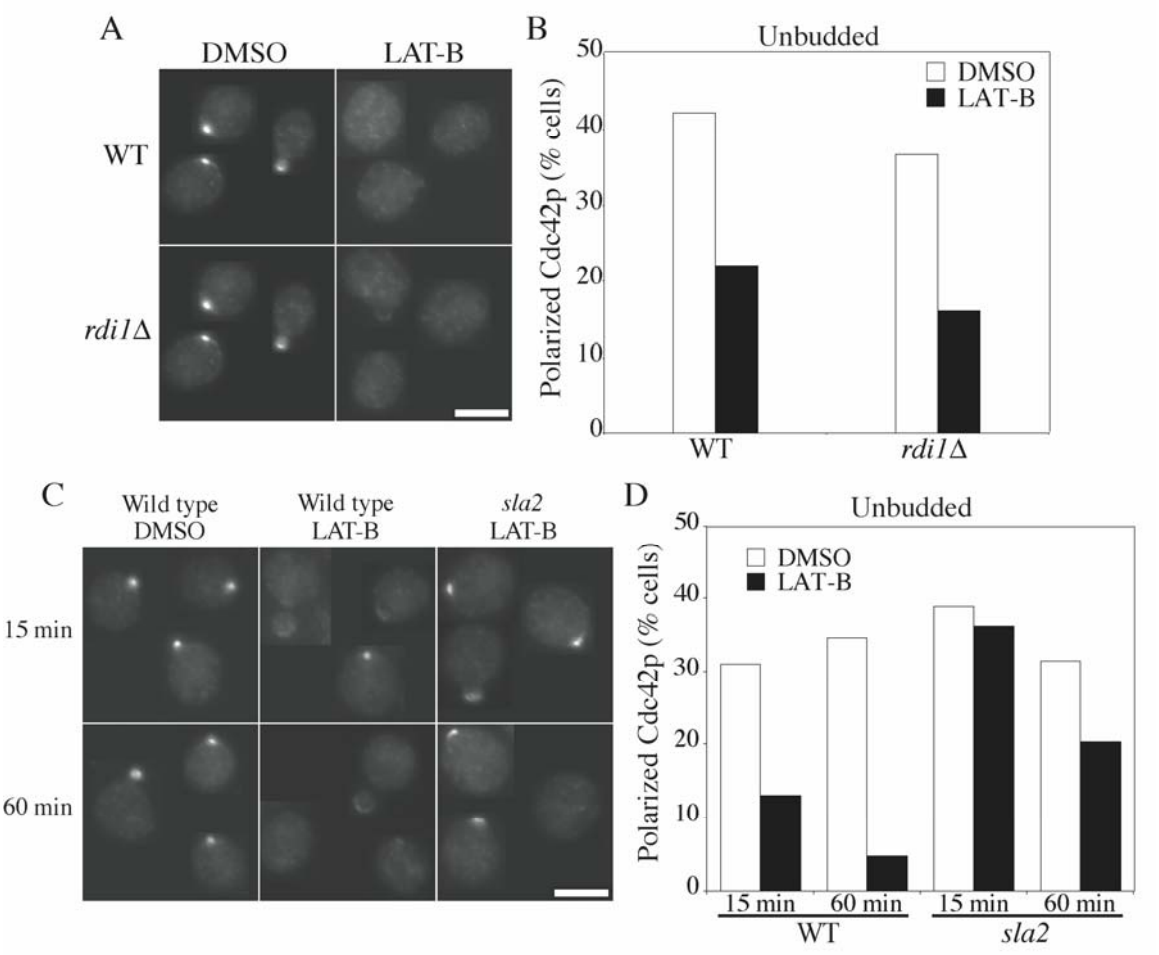

Figure 2.5 Cdc42p dispersal involves endocytosis but not Rdi1p.

(A,B) Wild-type (DLY1) and *rdi1*Δ (GPY10) cells were grown to exponential phase in YEPD at 30°C and treated with DMSO (control) or Lat B (100 μM) for 1 h, and then fixed and processed to visualize Cdc42p by indirect immunofluorescence**. (A)** Representative cells. Bar, 5 μM. **(B)** Quantitation: >100 cells were scored in each sample. **(C,D)** Wild-type (RH1800) and temperature-sensitive *sla2* (*sla2-41=end4-1*: DDY595) cells were grown to exponential phase in YEPD at 24°C, and shifted to 37°C (restrictive temperature) for 1 h, after which Cdc42p polarity had largely recovered from the temperature shift. Lat B (200 μM) was added for an additional 15 or 60 min at 37°C, as indicated, leading to dispersal of Cdc42p in the wild type but not in the *sla2* cells. **(C)** Representative cells. Bar, 5 μM. **(D)** Quantitation: >100 cells were scored in each sample.

dispersal mechanism and hence obviates the need for actin cables in maintaining Cdc42p polarization.

2.2.4 Cdc42p polarization becomes more resistant to dispersal after bud emergence

The studies described above focused on Cdc42p polarization to the presumptive bud site in unbudded cells. Following bud emergence, Cdc42p remains polarized to the bud tip until the activation of Cdc28p by mitotic cyclins triggers the apical-isotropic switch in bud growth, after which Cdc42p is dispersed until cytokinesis, when it accumulates at the mother-bud neck (Pruyne and Bretscher, 2000a; Richman et al., 2002). Like unbudded cells, small-budded cells also lost polarized Cdc42p staining following exposure to Lat B (data not shown) or prolonged shift of tropomyosin mutants to restrictive temperature (Fig. 2.6A). However, in the tropomyosin mutants this loss was significantly slower than the depolarization of Cdc42p in unbudded cells (compare Fig. 2.6A with Fig. 2.2F): Cdc42p initially depolarized due to temperature shift at the same rate in wild-type and tropomyosin mutant cells, then repolarized 50 minutes later, but was subsequently dispersed in the tropomyosin mutants. Although some of this dispersal likely reflects progress of the cell cycle to a point where Cdc42p normally becomes dispersed, recent evidence suggests that at least some of the budded tropomyosin mutants arrest the cell cycle prior to that stage (Pruyne et al., 2004). Thus, loss of actin cables leads to a delayed loss of Cdc42p polarization in budded cells.

To directly test whether budded cells at a cell cycle stage prior to the apical-isotropic switch would disperse Cdc42p upon loss of cable-directed traffic, we arrested

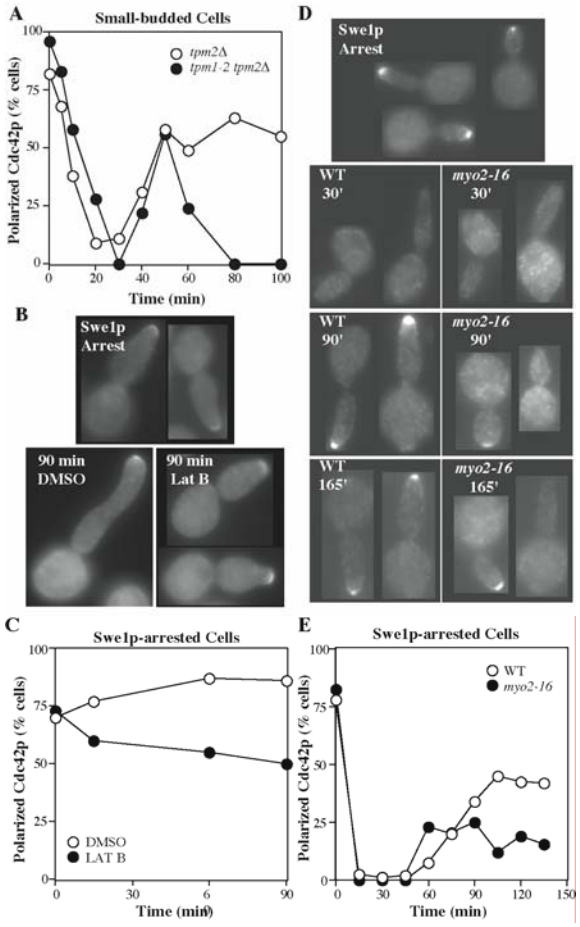

Figure 2.6 Cdc42p in budded cells is more resistant to dispersal by actin perturbation.

(A) Tropomyosin mutant (*tpm1-2 tpm2*Δ: ABY971) and control (*tpm2*Δ: ABY973) cells from the same experiment as in Fig. 2F above were scored to quantitate the proportion of small-budded cells displaying a tight patch of polarized Cdc42p. **(B, C)** Wild-type cells containing a *GAL1*-regulated *SWE1* gene (DLY3466) were grown to exponential phase in YEP-sucrose at 30°C and induced to express Swe1p by addition of galactose to 2% final concentration. After 1 h 40 min, many cells displayed large elongated buds characteristic of Swe1p-mediated G2 arrest (Lew and Reed, 1993), and at that time ("Swe1p Arrest") either DMSO or 100 μM Lat B was added. After 90 min, control (DMSO) cells continued to elongate their buds, whereas Lat B-treated cells ceased polarized growth and grew uniformly larger, although most did not disperse tip-localized Cdc42p. **(B)** Representative cells from the indicated samples. **(C)** Quantitation: >100 cells were scored for the presence or absence of Cdc42p polarization. **(D,E)** Wild-type and *myo2-16* cells containing a *GAL1*-regulated *SWE1* gene (DLY7543 and DLY7544, respectively) were grown to exponential phase in YEP-raffinose at 24°C and induced to express Swe1p by addition of galactose to 2% final concentration. After 2 h ("Swe1p Arrest"), the cells were shifted to 37°C, samples were fixed at 15 min intervals and processed to visualize Cdc42p. **(D)** Representative cells from the indicated samples. **(E)** Quantitation: >100 cells were scored for the presence or absence of Cdc42p polarization.

cells by overexpressing the mitotic cyclin/Cdc28p inhibitor Swe1p (Booher et al., 1993) and monitored Cdc42p localization following treatment with Lat B or shift-up of *myo2-16* mutants. As shown in Fig. 2.6B,C, most Swe1p-arrested cells treated with Lat B retained polarized Cdc42p staining. In *myo2-16* mutants, Cdc42p polarity was initially lost and then recovered following temperature shift as in wild-type cells. However, the degree of recovery was impaired in *myo2-16* cells compared to wild-type controls (Fig. 2.6D,E), indicating that myosin-mediated traffic contributes to Cdc42p polarity in budded cells. In summary, treatments that all caused dispersal of Cdc42p in unbudded cells had differing effects in budded cells, causing complete (tropomyosin mutant), partial (myosin mutant) or little (Lat B) dispersal. Even when dispersal did occur, it was much slower than in unbudded cells. Thus, the polarized Cdc42p in budded cells is significantly more resistant than that in unbudded cells to treatments that selectively disrupt actin cable-mediated traffic.

2.3 Discussion

2.3.1 Opposing effects of actin cables and actin patches on Cdc42p polarity

There are two clearly distinct types of F-actin structures in polarized yeast cells. Actin cables are polarized towards the pre-bud site and the bud tip, and serve as tracks for myosin-mediated traffic to those sites (Schott et al., 2002). Actin patches cluster at the pre-bud site and within the bud (Adams and Pringle, 1984), and are thought to mark sites of endocytosis as well as endocytic vesicles which have just been internalized (Kaksonen et al., 2003). F-actin is essential for both polarized traffic and endocytosis (Ayscough et

al., 1997). Previous studies documented the ability of Cdc42p to become polarized and to maintain polarity in the complete absence of F-actin in yeast (Ayscough et al., 1997; Irazoqui et al., 2003). However, we now report that selective impairment of actin cables caused dispersal of Cdc42p from the pre-bud site, and that such dispersal was dependent on actin patch-mediated endocytosis. Our results suggest that actin patches disperse Cdc42p through endocytosis, whereas oriented actin cables help to maintain Cdc42p polarization through myosin-mediated traffic. Thus, following its initial actin-independent polarization, subsequent maintenance of Cdc42p polarization at the pre-bud site involves an actin-mediated trafficking cycle.

We used three different perturbations that selectively disrupt actin cable function. Tropomyosin mutants eliminate cables without reducing the number or brightness of the patches (Pruyne et al., 1998). *myo2-16* mutants affect the major (though not the only) myosin that delivers cargo along actin cables, and do not affect actin patches (Schott et al., 1999). Lat B binds to G-actin (Ayscough et al., 1997), and appears to be more effective at sequestering the actin from cable nucleators than from patch nucleators, although it clearly does reduce the amount of F-actin in patches as well. These perturbations all dispersed Cdc42p from the pre-bud site, although there were differences in the rapidity and effectiveness of the dispersal (fast and complete in tropomyosin mutants, slower and incomplete upon Lat B treatment). Tropomyosin mutants were also more effective than Lat B at dispersing Cdc42p from the bud tip in budded cells, although in all cases dispersal was slower and less complete in budded than in unbudded cells (see below). These differences are consistent with the hypothesis that dispersal is mediated by

the actin patches, whose function is partly impaired upon Lat B treatment but not in tropomyosin mutants. Dispersal of Cdc42p from the pre-bud site was greatly reduced upon inactivation of the actin patch component Sla2p, which is required for endocytosis. In summary, our data indicate that if unopposed, actin-dependent endocytosis disperses Cdc42p. Endocytosed factors are normally recycled to the polarization site by vesicles trafficking on oriented actin cables, thereby maintaining Cdc42p polarity. As both endocytosis and polarized delivery are actin-dependent, actin perturbations exhibit different effects depending on the degree to which actin's opposing roles are affected by the perturbation. Thus, maintenance of Cdc42p polarization at the presumptive bud site involves a dynamic and antagonistic interplay between distinct F-actin structures.

We also confirmed previous work (Ho and Bretscher, 2001) showing that mild temperature shift of wild-type cells causes a transient, reversible dispersal of Cdc42p from polarization sites. Interestingly, temperature shift also induces a transient and partial actin depolymerization associated with selective loss of actin cables (Lillie and Brown, 1994), which may contribute to the dispersal of Cdc42p. However, temperature-shift-induced dispersal was also observed in *sla2* mutants (data not shown), indicating that it does not require endocytosis. Actin patches and glucan synthase complexes are also transiently dispersed upon temperature shift, and that dispersal has been ascribed to a Pkc1p-dependent stress signaling pathway (Delley and Hall, 1999), which may also act on Cdc42p.

2.3.2 Establishment versus maintenance of Cdc42p polarization

Once it is polarized, Cdc42p directs the orientation of actin cables towards the polarization site, most likely through formin proteins that are thought to be Cdc42p effectors as well as actin cable nucleators (Evangelista et al., 1997; Evangelista et al., 2002; Sagot et al., 2002). As we found that actin cables, in turn, contribute to maintaining Cdc42p polarity, there is potential for a positive feedback loop in which clustering of Cdc42p promotes actin cable orientation which reinforces Cdc42p clustering. Does this "actin-feedback" pathway contribute to the initial polarization of Cdc42p?

Wedlich-Soldner and colleagues have proposed that delivery of secretory vesicles carrying Cdc42p along actin cables concentrates Cdc42p at the polarization site, and that such actin-mediated positive feedback contributes to polarity establishment when bud site selection cues are absent (Wedlich-Soldner et al., 2003; Wedlich-Soldner et al., 2004). Initial support for this model came from the demonstration that polarization of an overexpressed GTP-locked mutant form of Cdc42p was absolutely dependent on F-actin, Myo2p, and secretory function, and that the GTP-locked Cdc42p was present on secretory vesicles (Wedlich-Soldner et al., 2003). However, wild-type Cdc42p can polarize in the absence of F-actin (Ayscough et al., 1997), even in the absence of bud site selection cues (Irazoqui et al., 2003), indicating that if such a feedback loop does operate, it is not absolutely required for polarization.

In a more recent study monitoring wild-type GFP-Cdc42p localization, Wedlich-Soldner at al. found that whereas most cells established and maintained robust Cdc42p polarization upon treatment with Lat A, a subset of cells established a "flickering"

Cdc42p polarity that was subsequently lost (Wedlich-Soldner et al., 2004). This observation suggests, consistent with our results, that actin can help to maintain Cdc42p polarization, making the polarization site more stable. In addition, they showed that in the absence of the scaffold protein Bem1p, F-actin was absolutely essential for any detectable polarization (Wedlich-Soldner et al., 2004). These observations suggested that the initial polarization of Cdc42p could occur either through an actin-independent pathway involving Bem1p (Irazoqui et al., 2003) or through an actin-dependent pathway. Distinguishing whether this actin-dependent pathway involves the proposed actin-Cdc42p feedback loop will require identification of the trafficking cargo relevant to Cdc42p polarization.

2.3.3 How do actin cables promote Cdc42p polarity?

Which cargo transported on actin cables is responsible for helping to maintain Cdc42p polarization? The simplest hypothesis would be that trafficking of Cdc42p itself is important: GTP-locked Cdc42p was found in a vesicle fraction (Wedlich-Soldner et al., 2003), and it seems likely that wild-type Cdc42p can also associate with vesicles. However, it appears that wild-type Cdc42p exchanges between membrane and cytosolic pools far more rapidly that GTP-locked Cdc42p (Wedlich-Soldner et al., 2004). In addition, polarization by the "actin-feedback" membrane recycling pathway illustrated in Fig. 1C will only be effective if diffusion is slow relative to endocytic recycling, as has been shown for some integral membrane proteins (Valdez-Taubas and Pelham, 2003), but fluorescence recovery after photobleaching experiments suggest that Cdc42p diffuses much more rapidly (Wedlich-Soldner et al., 2004). Thus, it is not clear whether vesicle

trafficking of Cdc42p itself would be a major contributor to Cdc42p polarization. Many integral and peripheral membrane proteins co-localize with Cdc42p (Irazoqui and Lew, 2004), and it seems likely that several of these proteins undergo both endocytosis and cable-mediated delivery. Thus, endocytosis may disperse Cdc42p by removing not only Cdc42p itself but several of its interacting factors from the polarization site. But because most known polarized factors are peripheral (not integral) membrane proteins, it is not clear whether they would need to be recycled to the polarization site via actin cables or whether they could return by diffusion through the cytoplasm. A recent study reported that in tropomyosin mutants, budded cells lost not only Cdc42p but also Rho1p polarization (as well as the ability to nucleate cables at the bud tip) after one hour without cables at the restrictive temperature (Pruyne et al., 2004). However, other peripheral components including Spa2p and the formin Bni1p were still largely polarized under those conditions, suggesting that these components either escape endocytosis or are able to return to the polarization site in a cable-independent manner.

2.3.4 Maturation of the polarization sites after bud emergence

To all appearances, the Cdc42p cap at the presumptive bud site and the cap at the tip of budded cells are very similar and share numerous components. However, we found that the cap in budded cells was considerably more resistant to dispersal upon selective loss of cable function than the cap in unbudded cells. In principle, this could be explained either by a difference in endocytic recycling or a difference in the cap itself. At present we cannot distinguish between these possibilities, but because extensive research into endocytosis has never (to our knowledge) revealed any differences between budded

and unbudded cells, we favor the hypothesis that the organization of the Cdc42p cap changes during or shortly after bud emergence. The nature and function of any such change remain to be discovered.

Author contribution: This chapter is the result of collaborative work. The author's contributions to this chapter include the data presented in Figures: 2.2 **A**, **D**, **E**; 2.3; 2.4, **B** and **D**; as well as Figures 2.5 and 2.6.

3. Characterization of the incipient bud site

3.1 Introduction

Cell cycle commitment at START results in the rapid reorganization of the yeast cytoskeleton. Within ~10 minutes of receiving the cell cycle cue, the actin cytoskeleton becomes polarized to a discrete site on the cell periphery (Lew and Reed, 1993). Over 30 proteins localize to the incipient bud site with the master polarity regulator Cdc42p to aid in the organization of the actin cytoskeleton and facilitate bud growth (Irazoqui and Lew, 2004). Dissecting what, if any, role these proteins play in polarity establishment (as defined either by Cdc42p polarization or actin cytoskeleton polarization) is difficult due to redundancies in the polarity establishment machinery. Mutation of Cdc42p or Cdc24p can block polarity establishment and budding (Adams et al., 1990; Sloat et al., 1981), but deletion of many other genes involved in polarity establishment results in relatively subtle phenotypes.

Live cell microscopy has been used to great effect to dissect assembly of other complex cellular structures, including the endocytic actin patch in budding yeast (Kaksonen et al., 2003) and the cytokinetic ring in *Schizosaccharomyces pombe* (Wu et al., 2003). By following pairs of fluorescently tagged proteins in live cells with a high degree of temporal resolution, Kaksonen, Wu and their colleagues were able to describe pathways for the assembly of the actin patch and contractile ring (Kaksonen et al., 2003; Wu et al., 2003). We sought to apply this type of analysis to polarity establishment. By mapping polarization of proteins with respect to one another and to bud emergence, we

hoped to determine whether there are different characteristic stages to polarity establishment and to create a pathway of relative protein polarization. Having a detailed map of polarity establishment would give us more descriptive power to analyze mutations that affect polarity establishment.

We chose to begin our analysis with four proteins that we could expect to have different polarization dynamics: Bem1p, Spa2p, Sec4p, and Abp1p. Bem1p is a scaffold protein that is a component in the amplification loop that helps to polarize Cdc42p (Kozubowski et al., 2008) and was chosen to represent the core polarity machinery. Like Cdc42p, Bem1p can polarize in the absence of a polymerized actin cytoskeleton (Ayscough et al., 1997). Spa2p is a component of the polarisome, which helps to organize the actin cytoskeleton (Sheu et al., 1998), and is one of the first proteins to polarize to the incipient bud site. Although Spa2p can polarize in the presence of the actin depolymerizing drug Latrunculin A, its polarization is delayed relative to cells containing an actin cytoskeleton (Ayscough et al., 1997). Sec4p is a secretory vesicle associated Rab-GTPase (Goud et al., 1988) that requires transport on actin cables to become polarized (Ayscough et al., 1997). Abp1p is an actin binding protein that labels actin patches (Drubin et al., 1990). Actin patches polarize to the incipient bud site along with actin cables (Adams and Pringle, 1984), presumably to endocytose cargo that is delivered along the actin cables.

Immunofluorescence studies have been unable to differentiate distinct stages of polarity establishment (Ford and Pringle, 1991); suggesting that the incipient bud site is assembled in a matter of minutes. This timeframe necessitated rapid filming if we hoped

to be able to describe relative protein polarization. Unfortunately, we found that the G1 phase of the yeast cell cycle was particularly sensitive to illumination. The frequency of image acquisition needed to differentiate between potential stages of polarity establishment often resulted in a failure of the cells to polarize or bud (Fig. 3.1). In some cases, cells were able to polarize one of the GFP-labeled proteins, however this polarization was a broad, occasionally motile crescent, which neither resembled the incipient bud site described by immunofluorescence studies, nor lead to bud emergence (data not shown). In order to film cells with the temporal resolution needed to follow polarity establishment we devised two synchrony methods to limit the amount of time cells were exposed to illumination prior to polarization. The first synchrony method utilized the *cdc24-1* temperature sensitive mutation to arrest cells just prior to polarization. We then moved to a pharmacological synchrony protocol using hydroxyurea, to arrest cells in the previous cell cycle.

3.2 Results

3.2.1 *cdc24-1* synchrony strategy

We first attempted to synchronize cells as close to the polarization event as possible using *cdc24-1* cells. Cdc24p is the guanine nucleotide exchange factor (GEF) for Cdc42p (Zheng et al., 1994) and at the restrictive temperature, *cdc24-1* cells arrest as large, unpolarized cells (Adams and Pringle, 1984; Sloat and Pringle, 1978). *cdc24-1* cells at the restrictive temperature will pass through START and progress through the cell cycle until G2. In the absence of a bud, yeast cells delay the cell cycle in G2 when cells

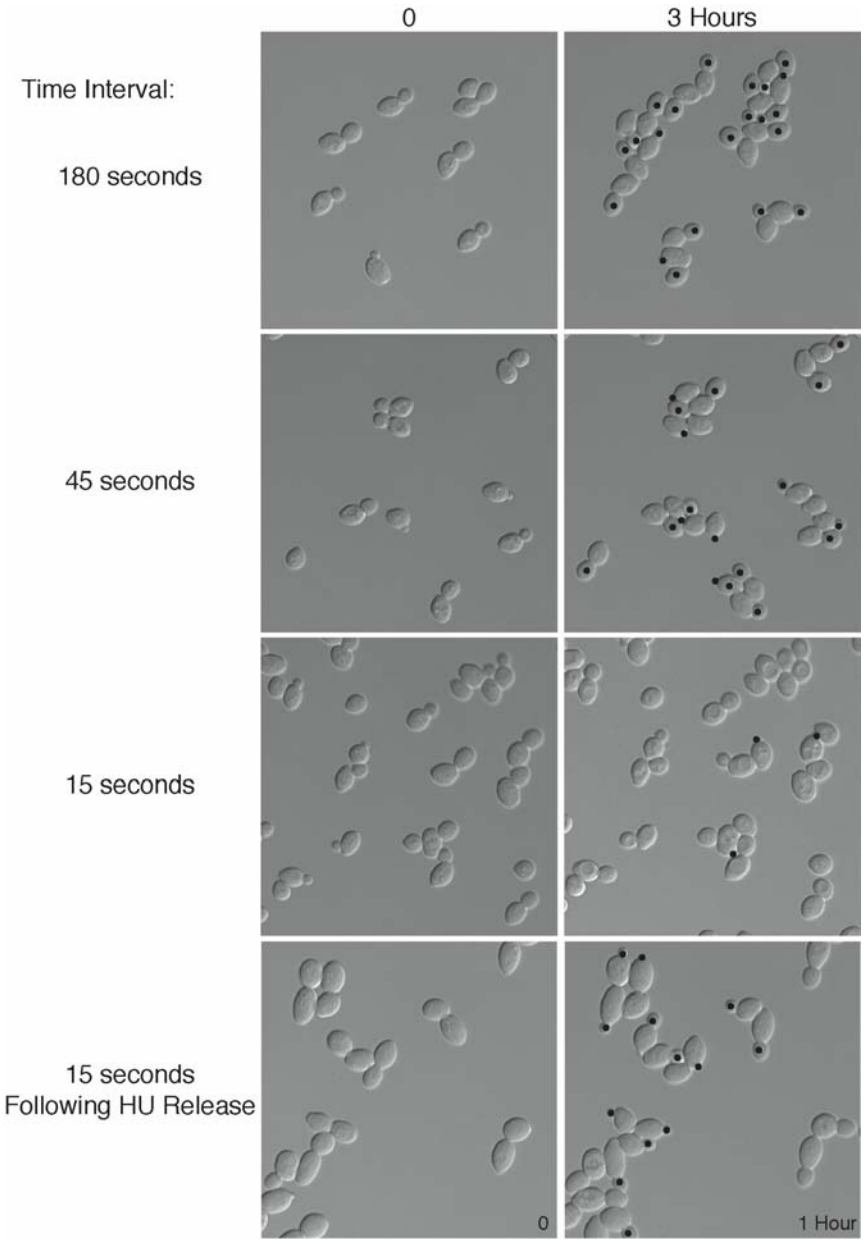

Figure 3.1 Blue-light induced phototoxicity

Frequent illumination to detect GFP signals results in a failure to bud in yeast cells, however prior arrest in HU can circumvent this phototoxicity. Cells were imaged as to detect Bem1p-GFP (11 z-planes with 0.5 μm steps, 200 ms exposure for each image) at the indicated intervals. Black circles mark the buds (or resultant cells) that polarized Bem1p-GFP to the incipient bud site after the timelapse began. Some bud sites had already polarized Bem1p-GFP at the start of filming and those buds were not marked.

are still polarization competent (Fig. 1.1) to allow bud emergence before entering mitosis (Lew and Reed, 1995). Therefore following release at the permissive temperature, *cdc24-1* cells rapidly establish an axis of polarity. We introduced functional constructs of *BEM1-GFP* and *SEC4-GFP* under the control of their own promoters into the *cdc24-1* background in addition to the endogenous copies of *BEM1* and *SEC4*. The functional *SPA2-GFP* replaced the endogenous copy of *SPA2* in our *cdc24-1* haploids. Asynchronous *cdc24-1* cultures were shifted to the restrictive temperature of 37°C for 2.5 h. Once these synchronized cells were shifted back down to the permissive temperature, they rapidly polarized (within approximately 10 minutes) and budded. By synchronizing the cells just prior to polarity establishment, we were able to acquire a GFP image every 10 s without preventing polarization or budding. Due to equipment constraints at the time, we were only able to acquire a single GFP image at every timepoint. Therefore having a large number of cells prepared to polarize also enabled us to image a single field of cells at a single focal plane and still find some cells that polarized in our view. We only analyzed the cells that grew a bud in the correct focal plane.

Bem1p-GFP and Spa2p-GFP rapidly accumulated at the incipient bud (Fig. 3.2), with the majority of cells dramatically increasing in signal intensity at the bud site within 20 – 30 s. Once Spa2p-GFP and Bem1p-GFP were polarized, they sometimes appeared to "flicker" in intensity. In contrast, vesicle-associated Sec4p-GFP did not have these periods of decreased signal intensity (Fig. 3.2). Sec4p-GFP generally appeared to gradually increase in intensity at the bud site over the course of polarization and bud emergence (Fig. 3.2).

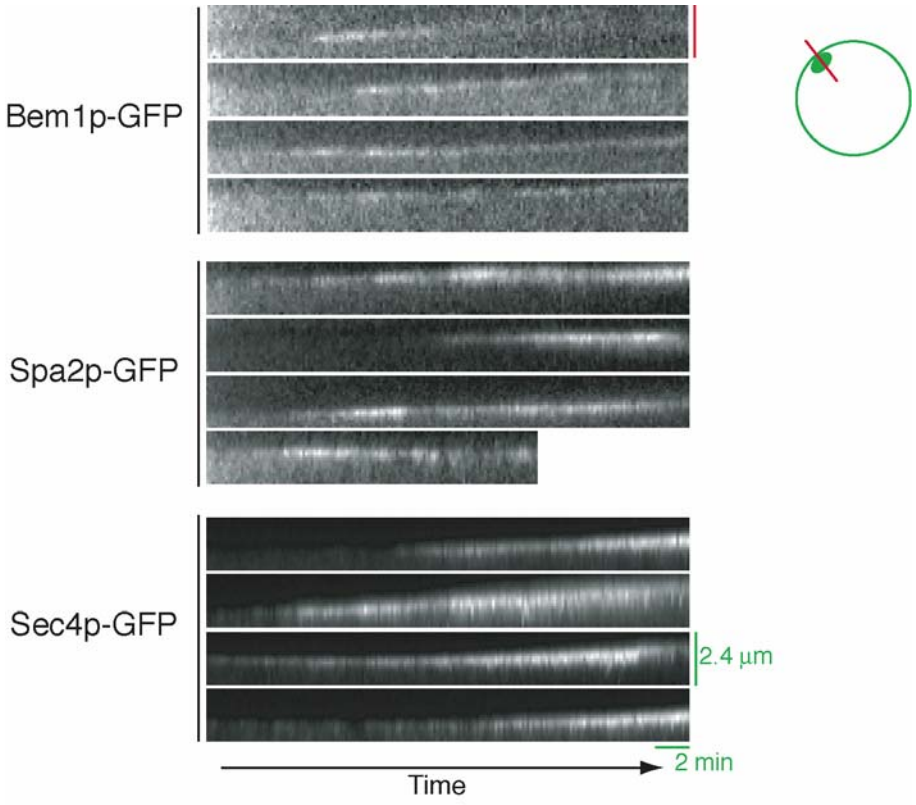

Figure 3.2 *cdc24-1* cells rapidly polarize following release from the restrictive temperature

cdc24-1 cells containing the indicated fluorescently labeled proteins were arrested in a depolarized state for 2 h at 37°C before being returned to room temperature and mounted on slides for live-cell microscopy. Single GFP images through the center of the cell were acquired every 10 s for a total of 30 minutes. Kymographs were constructed by drawing a 1 pixel-wide line through the polarization site, perpendicular to the plasma membrane. Representative kymographs are shown. The kymographs are aligned based on release from the restrictive temperature. Each kymograph starts approximately 8 minutes after release from 37°C. Bud emergence is apparent in the increasing slope of the polarized signal over time. The third Spa2p-GFP kymograph is abbreviated due to cell movement.

Although synchronizing cells with the *cdc24-1* mutation allowed rapid filming of polarizing proteins, there were significant caveats that diminished the protocol's utility. Primarily, although using a temperature sensitive mutation in the GEF for Cdc42p did arrest cells just prior to point we wished to film; it also required using a mutant version of one of the key regulators of polarity. In addition, growing *cdc24-1* cells at the restrictive temperature results in cell wall defects (Sloat et al., 1981). The potential problem these cell wall defects could pose was highlighted when we attempted to expand our analysis to include mutations in additional polarity genes. *rsr1*Δ cells bud randomly with respect to the bud site selection cues but otherwise appear healthy and wild type (Bender and Pringle, 1989; Chant and Herskowitz, 1991). Cells that contained both the *cdc24-1* and *rsr1Δ* mutations in our strain background, however, lysed at the restrictive temperature needed to synchronize the cells (data not shown). In part to avoid potential problems associated with the *cdc24-1* mutation, we devised a second synchrony protocol.

3.2.2 Hydroxyurea synchrony strategy

Our second synchrony strategy to avoid the phototoxic effects of frequent illumination utilized the drug hydroxyurea. Yeast cells treated with hydroxyurea (HU) arrest in the S-phase of the cell cycle (Slater, 1973). HU is an inhibitor of ribonucleotide reductase and that stalls replication forks by depleting pools of dNTP (Elledge et al., 1993). Single-stranded DNA resulting from the stalled replication forks activates the DNA damage checkpoint leading to cell cycle arrest, upregulation of DNA repair genes and ribonucleotide reductase (Branzei and Foiani, 2006; Elledge et al., 1993). We synchronized cultures by arresting them in S-phase for 2.5 h with 200 mM HU. Once

cells were released from the HU arrest into fresh medium they remained synchronous enough as they went through mitosis and entered the next cell cycle for us to determine the appropriate point to begin filming to catch polarity establishment and budding (Fig. 3.1). In addition to providing a synchronous population of cells, prior arrest in HU appears to imbue the cells with some resistance to the damaging effects of illumination. We could continue to image cells with very frequent timepoints even until they entered the second cell cycle after HU release.

Using the HU synchrony protocol, we first attempted to determine whether we could create a temporal hierarchy of polarization to the incipient bud site. Following release from HU, both fluorescence and DIC images were acquired every 15 seconds and the interval between polarization and budding was determined for Bem1p-GFP, Spa2p-GFP and Sec4p-GFP. In diploid cells that were otherwise wild type, Bem1p-GFP (as the only Bem1p in the cell, expressed from the endogenous locus) polarized the earliest in relation to budding (9.75 $\pm$ 1.46 minutes before budding, mean $\pm$ SD, N=10, $p < 0.01$). Spa2p-GFP and Sec4p-GFP appeared to have a shorter interval between polarization and budding and appeared to polarize at approximately the same time. Spa2-GFP polarized 7.47 $\pm$ 1.25 minutes before bud emergence (N=8) and Sec4p-GFP polarized 7.93 $\pm$ 0.8 minutes prior to bud emergence (N=8). To more precisely determine when the proteins described above arrived at the bud site in relation to one another we imaged strains containing pairs of GFP and mCherry-labeled proteins with 20 s between timepoints. By using these pair-wise comparisons, we observed that Bem1p-GFP polarized 20 - 100 s before Spa2p-mCherry appeared at the incipient bud site (Fig. 3.3A).

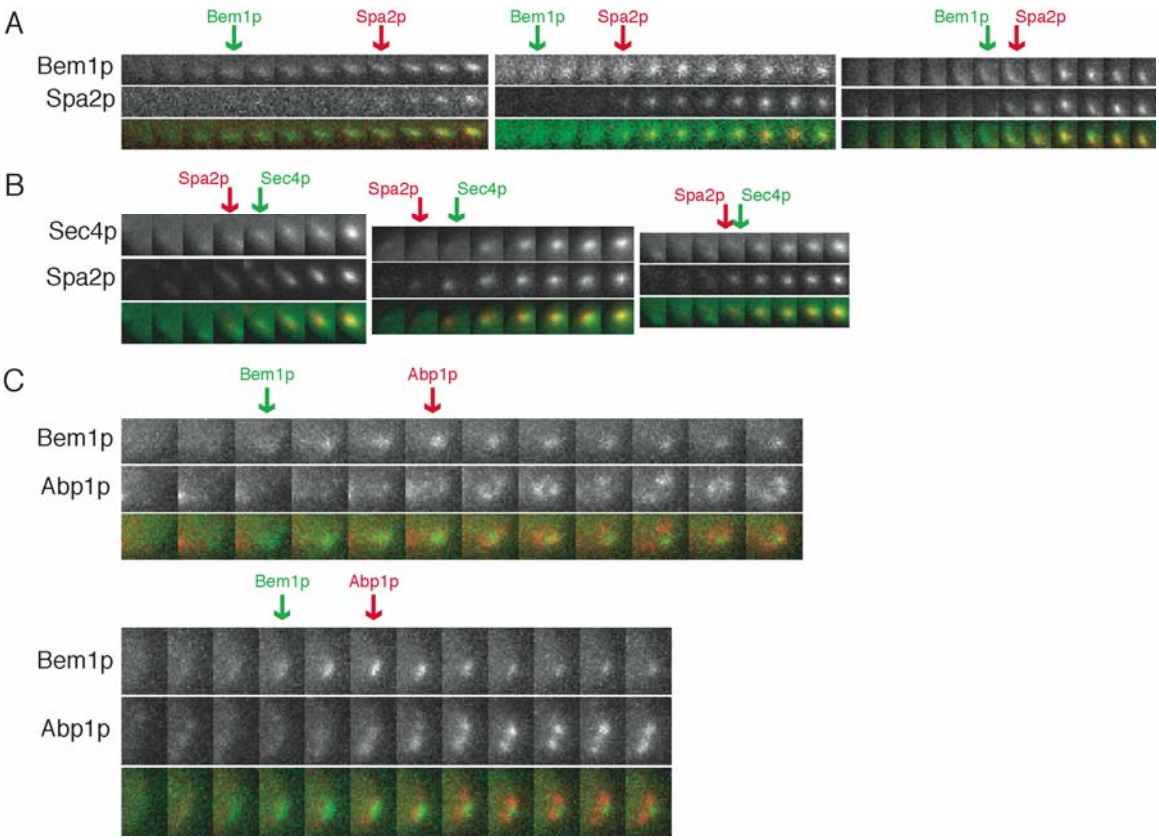

Figure 3.3 Bem1p polarizes to the incipient bud site before Spa2p, Sec4p and actin patches

Cells containing pairs of fluorescently tagged proteins were arrested in HU and released into fresh medium. The cells were then mounted for live-cell microscopy and imaged at ~24°C. GFP, RFP and DIC images were acquired for 11 z-planes with 0.5 μm steps every 20 s. Maximum projections of the fluorescent images were created and representative montages of the incipient bud site are shown. **(A)** Bem1p-GFP polarizes 20 – 100 s before Spa2p-mCherry arrives at the bud site. **(B)** Spa2p-mCherry and Sec4p-GFP polarize at approximately the same time, however Spa2p-mCherry can sometimes be detected at the bud site first. **(C)** Bem1p-GFP polarizes before there are organized actin patches at the bud site.

Spa2p-mCherry and Sec4p-GFP appeared to arrive the bud site at approximately the same time, but Spa2p-mCherry could be seen at the incipient bud site one timepoint (20 seconds) before there was detectable Sec4p-GFP in some cells (37% of cells, N=8) (Fig. 3.3B). Bem1p-GFP also polarized to the incipient bud site before a ring of actin patches polarized, as determined by Abp1p-mCherry localization (N=8, Fig. 3.3C). The combination of single-color data on the interval between polarization and budding and the two-color data on relative polarization allowed us to create a rough hierarchy of protein polarization to the bud site. We propose that Bem1p (and presumably Cdc24p and Cdc42p) polarizes to the incipient bud site first, followed by Spa2p and finally Sec4p and the actin patches.

We next examined the single-color polarization data for information on the dynamics of polarization. Sec4p-GFP polarization following HU-mediated cell synchrony appeared very similar to the results we observed in *cdc24-1* cells. Sec4p-GFP intensity appeared to increase over several minutes at the polarization site (Fig 3.4A). Spa2-GFP polarization was also superficially similar to what we observed in *cdc24-1* cells, in that it appeared to rapidly accumulate at the bud site in 30 – 45 seconds (Fig 3.4B). Using HU-arrested cells, Bem1p-GFP polarization appeared to have an initial, dimmer, broader period of localized protein accumulation before clearly polarizing to a spot (Fig 3.4C). This dim phase was not apparent in the *cdc24-1* cells, however the discrepancy may be due to the different *BEM1-GFP* constructs used and less sensitive equipment used to acquire images following *cdc24-1* arrest. In wild-type cells arrested in

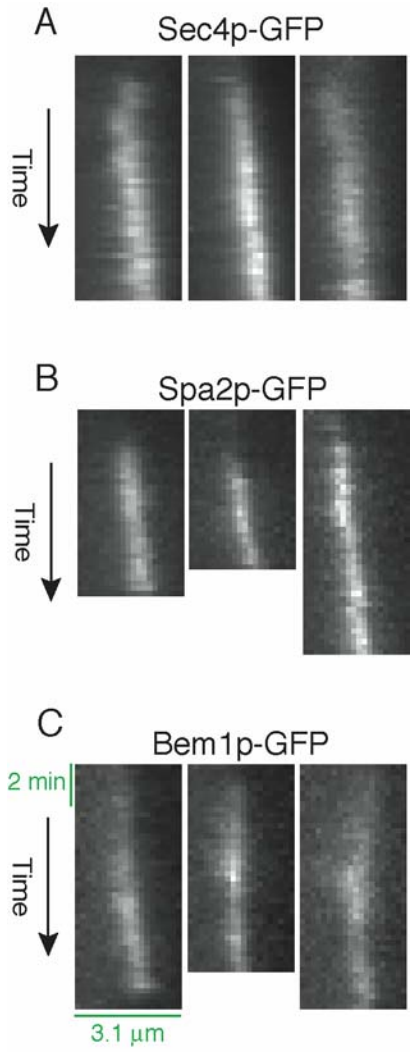

Figure 3.4 Bem1p, Spa2p and Sec4p rapidly concentrate at the incipient bud site

Cells containing the indicated GFP-labeled proteins were arrested in HU and released into fresh medium. The cells were then mounted for live-cell microscopy and imaged at ~24°C. GFP and DIC images were acquired for 11 z-planes with 0.5 µm steps every 15 s. Kymographs were constructed by drawing a 1 pixel-wide line through the polarization site, perpendicular to the plasma membrane. Representative kymographs are shown. **(A)** Kymographs from diploid cells in which one copy of *SEC4-GFP* was integrated at *URA3*. Sec4p-GFP rapidly localizes to the incipient bud site and continues to increase in intensity over the course of several minutes. **(B and C)** Kymographs from diploid cells in which both copies of *BEM1* or *SPA2* was replaced with GFP-tagged versions of the genes. **(B)** Spa2p-GFP rapidly (within 15-30 s) localizes to the incipient bud site. Spa2p-GFP does not appear to flicker in intensity following release from HU. **(C)** Bem1p-GFP rapidly localizes to the incipient bud site. There is a 15 – 45 s period when there is an increase in local Bem1p-GFP concentration, but not yet pronounced polarization. Bem1p-GFP does not appear to flicker in intensity following release from HU.

HU we did not observe the "flickering" in signal intensity that we saw using the *cdc24-1* mutation (Fig 3.4).

When we expanded our analysis to *rsr1Δ* cells, we were surprised to see that Bem1p-GFP appeared to have remarkably different polarization dynamics in the absence of Rsr1p. In *rsr1Δ* cells, Bem1p-GFP appeared to oscillate in signal intensity at the polarization site (Fig 3.5 A and B). These oscillations were even more striking when we filmed Bem1p-GFP in *RSR1* cells and *rsr1Δ* cells side by side on the same slide where the signal clearly oscillated in intensity only in the absence of Rsr1p (genotypes were distinguished by Alexa-Concanavalin A staining prior to mixing, Fig3.5 C). When we imaged Bem1p-GFP in asynchronous *rsr1Δ* cells with less temporal resolution, an initial unusually bright Bem1p-GFP signal followed by a dim period was often detected (Fig 3.5D). Therefore, we do not believe that the oscillations were due to HU treatment.

3.3 Discussion

Synchronizing cells to begin imaging just prior to polarity establishment is an effective means to circumvent the phototoxicity associated with rapid filming during the G1 phase of the cell cycle. Although we do not know why G1 appears to be more sensitive than other phases of the cell cycle in yeast, recent studies in mammalian cells suggest that p38 may be responsible for arresting cells in G1 in response to imaging-induced stress (Uetake et al., 2007). Prior cell cycle arrest in HU may have been able to impart some resistance to the damaging effects of imaging in G1 by "priming" the cells to respond to stress through prior up-regulation of stress response pathways.

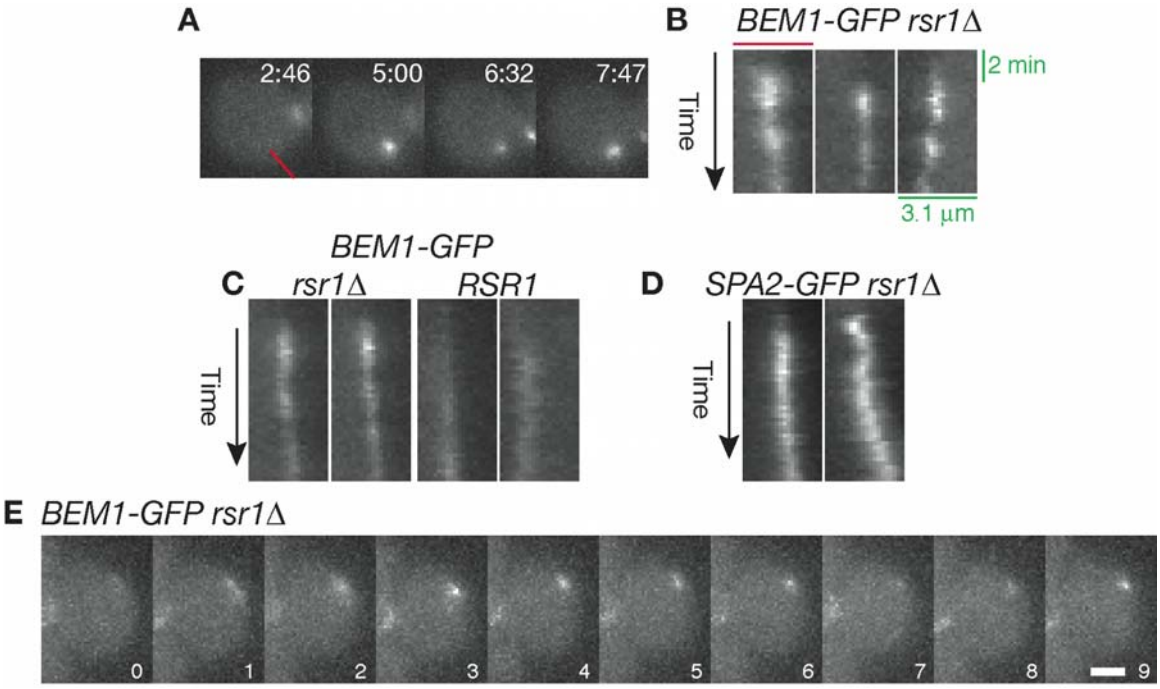

Figure 3.5 Bem1p-GFP oscillates in intensity in the absence of Rsr1p

(A and B) Diploid *rsrΔ* cells were arrested in HU, released into fresh medium and prepared for live-cell microscopy at ~24°C. GFP and DIC images were acquired for 11 z-planes with 0.5 μm steps every 15 s. **(A)** Frames from a timelapse show Bem1p-GFP decreasing in intensity at the bud site following polarization. Time is shown as min:s. **(B)** Representative kymographs constructed by drawing a 1 pixel-wide line through the polarization site, perpendicular to the plasma membrane are shown. **(C)** *rsr1Δ* cells were stained with Alexa-Concanavalin A (to label the cell wall); mixed with un-labeled *BEM1-GFP RSR1* cells; and prepared for live-cell microscopy as above. Kymographs from *RSR1* and *rsr1Δ* cells imaged side by side are shown. The oscillations in signal intensity observed in *rsr1Δ* cells are not apparent in *RSR1* cells. **(D)** Fluctuations in Bem1p-GFP intensity at the bud site are also apparent in cells not treated with HU and imaged every minute. Time is shown in min.

Despite challenges associated with phototoxicity, we were able to delineate a rough hierarchy of protein localization to the bud site. The fact that we were able to differentiate the timing of polarization between proteins utilizing different polarization mechanisms (i.e. Bem1p, which polarizes through a diffusion-based mechanism and Sec4p, which polarizes through an actin-mediated mechanism) supports the hypothesis that the initial stages of polarity establishment are actin independent. Although we were able to differentiate relative polarization of different proteins to the incipient bud, our results were highly variable. Our initial models for the characterization of the incipient bud site were the studies on actin patch and cytokinetic ring assembly (Kaksonen et al., 2003; Wu et al., 2003). Both the actin patch and the cytokinetic ring are structures with specific mechanical functions in the cell. It is possible that the incipient bud site is not assembled through similar stereotypical steps, but through a variable process that will differ somewhat from cell to cell.

Synchronizing cells through the use of the temperature sensitive *cdc24-1* mutation enabled us to follow polarization with a high degree of temporal resolution. However, the fact that arresting cells just prior to polarization requires the use of a mutant version of one of the key regulators of polarity establishment (and whose polarization we would, ideally like to follow) reduces the utility of this protocol. Due to the effectiveness of arrest in HU, the *cdc24-1* protocol has been abandoned.

Through the use of the HU synchrony protocol we were able to image cells at 6 times the temporal resolution available in asynchronous cells. We did not observe a motile crescent of Bem1p-GFP polarization in the absence of Rsr1p as reported by

Ozbudak et al. (Ozbudak et al., 2005). Instead, we found that Bem1p-GFP polarizes with different dynamics, but a stable location, in the presence or absence of Rsr1p. The oscillations in Bem1p-GFP signal intensity in *rsr1Δ* cells suggest that there is a delayed negative feedback loop whose activity is either stronger, or simply more visible, when cells are forced to break symmetry. What is the basis of this negative feedback loop? In Chapter 2 we discussed the negative effect that actin patch mediated endocytosis can have on the polarization site. The GTPase activating proteins (GAPs) for Cdc42p also localize to sites of polarized growth, providing another possible group of candidates for the negative regulators in polarity establishment. We also observed a "flickering" Bem1p-GFP and Spa2p-GFP signal in *cdc24-1* cells, however it is unclear whether the instability in the polarized signal is due to the same mechanisms responsible for the unstable polarization in *rsr1Δ* cells.

4. Re-wiring yeast cells to make two buds

4.1 Introduction

A polarized cell usually has a single directional axis: a “front” and a “back”. One of the central questions in polarity establishment concerns how cells polarize to one and only one "front" (here referred to as singularity). Singularity does not depend on pre-oriented polarization cues, because in many cases cells deprived of such cues polarize spontaneously towards a randomly oriented, but nevertheless unique, "front" (Wedlich-Soldner and Li, 2003). Although much has been learned about the molecular components responsible for polarity establishment, the basis for the singularity of polarization remains unclear.

Polarity establishment in animals and fungi involves the highly conserved Rho-family GTPase, Cdc42p (Etienne-Manneville, 2004). Polarization signals act through Cdc42p-directed guanine nucleotide exchange factors (GEFs) and/or GTPase activating proteins (GAPs) to trigger the localized accumulation of membrane-bound GTP-Cdc42p at the site destined to become the "front" of the cell. This localized GTP-Cdc42p then organizes cytoskeletal elements through a variety of effectors to yield the polarized morphology appropriate to the cell type (Etienne-Manneville, 2004).

The budding yeast *Saccharomyces cerevisiae* has served as a tractable model system to investigate the mechanism of polarity establishment (Park and Bi, 2007). In this system, the physiological polarization signal comes from cell cycle regulators. When a cell commits to begin a new cell cycle, activation of G1 cyclin/cyclin-dependent kinase

(CDK) complexes triggers rapid actin polarization leading to bud formation (Lew and Reed, 1993). Polarization is normally directed to predictable sites by an internal "bud site selection" machinery. However, mutational inactivation of that machinery (e.g., in *rsr1*Δ mutants) does not block polarization: it simply randomizes the budding location (Park and Bi, 2007). Importantly, such "symmetry breaking" polarization occurs with a timing, efficiency, and singularity similar to that in wild-type cells (Bender and Pringle, 1989; Chant and Herskowitz, 1991).

Theoretical analyses of how cells with initially homogeneous distributions of polarity factors might develop asymmetric patterns date back to a landmark paper by Alan Turing (Turing, 1952). Turing pointed out that small clusters of "morphogens" (in our context, polarity factors) would arise at random sites due to stochastic fluctuations, and that if an autocatalytic amplification mechanism were present, then a stochastic cluster could grow by positive feedback to generate a dominating asymmetry.

We recently proposed a molecular mechanism for the positive feedback that amplifies a stochastic cluster of GTP-Cdc42p at a random cortical site during symmetry breaking in yeast (Kozubowski et al., 2008). This mechanism involves assembly of complexes centered on a scaffold protein, Bem1p, which links the Cdc42p-directed GEF to a Cdc42p effector kinase (p21-activated kinase, or PAK) (Kozubowski et al., 2008). GTP-Cdc42p at the cortex binds and thereby recruits the PAK, activating it to phosphorylate the associated GEF, which induces neighboring Cdc42p molecules to exchange their GDP for GTP. The Bem1p-GEF-PAK complex thereby "grows" a cluster of GTP-Cdc42p at the cortex (Fig. 4.1A). This mechanism requires that

Figure 4.1. Re-wiring the yeast polarization feedback loop.
(A) Feedback by the Bem1p-GEF-PAK complex (Kozubowski et al., 2008). The panels represent sequential snapshots of the plasma membrane as seen from the cell interior. GTP-Cdc42p arising stochastically at random sites may recruit a GEF-PAK complex from the cytoplasm through direct binding of the PAK (a Cdc42p effector). The activated PAK phosphorylates and perhaps activates the associated GEF, leading to enhanced local GTP-loading of Cdc42p in the immediate vicinity and causing growth of a GTP-Cdc42p cluster. **(B)** Feedback by actin-mediated delivery of an actin cable nucleator (Wedlich-Soldner et al., 2003). (1) A local increase in concentration of a membrane protein able to promote actin cable nucleation would lead to (2) nucleation of an actin cable, delivering vesicles containing more of the protein towards that site on the plasma membrane and growing a focus. (3) Slow diffusion and balanced endocytosis would maintain the polarized state. **(C)** Schematic of the Bem1p-GFP-Snc2p fusion protein used to re-wire cells to employ actin-mediated amplification. In subsequent Figures, the oval denotes Bem1p, a green oval denotes Bem1p-GFP, and a green oval with a purple transmembrane tail denotes Bem1p-GFP-Snc2p. The red star denotes mutations in the Snc2p endocytosis motif. **(D)** FRAP analysis of diploid yeast homozygous for *BEM1-GFP-SNC2* or *BEM1-GFP*. Average intensities are plotted relative to the pre-bleach signal. Half-times of recovery are presented as mean $\pm$ standard deviation. The inset displays the same data on a timescale appropriate for the Bem1p-GFP recovery. **(E)** Bem1p-GFP-Snc2p, but not the endocytosis-deficient Bem1p-GFP-Snc2p^{V39A,M42A}, concentrates at the incipient bud site and in small buds marked with PBD-RFP, a probe for GTP-Cdc42p (arrows). GFP and RFP images of live cells are shown. Bar = 5 μm.

Figure 4.1 Re-wiring the yeast polarization feedback loop.

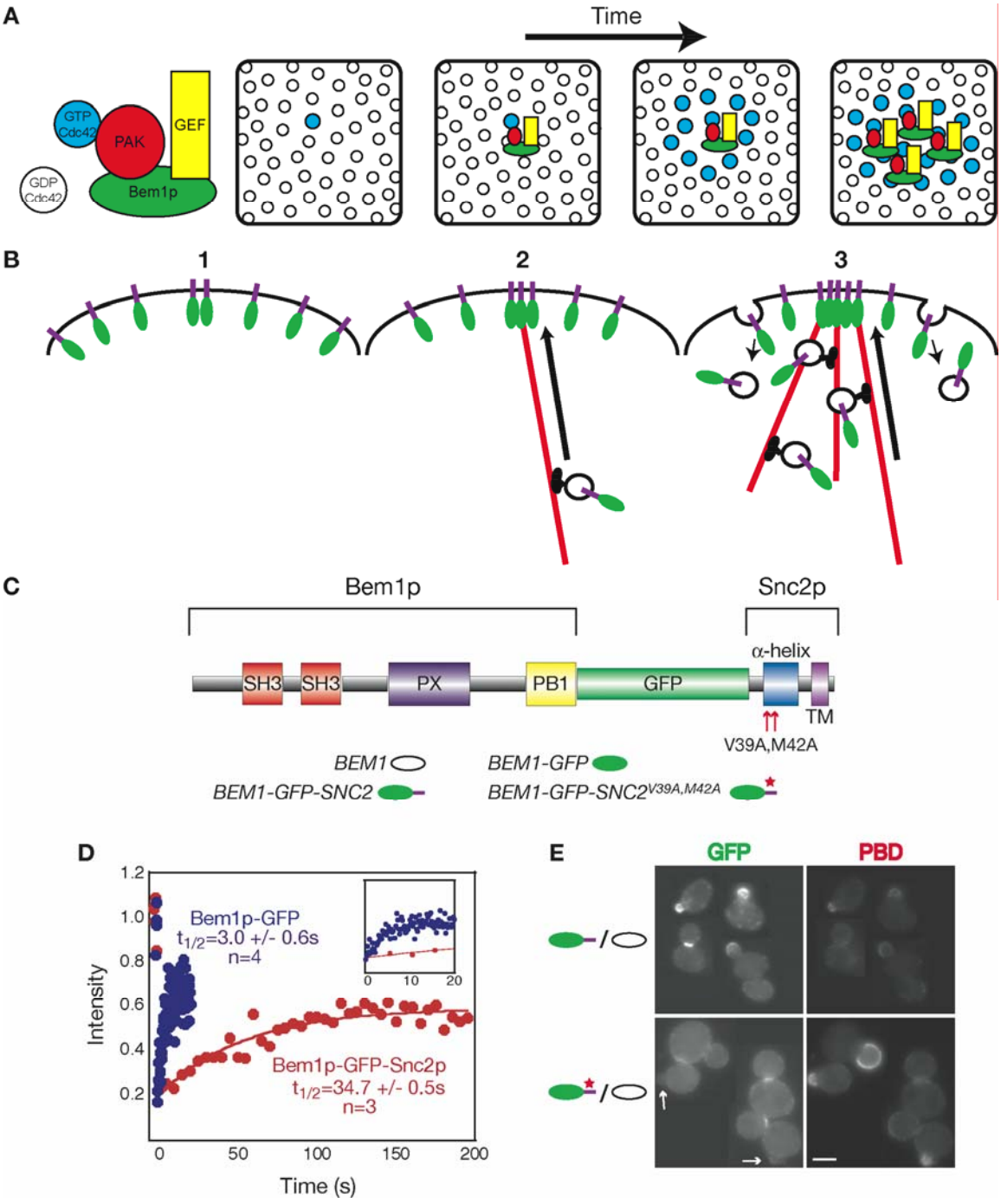

Bem1p-GEF-PAK complexes diffuse rapidly in the cytoplasm, so that they can be recruited to GTP-Cdc42p molecules already resident at the cortex: for that reason we refer to this as the “diffusional” amplification mechanism in what follows.

Amplification mechanisms can explain how it is that a random site, benefiting from a stochastic initial advantage, can develop a concentrated cluster of polarity factors. However, amplification could in principle allow several sites to develop such clusters: why does only a single site become the "front"? Theoretical analyses indicate that singularity could arise via competition between “fronts” for factors needed to establish a successful front, or by dissemination of anti-polarity factors that squelch polarity establishment at other sites (Gierer and Meinhardt, 1972; Goryachev and Pokhilko, 2008; Onsum and Rao, 2009). A wide variety of potential squelching mechanisms can be envisaged. In the fast block to polyspermy during sea urchin fertilization (another process in which singularity is important), ion fluxes induced by the first sperm to fuse with the egg rapidly make the entire cortex unwelcoming for new sperm (Jaffe, 1976). One could imagine that similarly rapid processes (which could involve ion fluxes, or changes in cell wall tension induced by local cell wall remodeling (Klis et al., 2006), or other factors) would favor a single cluster of GTP-Cdc42p. In these scenarios, a downstream consequence of GTP-Cdc42p cluster formation guarantees singularity. Alternatively, it may be that some aspect of the Cdc42p amplification mechanism itself (e.g., competition between clusters for limiting feedback components) assures singularity.

To address the singularity problem, yeast geneticists sought to identify mutants that cause cells to form more than one bud. Most "multibudded" mutants turned out to be

uninformative, involving defects in cell abscission such that buds from sequential cell cycles remained attached to the mother. However, a pioneering 2002 study identified a mutant, *cdc42-22*, in which multiple buds could grow simultaneously (Caviston et al., 2002). In that mutant, polarization is no longer dependent on the Cdc42p-directed GEF, suggesting that it must employ an amplification mechanism distinct from the GEF-mediated diffusional mechanism discussed above. Precisely what leads *cdc42-22* cells to make >1 bud has remained unclear, in part because the mutant displays pleiotropic defects (see Discussion). Nevertheless, the mutant demonstrates that perturbations affecting Cdc42p can cause a violation of the singularity rule, consistent with the idea that singularity is conferred by the Cdc42p amplification mechanism itself.

To address whether specifically altering the Cdc42p amplification mechanism would impact singularity, we created a novel fusion protein designed to "re-wire" the endogenous yeast polarization pathway to use an engineered feedback loop to break symmetry. We show that such re-wired cells can polarize and successfully proliferate. However, they often polarize to two sites simultaneously and can make two buds. Our findings suggest that singularity is an intrinsic property of the Cdc42p positive feedback mechanism that underlies polarity establishment.

4.2 Results

4.2.1 Re-wiring the yeast polarization feedback loop

Previous work on an artificial system involving overexpression of $Cdc42p^{Q61L}$ (a "constitutively active" GTP-locked mutant that no longer needs a GEF to become GTP-

loaded and is therefore unable to engage the diffusional feedback loop used by endogenous Cdc42p) suggested that an alternative amplification pathway, quite distinct from the diffusional pathway, could be used to grow clusters of GTP-Cdc42p (Wedlich-Soldner et al., 2003). Because overexpression of $Cdc42p^{Q61L}$ is lethal, we did not use that system, but we did follow the conceptual model emerging from it, which is illustrated in Fig. 4.1B. In this model, a membrane-bound polarity factor is able to influence actin cable attachment to the plasma membrane. Delivery of vesicles containing the polarity factor along the attached actin cable can increase the local concentration of the factor (assuming that it diffuses slowly from its site of delivery), leading to further actin cable attachment in a positive feedback loop. Eventually, of course, the membrane protein will diffuse away, but a stable focused polarization site can persist if endocytosis removes the polarity factor from the membrane before it diffuses too far (Marco et al., 2007)(Fig. 4.1B).

The actin-mediated feedback loop (Fig. 4.1B) relies on the presence of a protein with the following characteristics: it must (i) traffic on secretory vesicles, (ii) diffuse slowly in the plasma membrane, (iii) enhance the local attachment of actin cables, and (iv) undergo endocytosis before it diffuses too far from its site of delivery. The yeast exocytic v-SNAREs (Snc1p and Snc2p) fulfill three (i, ii, and iv) of the four requirements (Valdez-Taubas and Pelham, 2003), but cannot influence attachment of actin cables to the membrane. To create a protein that fulfills all four requirements, we fused the scaffold protein Bem1p (which can influence local actin cable attachment via Cdc42p) to the v-SNARE Snc2p, incorporating a GFP tag in between to allow visualization of the protein

in living cells (Fig. 4.1C). Our goal was to drive an actin-mediated amplification pathway in yeast cells without the toxic side-effects of Cdc42p^{Q61L} overexpression.

Using fluorescence recovery after photobleaching (FRAP), we found that whereas Bem1p-GFP was highly dynamic (recovery $t_{1/2}$~3 s), recovery of Bem1p-GFP-Snc2p was much slower ($t_{1/2}$~35 s) (Fig. 4.1D). These data are consistent with previous FRAP studies on Bem1p-GFP (Wedlich-Soldner et al., 2004) and v-SNAREs (Valdez-Taubas and Pelham, 2003), respectively. Thus, the dynamics of the Bem1p-GFP-Snc2p fusion protein are dominated by the Snc2p moiety, as expected.

When expressed in wild-type cells, Bem1p-GFP-Snc2p displayed a polarized distribution, concentrating together with GTP-Cdc42p (assessed using the reporter PBD-RFP (Tong et al., 2007)) at pre-bud sites and bud tips early in the cell cycle, and at the mother-bud neck late in the cell cycle (Fig. 4.1E). However, a version of Bem1p-GFP-Snc2p carrying point mutations that inactivate the Snc2p endocytosis signal (Fig. 4.1C) (Grote et al., 2000; Lewis et al., 2000) was no longer polarized to pre-bud sites or bud tips (Fig. 4.1E). This result indicates that, as expected, Bem1p-GFP-Snc2p diffusion is too slow to allow it to concentrate at polarization sites through binding interactions. Thus, unlike Bem1p, Bem1p-GFP-Snc2p would diffuse too slowly to locate and amplify GTP-Cdc42p clusters using the diffusional amplification mechanism (Fig. 4.1A). At the same time, by creating a synthetic protein with all four of the requisite properties listed above, Bem1p-GFP-Snc2p should enable cells to employ the actin-mediated amplification mechanism (Fig. 4.1B).

4.2.2 Bem1p-GFP-Snc2p promotes polarization and proliferation of *rsr1Δ* cells

To ask whether the actin-mediated amplification loop could replace the diffusional amplification loop to promote polarization in yeast, we replaced one copy of *BEM1* in a diploid with the *BEM1-GFP-SNC2* fusion construct. Upon tetrad dissection, all haploid spores containing *BEM1-GFP-SNC2* instead of *BEM1* were viable (Fig. 4.2A) and displayed normal cell morphology (Fig. 4.2B), even if they were also *rsr1*Δ and lacked spatial cues for bud emergence. Bem1p-GFP-Snc2p was expressed at similar levels to Bem1p-GFP (Fig. 4.2C), and localized to polarization sites as well as to the mother-bud neck during cytokinesis (Fig. 4.2B). Haploid *BEM1-GFP-SNC2 rsr1*Δ cells proliferated with a normal cell cycle profile (Fig. 4.2D) and a doubling time only slightly longer than that of control *BEM1-GFP rsr1*Δ cells (102 min versus 90 min). Thus, Bem1p-GFP-Snc2p can sustain cell polarization and proliferation.

4.2.3 Bem1p-GFP-Snc2p biases polarization towards the previous division site

Given the successful proliferation of *BEM1-GFP-SNC2 rsr1*Δ cells, we expected that they would break symmetry and pick random bud sites like *rsr1*Δ cells. However, bud scar and birth scar staining indicated that new buds generally formed adjacent to previous division sites (Fig. 4.3A). We speculate that because of its concentration at the neck during cytokinesis and its slow diffusion, Bem1p-GFP-Snc2p remains concentrated near the division site, seeding polarization towards that site in the next cell cycle. Consistent with this view, when Bem1p-GFP-Snc2p was expressed in diploid *RSR1/RSR1* cells containing positional cues (in which daughters almost always

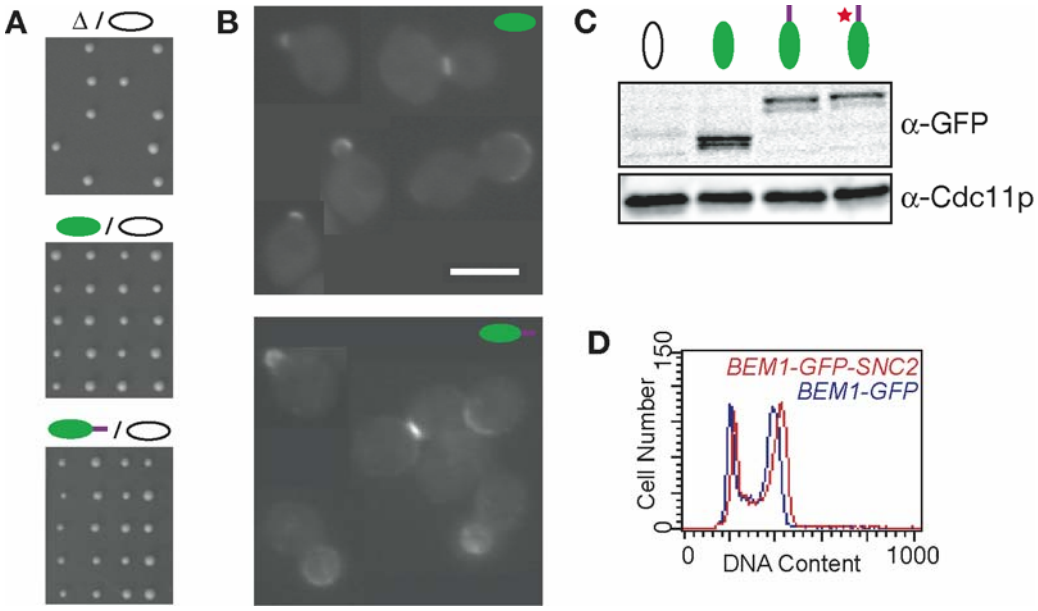

Figure 4.2 Bem1p-GFP-Snc2p promotes polarization and proliferation of *rsr1Δ* cells.

(A) Tetrads from sporulation of strains heterozygous for *bem1Δ*, *BEM1-GFP*, or *BEM1-GFP-SNC2* as indicated. **(B)** Cells with Bem1p-GFP-Snc2p as their only source of Bem1p displayed wild-type morphology and polarized Bem1p-GFP-Snc2p. GFP images of live cells are shown. Bar = 5 µm. **(C)** Bem1p-GFP, Bem1p-GFP-Snc2p and Bem1p-GFP-Snc2p^{V39A,M42A} were expressed at similar levels. Blot probed with anti-GFP and anti-Cdc11p (loading control). **(D)** Proliferating *BEM1-GFP-SNC2* cells displayed a similar cell cycle profile to *BEM1-GFP* cells by flow cytometry.

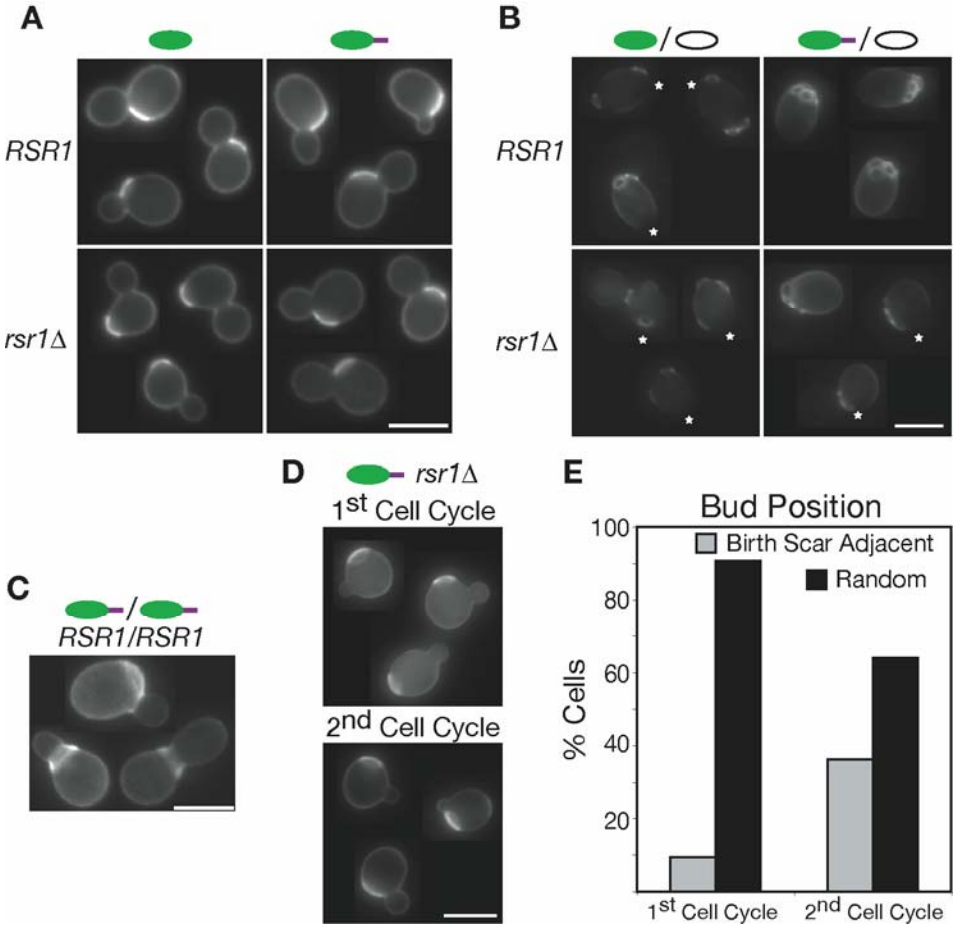

Figure 4.3 Bem1p-GFP-Snc2p biases polarization towards the previous division site, but can also break symmetry.

(A) Budding of *BEM1-GFP-SNC2 rsr1*Δ is biased towards the previous division site. First-time mothers stained to label the cell wall and birth scar (bright patch, marks the initial division site) are shown. The presence/absence of Rsr1p and the Bem1p fusion are indicated. (**B)** Budding of *BEM1*/*BEM1-GFP-SNC2* diploids is biased towards the previous division site. Multiple-time mothers stained to label bud scars are shown (birth scars are indicated by * when not obscured by bud scars). Bud scars show the location of previous division sites in mother cells that have previously budded. **(C)** Budding of *BEM1-GFP-SNC2/ BEM1-GFP-SNC2* diploids can occur directly into birth scar. (**D)** Following centrifugal elutriation and release into fresh medium at 37° C, budding was random (indicative of symmetry breaking) in *BEM1-GFP-SNC2 rsr1Δ* cells. In the second cell cycle following elutriation budding was again biased towards the previous division site. Cells were fixed and stained to label the cell wall and birth scar at 80 min and 180 min after elutriation. Bar = 5 μm in all panels. **(E)** Bud site position for > 100 first- and second-time mothers from D.

bud towards the distal site marked by the landmark Bud8p (Chant and Pringle, 1995; Zahner et al., 1996)), it skewed the budding pattern towards the division site instead (Fig. 4.3B). Some cells even budded directly within the previous division site (Fig. 4.3C), a behavior that is normally prevented by the Cdc42p GAP, Rga1p (Tong et al., 2007).

4.2.4 Bem1p-GFP-Snc2p can promote symmetry breaking polarization

If slow diffusion of Bem1p-GFP-Snc2p from the division site is responsible for biasing polarization towards the division site in *BEM1-GFP-SNC2 rsr1*Δ cells, then a sufficient lengthening of the early G1 interval (before G1 cyclin/CDK activation) should provide time for dissipation of the Bem1p-GFP-Snc2p gradient to a homogeneous distribution, forcing the cells to break symmetry in order to polarize. We used centrifugal elutriation (a size-selection procedure) to isolate small early-G1 daughter cells that have a longer G1 interval, and shifted the cells to 37°C to depolarize actin following elutriation (Lillie and Brown, 1994). Elutriated *BEM1-GFP-SNC2 rsr1*Δ cells budded at random sites in the first cycle after elutriation, although the preference for budding towards the division site returned in the second cycle (Fig. 4.3D,E). Thus, Bem1p-GFP-Snc2p can promote symmetry breaking.

4.2.5 Actin-dependent polarization by Bem1p-GFP-Snc2p

If Bem1p-GFP-Snc2p uses actin-mediated amplification instead of the diffusional mechanism, then polarity in this strain (unlike in wild-type or *rsr1*Δ cells) should be abolished upon depolymerization of F-actin by Latrunculin A. Indeed, whereas Latrunculin-treated control cells polarized GTP-Cdc42p, Spa2p (a polarisome component

(Sheu et al., 1998)), and Cdc3p (a septin (Gladfelter et al., 2001)), as well as Bem1p-GFP itself, none of these markers became polarized in Latrunculin-treated Bem1p-GFP-Snc2p cells (Fig.4. 4A,B). Thus, Bem1p-GFP-Snc2p can break symmetry, and it does so by an actin-based amplification mechanism instead of the diffusional mechanism.

As polarity establishment was actin-dependent in *BEM1-GFP-SNC2* cells, we tested what effect actin cytoskeleton perturbation, but not complete depolymerization, would have on cell viability. Mutations that normally result in relatively mild actin cytoskeleton perturbations were introduced into diploid cells containing *BEM1-GFP-SNC2*. Upon tetrad dissection we found that deletion of either tropomyosin (*TPM1* or *TPM2* (Drees et al., 1995)), or the polarisome components *SPA2* ad *PEA2* had very little, if any effect on cell viability (Table 1). In contrast, deletion of either fimbrin (*SAC6* (Adams et al., 1991)), or a subunit of capping protein (*CAP2* (Amatruda et al., 1990)) resulted in a reduction in the number of viable spores and generally very sick cells that were difficult to grow for further characterization (Table 1). Not surprisingly given the importance of localized actin cable nucleation to the actin-mediated feedback loop, both *bni1Δ* (formin) and its interactor *bud6Δ* (Evangelista et al., 1997) were synthetically lethal with *BEM1-GFP-SNC2* (Table 1).

The demonstration that a synthetic re-wiring of the yeast polarization pathway to employ an actin-based mechanism can work to break symmetry provides an important validation of the actin-mediated positive feedback concept (Wedlich-Soldner et al., 2003), and indicates that such polarization can occur in a sufficiently rapid timeframe to be useful to yeast, which was unclear from the previous work. We then used time-lapse

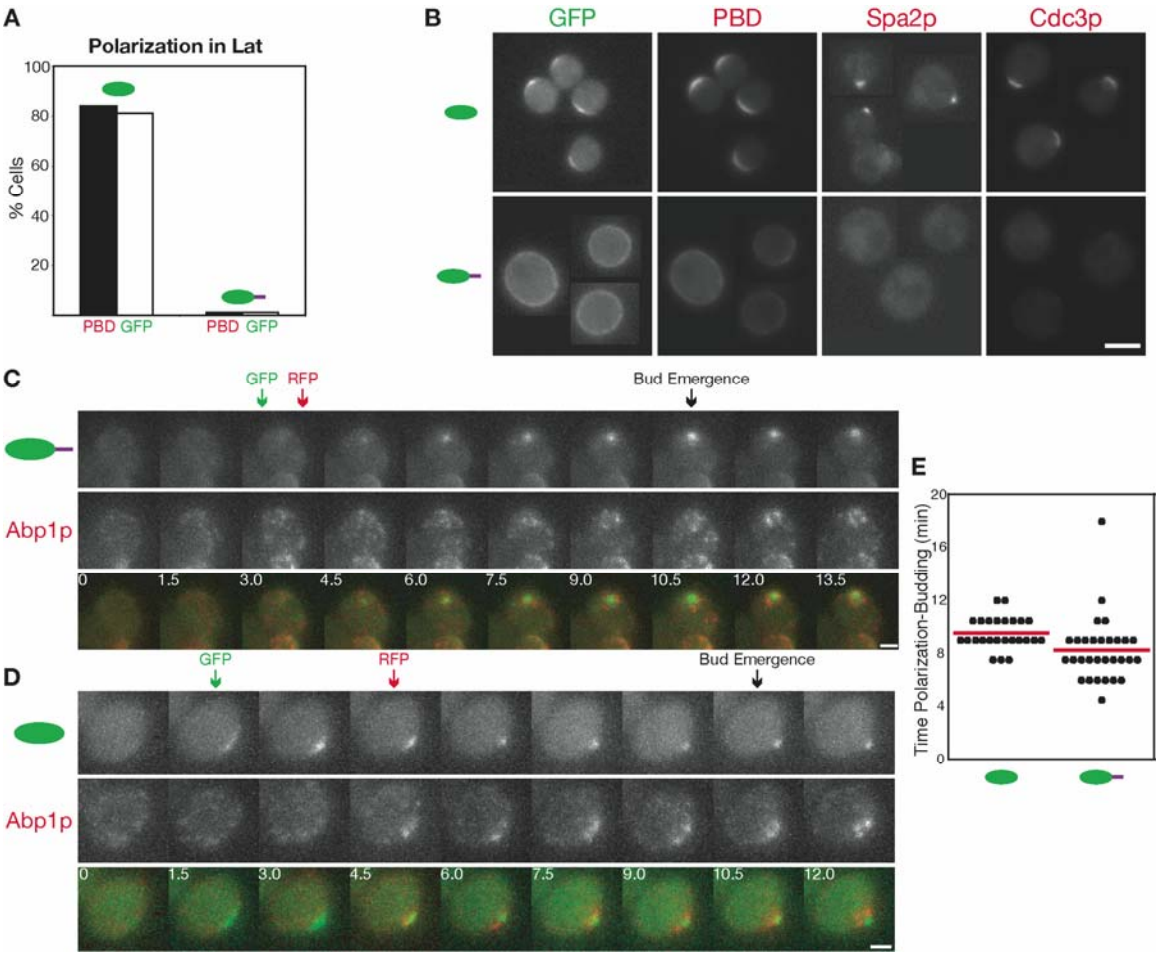

Figure 4.4 Actin-dependent polarization by Bem1p-GFP-Snc2p

(A) Polarization following Lat A treatment in cells containing PBD-RFP and either Bem1p-GFP or Bem1p-GFP-Snc2p. >90 cells were scored for polarized signal from live-cell images. **(B)** Cells that failed to polarize Bem1p-GFP-Snc2p also failed to polarize PBD-RFP, Spa2p-RFP, and Cdc3p-RFP. Montages of live-cell images Bar = 5 µm **(C and D)** Cells containing Abp1p-mCherry (actin patches) and either Bem1p-GFP or Bem1p-GFP-Snc2p were imaged by live-cell microscopy. Arrows indicate times of Bem1p-GFP-Snc2p or Bem1p-GFP polarization (green), actin patch polarization (red), and bud emergence (black: scored from DIC images). Maximum projections of 11 z-planes are shown for GFP and RFP. Time is in min. Bar = 2 µm. **(C)** Bem1p-GFP-Snc2p polarization is coincident with actin patch accumulation. **(D)** Bem1p-GFP polarization precedes actin patch accumulation. **(E)** Time from polarization of GFP signal to bud emergence in *BEM1-GFP* and *BEM1-GFP-SNC2 SPC42-mCherry* cells at 30°C (red signal used to distinguish genotypes of cells mixed and imaged on the same slab). Line indicates average.

Table 1 *BEM1-GFP-SNC2* cells are sensitive to actin cytoskeleton perturbations

	Viable Spore Colonies (Inviable)	
	BEM1-GFP-SNC2	*BEM1-GFP*
bni1Δ	**2*** (24)	**9** (0)
bud6Δ	**0** (19)	**7** (0)
sac6Δ	**13** (14)	**22** (0)
cap2Δ	**12** (8)	**18** (0)
tpm1Δ	**16** (0)	**14** (2)
tpm2Δ	**16** (0)	**18** (0)
spa2Δ	**15** (2)	**16** (0)
pea2Δ	**19** (1)	**11** (1)

Diploid cells with the indicated genotypes were sporulated and tetrads dissected. Spore colonies were scored for markers associated with each mutation and the number of inviable spore colonies recovered from each genotype is shown. *projected to be of this genotype based on segregation of markers in other spores from the tetrad, however the colonies were too small to replica plate.

microscopy to directly compare the kinetics of polarization in wild-type and re-wired cells.

4.2.6 Dynamics of polarization by Bem1p-GFP-Snc2p compared to Bem1p-GFP

Bem1p-GFP-Snc2p accumulated at the pre-bud site coincident with actin patch accumulation (visualized using the patch marker Abp1p-mCherry) (Fig. 4.4C). Bem1p-GFP-Snc2p accumulated over 2-5 min at a small focus (Fig.4. 4C), with bud emergence first detected 8.3 $\pm$ 2.5 min (mean $\pm$ standard deviation, n = 30) after focus formation was first detected (Fig. 4.4E).

Although superficially similar, polarization in cells containing wild-type Bem1p-GFP displayed three notable differences. First, polarization of Bem1p-GFP occurred initially in a wider zone (~1.9 μm diameter) that subsequently condensed to a small focus (<1 μm diameter: Fig. 4.4D). Second, Bem1p-GFP routinely polarized 1.5-3 min before detectable accumulation of Abp1p-mCherry (Fig. 4.4D). Third, bud emergence was detected 9.5 $\pm$ 1.2 min (mean $\pm$ standard deviation, n = 25, $p<0.001$) after Bem1p-GFP polarization was first detected (Fig. 4.4E). To avoid potential differences stemming from day-to-day variations in temperature or slide composition, the data in Fig. 4.4E were collected from mixed-cell experiments where *BEM1-GFP rsr1Δ* and *BEM1-GFP-SNC2 rsr1Δ* cells were imaged simultaneously (the cells were distinguished by the presence of an mCherry marker in the *BEM1-GFP-SNC2 rsr1Δ* strain). We conclude that in wild-type cells, polarization of Bem1p precedes actin polarization by 1.5-3 min, whereas in the

re-wired cells, polarization of Bem1p-GFP-Snc2p is coincident with (and dependent on) actin polarization.

4.2.7 Bem1p-GFP-Snc2p can lead cells to make two buds simultaneously

In diploid *BEM1-GFP-SNC2 rsr1*Δ cells growing on minimal media at 24°C, 4.9% of budded mothers had two buds (n > 1000). This number was reduced to ~1-2% under optimal growth conditions (rich media at 30°C), in which the cells budded predominantly towards the division site (see above). Time-lapse analysis revealed that the two buds emerged and grew simultaneously, though at a reduced rate compared to neighboring single-budded cells (Fig. 4.5A,B). The two buds in such cells were both "true buds" in the sense that they displayed polarized actin patches, septin hourglass structures at the neck, and polarized localization of a GTP-Cdc42p reporter as well as Spa2p (Fig. 4.5C). The location of the two buds relative to each other varied widely: some cells had buds right next to each other while other cells had buds at opposite ends (Fig. 4.5C). Thus, switching from a diffusional amplification mechanism (Fig. 4.1A) to an actin-based amplification mechanism (Fig. 4.1B) caused the occasional breakdown of singularity, suggesting that the normal prohibition restricting cells to form only one bud is conferred by the nature of the amplification mechanism itself. We tested whether the two-budded phenotype of *BEM1-GFP-SNC2* cells could be suppressed either by reinstating the diffusional positive feedback loop (through addition of *BEM1-GFP*) or by restoring bud site selection (through addition of *RSR1*). An additional copy of *BEM1-GFP* reduced the frequency of two-budded cells (2.5% as opposed to 4.9%, n > 1000 in

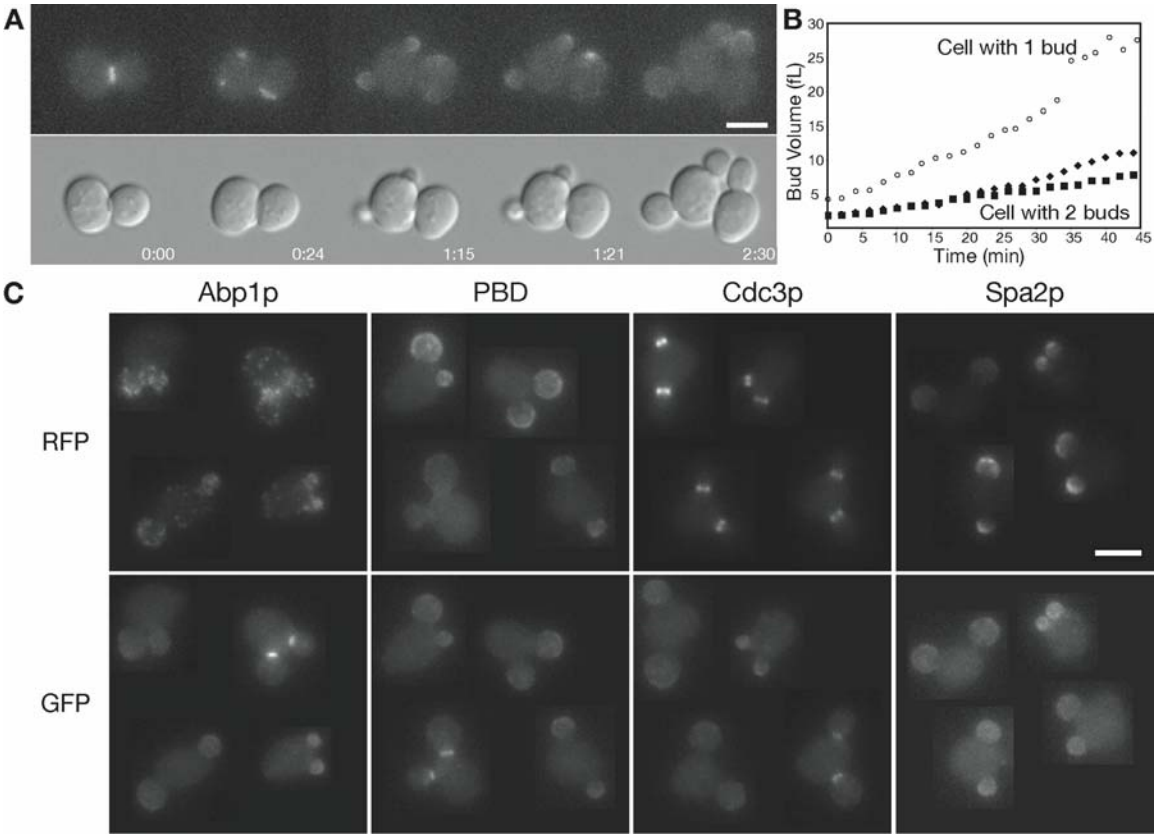

Figure 4.5 *BEM1-GFP-SNC2* cells can make two buds simultaneously.

(A) Bem1p-GFP-Snc2p could polarize to two sites and result in two simultaneously growing buds. A *BEM1-GFP-SNC2* mother-daughter pair was imaged for GFP and DIC and selected frames are shown. Elapsed time is shown as h:min. Bar = 5 µm **(B)** Graph comparing bud growth in a cell with one bud as compared to a cell with two buds. Bud growth was measured from DIC images taken of cells growing side by side. Open symbols denote bud volume in a cell with only one bud. Closed symbols denote bud volume in a cell with two growing buds. **(C)** Localization of polarity and cytoskeletal proteins to both buds. Maximum projections of 13 z-planes with 0.5 µm steps were selected for a montage of cells containing *BEM1-GFP-SNC2* and *ABP1-mCherry*, *CDC3-mCherry*, *PBD-RFP*, or *SPA2-mCherry*. Bar = 5 µm.

minimal media at 24°C), whereas *RSR1* had little effect (5.6% as opposed to 4.9%, n > 1000).

4.2.8 Competition between polarization foci

Time-lapse microscopy of polarization in 136 *BEM1-GFP-SNC2 rsr1Δ* cells revealed that 24 (17.6%) of the cells initiated polarization at two foci, yet only 4 (2.9%) made two buds. Thus, in a majority of the cells that generated two Bem1p-GFP-Snc2p foci, one of the foci subsequently disappeared, and the cells formed a single bud (Fig. 4.6A). Two foci could coexist for 4.5 – 7.5 min (n = 19: one outlier appeared to take 10 min), before one focus disappeared leaving a single bud site.

In contrast to cells with two foci, we never saw the focus disappear in the 112 cells that only made a single focus. This suggests that the "disappearance" of one focus was due to the presence of the second focus, implicating some form of competition between foci as the basis for the disappearance of one focus.

Cells that established two foci of Bem1p-GFP-Snc2p always did so within < 3 min of each other, and in most cases any potential differences in the focus initiation times were not resolved by our 1.5 min image acquisition intervals. Thus, it appears that once a dominant focus becomes established, new foci do not arise. This was not due to progression of the cell cycle (which eventually terminates polarization) because new foci did not arise even if the cell cycle was arrested at a polarizing stage (Fig. 4.7). A competitive mechanism that favored the larger focus could account for this observation, as a newly-growing focus would be unable to compete with a well-established one.

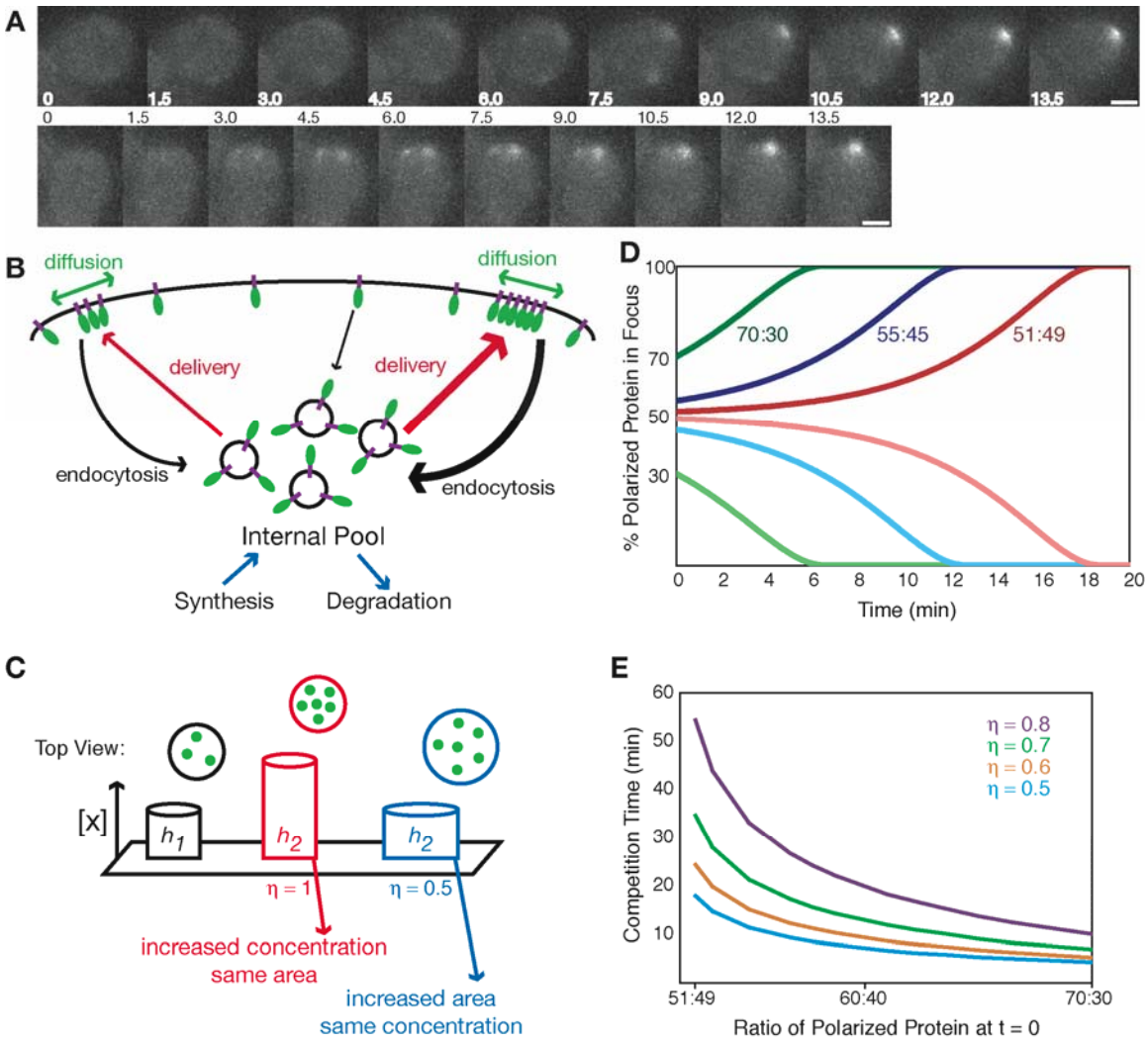

Figure 4.6 Competition between foci of Bem1p-GFP-Snc2p can lead to singularity.

(A) When Bem1p-GFP-Snc2p polarized to two foci simultaneously, one focus usually disappeared and the other became the sole bud site. Selected frames from timelapse of *BEM1-GFP-SNC2 rsr1Δ* cells. Time is shown in min. Scale bar = 2 μm. **(B)** Model describing Bem1p-GFP-Snc2p trafficking in cells with two foci. Red arrows indicate vesicular trafficking along actin cables. Black arrows indicate endocytosis. Green arrows indicate diffusion in the plane of the membrane. **(C)** Effect of focus geometry on diffusional escape of Bem1p-GFP-Snc2p. The circles represent a top-down view of the cylinders illustrating the distribution of Bem1p-GFP-Snc2p (green dots). **(D)** Simulation of competition between foci, using the model described in the supplement with $\eta = 0.5$. Similar-colored lines indicate Bem1p-GFP-Snc2p content of two foci seeded with the indicated ratios of protein. **(E)** Dependence of the resolution time (the time taken for the smaller focus to effectively disappear) on the initial ratio and on η.

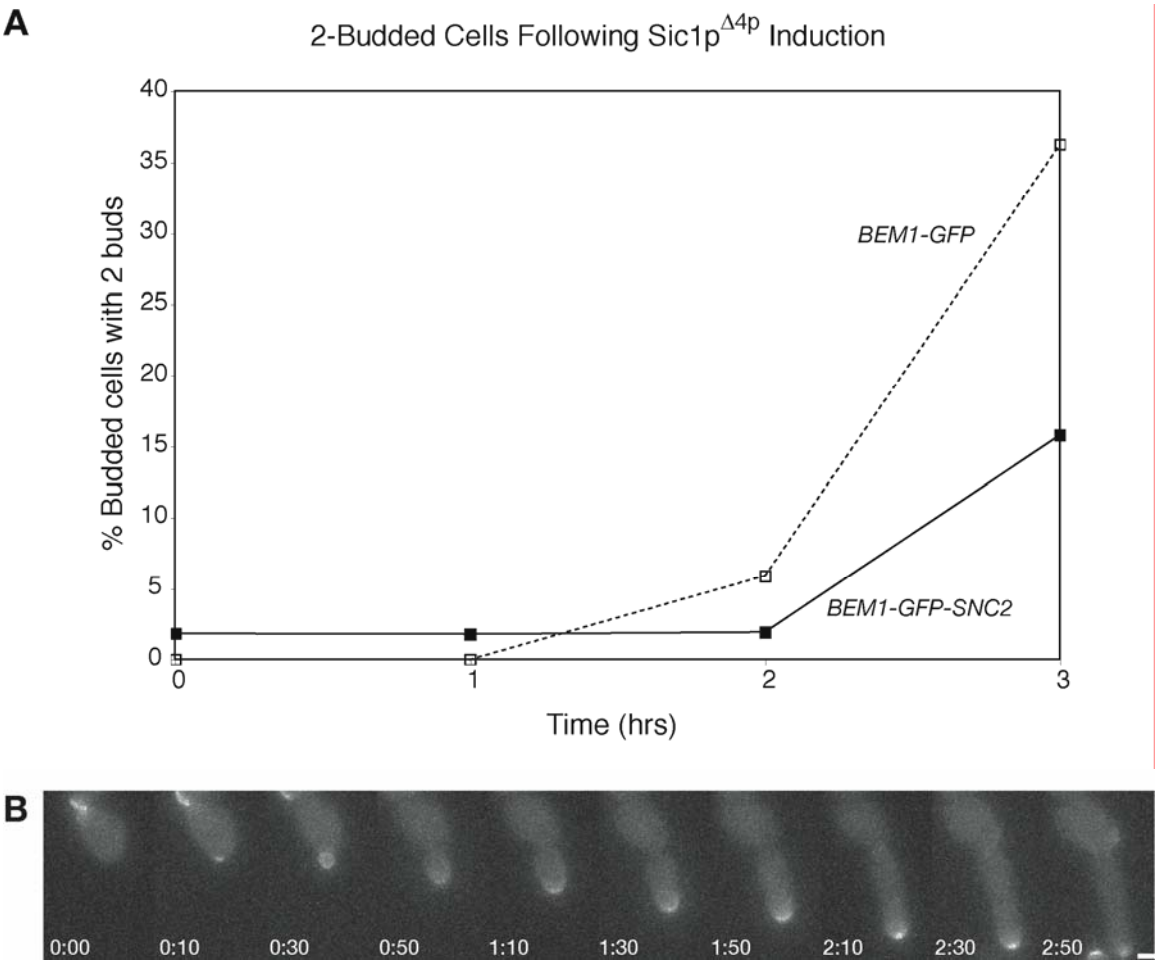

Figure 4.7 Sic1pΔ^{4p} overexpression does not lead to an increase in 2-budded cells within 2 hours.

Prolonging the period of polarized growth did not increase the number of polarization foci or buds within 2 h. **(A)** Exponentially growing cells expressing either Bem1p-GFP (open symbols) or Bem1p-GFP-Snc2p (closed symbols) were induced to overexpress Sic1p$^{\Delta 4p}$ by the addition of 75 nM β-estradiol. Aliquots (1 mL) were taken every hour and fixed with 3.7% formaldehyde. Cells were scored for number of buds by DIC microscopy, n>1000. The percentage of budded cells with 2 buds is shown. **(B)** Frames from GFP timelapse of a cell expressing Bem1p-GFP-Snc2p and Sic1p$^{\Delta 4P}$. Elapsed time is shown as h:min. Bar = 2 μm

What is the basis for the observed competition between foci? In cells with two foci, secretory vesicles carrying Bem1p-GFP-Snc2p would encounter actin cables oriented towards either focus. If we assume (as seems likely) that more intense foci (i.e. those containing more Bem1p-GFP-Snc2p) sustain greater numbers of actin cables, then delivery will be biased towards the more intense focus, forming a potential basis for a competition mechanism (red arrows in Fig. 4.6B). To assess whether simple competition for Bem1p-GFP-Snc2p itself would yield the observed behavior, we turned to mathematical modeling.

4.2.9 Mathematical model for competition between Bem1p-GFP-Snc2p foci

A mathematical model incorporating delivery of Bem1p-GFP-Snc2p from internal pools to the polarization site by actin cables, diffusion in the plasma membrane, and retrieval by endocytosis (Fig. 4.6B) is presented in the supplement. We assume that in the relevant timeframe for polarization (a few minutes), the system is at a global steady state in which synthesis and degradation of Bem1p-GFP-Snc2p are balanced, and can be ignored.

The simplest scenario is that delivery of Bem1p-GFP-Snc2p is biased in a manner proportional to the amount of Bem1p-GFP-Snc2p that is already polarized in each focus. However, because endocytic retrieval of Bem1p-GFP-Snc2p (black arrows in Fig. 4.6B) is also expected to be proportional to the amount already polarized, this would not necessarily lead to a net change in the relative amounts of protein at the two different foci. The outcome in such a scenario will depend on a third element, diffusion in the plasma membrane (green arrows in Fig. 4.6B).

The rate of diffusional "escape" of Bem1p-GFP-Snc2p from a focus will depend on the precise geometry of the focus (i.e. the concentration profile in two dimensions). An unrealistic but instructive geometry is illustrated in Fig. 4.6C, where a reference focus (black) is depicted as a circular region containing evenly-distributed Bem1p-GFP-Snc2p. With this geometry, diffusional escape of Bem1p-GFP-Snc2p from the focus would be proportional both to the length of the circle's perimeter and to the concentration of Bem1p-GFP-Snc2p within the focus.

We now consider two extreme scenarios for the distribution of Bem1p-GFP-Snc2p in a focus that contains more molecules of Bem1p-GFP-Snc2p (depicted in red or blue in Fig. 4.6C). At one extreme (red), we imagine that the size (and hence perimeter) of the circle remains unchanged, and the circle contains a higher concentration of Bem1p-GFP-Snc2p. In that case, diffusional escape from each focus will simply be proportional to the total protein content in the focus, just as we assumed for delivery and endocytosis. It can then be demonstrated that in cells with two foci containing amounts of Bem1p-GFP-Snc2p designated as h_1 and h_2, the ratio h_1/h_2 will tend to remain the same regardless of the fraction of Bem1p-GFP-Snc2p in each focus (Chapter 7: Analysis of the proportional model). Thus, in this scenario there will be no net competition between foci.

In the second scenario (Fig. 4.6C, blue), we imagine that the concentration of Bem1p-GFP-Snc2p within the focus remains the same as in the reference focus, but that the area of the circle is increased. Because protein content is proportional to area, and diffusional escape is proportional to the length of the circle's perimeter, in this scenario diffusional escape would be proportional to [total protein in focus]$^{0.5}$. These extremes

(red, blue) allow us to infer the general form of a diffusional escape term for a realistic focus geometry in between these extremes: diffusional escape will be proportional to [total protein in focus]$^{\eta}$, where $0.5 < \eta < 1$. It can then be shown that the ratio, h_1/h_2, of protein content in one focus to protein content in the other, will change according to

$$\frac{d(h_1/h_2)}{dt} = k\left(\left(\frac{h_1}{h_2}\right) - \left(\frac{h_1}{h_2}\right)^{\eta}\right)$$

where k is a positive quantity dependent on diffusion rate and focus geometry (Chapter 7: Analysis of the non-proportional model).

This means that if $h_1/h_2 > 1$ (i.e. focus 1 is more intense than focus 2), $d(h_1/h_2)/dt$ will be positive and focus 1 will grow at the expense of focus 2. Conversely, if $h_1/h_2 < 1$ (i.e. focus 2 is more intense than focus 1), $d(h_1/h_2)/dt$ will be negative and focus 2 will grow at the expense of focus 1. Unless the foci have precisely equal content ($h_1/h_2 = 1$, in which case $d(h_1/h_2)/dt = 0$), the bigger focus will out-compete the smaller focus. Thus, inclusion of a realistic diffusion scenario ($0.5 < \eta < 1$) in a simple model of Bem1p-GFP-Snc2p behavior is sufficient to promote competition and guarantee singularity if given sufficient time.

To assess the timeframe in which the competitive mechanism proposed above would operate, we constrained model parameters based on published observations and experimental data (Fig. 4.1D and Fig. 7.1; see Chapter 7: Parameter estimation). Examples of model behavior using these parameters and setting $\eta = 0.5$ are shown in Fig. 4.6D. When two foci of Bem1p-GFP-Snc2p were initiated at different ratios, the larger focus grew while the smaller disappeared. The bigger the initial asymmetry, the faster the

resolution of two foci to one (Fig. 4.6D,E). With increasing η, competition took progressively longer (Fig. 4.6E). This simple model indicates that with realistic parameter values, competition can lead to growth of one focus at the expense of the other within a biologically relevant (several minute) timeframe.

When two foci start out with almost equivalent amounts of Bem1p-GFP-Snc2p, competition takes longer (Fig. 4.6D,E), and one would expect two buds to emerge. The fact that we detected 2-budded cells indicates that competition is not always completed within the allotted ~8 min interval between polarization and bud emergence. We observed a total of 38 Bem1p-GFP-Snc2p cells in which two buds emerged (including both *RSR1* and *rsr1*Δ strains). In two cases, a tiny bud was then "abandoned", but in the other 36 instances both buds grew for prolonged periods (Fig. 4.5). This observation suggests that competition is terminated soon after bud emergence.

4.2.10 Competition between Bem1p-GFP foci

The finding that competition between polarity sites alone, could theoretically describe singularity in the actin-mediated feedback loop encouraged us to ask whether or not competition could be occurring in wild-type cells (in the presence of the GEF-PAK diffusional feedback loop). As predicted by the Goryachev and Pokhilko model, in which polarization sites compete for Bem1p-Cdc24p complexes, *BEM1-GFP rsr1Δ* cells could indeed grow two buds simultaneously when Bem1p-GFP was overexpressed from a 2 μm plasmid (Fig. 4.8A). Approximately 1.8 % of budded cells overexpressing Bem1p-GFP had two buds (n>500). We did not observe multiple Bem1p-GFP foci in our timelapse analysis with 90 s time intervals, however, it is possible that competition between

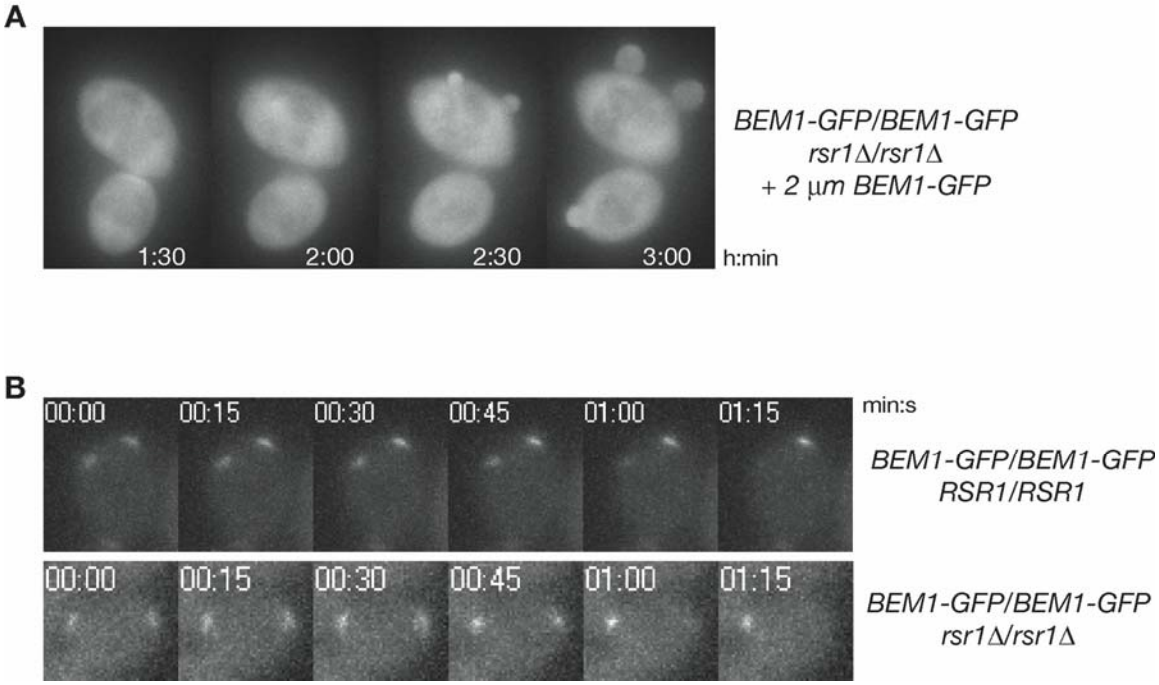

Figure 4.8 Competition between Bem1p-GFP foci

Competition for Bem1p-GFP may guarantee singularity in the presence of the GEF-PAK feedback loop. **(A)** Cells overexpressing Bem1p-GFP can grow two buds simultaneously. Selected frames from a timelpase of *BEM1-GFP/BEM1-GFP rsr1Δ/rsr1Δ* cells overexpressing Bem1p-GFP a 2 μm *BEM1-GFP* plasmid. Elapsed time is shown as h:min. **(B)** Multiple Bem1p-GFP polarization sites can form before leading to a single polarization site and bud. Selected frames from timelapses of cells imaged following release from HU arrest. Note that the two polarization sites are resolved to one within the span of 1 – 2 minutes. Elapsed time is shown in min:s.

Bem1p-GFP foci occurs much faster than in between Bem1p-GFP-Snc2p foci. When we decreased the time interval to 15 s by arresting cells in hydroxyurea prior to filming, we observed cells with multiple Bem1p-GFP foci that resolved to a single bud site within 90 s (Fig. 4.8B).

4.3 Discussion

4.3.1 Singularity in polarization

A key finding of this work is that cells synthetically re-wired to use a different positive feedback loop to polarize Cdc42p sometimes violated the singularity rule and made two buds simultaneously. This finding suggests that singularity is an intrinsic property of the Cdc42p-amplifying positive feedback system, and that there is no separate singularity-guaranteeing process.

What aspect of the Cdc42p amplification pathway guarantees singularity? As mentioned in the Introduction, theoretical analyses have stressed the idea that some form of competitive interaction between Cdc42p clusters could act to ensure singularity when two or more clusters arise. For example, a mathematical model of the Bem1p-based diffusional amplification mechanism (Goryachev and Pokhilko, 2008) indicated that competition between Cdc42p clusters for a limiting cytoplasmic pool of Bem1p complexes would lead to the eventual growth of the biggest cluster at the expense of the others. An alternative strategy to promote singularity, supported by another recent theoretical analysis (Altschuler et al., 2008), concerns the stochastic events that kick off the positive feedback loop. Positive feedback is initiated when a random cortical site

accumulates key polarity factors above some threshold concentration. If this stochastic "initiation" were sufficiently infrequent, then a second initiation event would be unlikely to occur in the time between the first event and bud emergence. The finding that overexpression of Bem1p-GFP could result in two simultaneously growing buds supports the model in which competition for Bem1p-containing complexes guarantees singularity. However, we cannot rule out the possibility that overexpression of Bem1p-GFP results in increased levels of initiation.

The competition model makes the prediction that symmetry-breaking polarization should (at least in some cells) occur through an intermediate “multiple cluster” stage. In wild-type cells filmed at > 90 s time-lapse intervals, this stage is not apparent. However, by synchronizing cells prior to imaging in HU, we were able to decrease the timelapse interval and detect the “multiple cluster” stage in wild-type cells. In these cells, competition between multiple Bem1p-GFP foci was resolved in < 90 s, potentially explaining why multiple Bem1p-GFP foci have not been reported in wild-type cells. Interestingly, competitive interactions between clusters were more easily detectable, and hence experimentally accessible, in the cells re-wired to perform actin-mediated instead of diffusional symmetry breaking.

4.3.2 Competition between polarization foci

Many of the re-wired cells formed two polarization foci, but in most cases one of the foci disappeared before bud emergence, and two-budded cells were infrequent. This finding provides strong evidence that foci interact with each other in a competitive manner that eventually leads to the growth of one focus at the expense of the other. Cells

that did establish two foci did so almost simultaneously, and new foci no longer appeared once a strong focus had formed, even if the cell cycle was arrested at a polarization-competent stage. This observation is also consistent with a competition model, as the first focus would effectively prevent the growth of subsequently-initiated foci. What is the basis for the observed competition?

The simplest possibility to explain competition in the re-wired cells is that foci compete (via their attached actin cables) for the vesicles that deliver additional Bem1p-GFP-Snc2p to the foci. Because foci are constantly losing Bem1p-GFP-Snc2p by diffusion and by endocytosis, delivery of new vesicles is required to maintain a focus. We present a simple mathematical model for such competition, and show that if delivery and loss are both proportional to the Bem1p-GFP-Snc2p content of a focus, then the situation is balanced and different foci can co-exist indefinitely. However, if foci with more Bem1p-GFP-Snc2p are also larger in extent (even if only slightly so) than foci with less Bem1p-GFP-Snc2p, then diffusional loss will no longer be proportional to protein content, and the larger focus will always grow at the expense of the smaller focus. This simple and realistic assumption about focus geometry suffices to make the 2-focus situation competitive rather than balanced. When model parameters were estimated based on experimental findings, the mathematical model was able to promote competition in a relevant timeframe, suggesting that this mechanism is powerful enough to account for competition in the re-wired cells. Of course, it remains entirely possible that there are other factors that could enhance competition.

After bud emergence, it appears that competition is no longer in effect, as both buds continued to grow in almost all cases. We speculate that once buds emerge the recycling pools of Bem1p-GFP-Snc2p in each bud are "insulated" from each other. Internal membranes including endosomes and golgi quickly enter small buds (Preuss et al., 1992), allowing the recycling of Bem1p-GFP-Snc2p within one bud to become independent from that in the other.

4.3.3 Comparison of re-wired cells with *cdc42-22* mutants

Prior to this work, the major experimental study to address singularity in polarization was focused on *cdc42* mutants capable of growing two or even more buds simultaneously (Caviston et al., 2002). The fact that single point mutations in *CDC42* could cause a breakdown in singularity supports our conclusion that singularity is conferred by the positive feedback mechanism that amplifies Cdc42p foci. However, there are a number of interesting and instructive differences between the phenotypes of our re-wired cells and those of *cdc42-22* mutants.

One major difference is that whereas polarization by Bem1p-GFP-Snc2p was still regulated by the normal cell cycle cues, polarity establishment by Cdc42p-22 was no longer appropriately regulated (Caviston et al., 2002). Recent work suggests that CDK activation may down-regulate Cdc42p-directed GAPs (Knaus et al., 2007; Sopko et al., 2007), potentially allowing stochastic GTP-loading of Cdc42p to initiate a polarizing positive feedback loop. Bem1p-GFP-Snc2p would not influence actin until levels of GTP-Cdc42p had built up in the cell, making Bem1p-GFP-Snc2p responsive to the cell cycle cue. However, Cdc42p-22 is thought to be very defective in GTP hydrolysis, and

can load and retain GTP without need of the Cdc24p GEF (Caviston et al., 2002). This may explain why Cdc42p-22 no longer needs the CDK signal in order to initiate polarization.

A second difference between our re-wired cells and *cdc42-22* mutants is that the latter generally polarized to random locations, whereas Bem1p-GFP-Snc2p biased polarization towards the previous division site. Both Cdc42p and Bem1p-GFP-Snc2p are concentrated at division sites, and we speculate that the bias towards that site is due to the slow diffusion of Bem1p-GFP-Snc2p from that site. Previous work (Marco et al., 2007; Valdez-Taubas and Pelham, 2003) suggested that lateral diffusion of Cdc42p is an order of magnitude faster than that of integral membrane proteins (including v-SNARES: $D \sim 0.0025\ \mu m^2/s$ versus $D \sim 0.036\ \mu m^2/s$ for Cdc42p), potentially explaining the lack of division-site bias in *cdc42-22* cells. In addition, it is clear that our re-wired cells retain some responsiveness to the Rsr1p-dependent bud site selection machinery whereas *cdc42-22* mutants do not (Caviston et al., 2002). As with cell cycle control, bud site selection is thought to influence Cdc42p GTP-loading (Park and Bi, 2007), which would impact the Bem1p-GFP-Snc2p mediated amplification but not that of Cdc42p-22.

The third and most interesting difference between re-wired cells and *cdc42-22* mutants is that the latter did not appear to show competition between foci, as new Cdc42p-22 buds could form even after one bud was well established (Caviston et al., 2002). The amplification mechanism used by *cdc42-22* mutants is not known. Because the mutant no longer needs the GEF, it clearly does not use the diffusional Bem1p-GEF-PAK complex mechanism (Fig. 4.1A). It may, however, use an actin-based amplification

mechanism similar to that of Bem1p-GFP-Snc2p (Fig. 4.1B). The actin-mediated positive feedback mechanism was first proposed for cells overexpressing GTP-locked Cdc42p^{Q61L} (Wedlich-Soldner et al., 2003), and Cdc42p-22 both accumulates to high levels (relative to wild-type Cdc42p) and is defective in GTP hydrolysis (though perhaps not to the degree of Cdc42p^{Q61L}) (Caviston et al., 2002). If Cdc42p-22 does employ an actin-mediated amplification mechanism, why does it not display competition between foci like Bem1p-GFP-Snc2p? A potential answer is suggested by our mathematical model of competition in re-wired cells, which shows that the timeframe for competition depends on focus geometry. If Cdc42p-22 foci tend to be of about the same size regardless of Cdc42p-22 content (η near 1 in our model), then foci could co-exist without competing.

Given the above considerations, it is tempting to speculate that the singularity rule boils down to having an efficient competitive mechanism. *cdc42-22* mutants with little or no competition break the singularity rule in ~45% of cells (Caviston et al., 2002). Our re-wired cells, with a competition mechanism operating in the timeframe of several minutes, break singularity in less than 5% of cells. Competition in wild-type cells operates in the timeframe of seconds to minutes, potentially explaining why they never break the singularity rule.

4.3.4 Tuning competition to obey or flout singularity

Not all polarized cells obey the singularity rule. Filamentous fungi can sustain many growing tips in the same (multinucleate) cell (Harris, 2008), and neurons initially form several neurite extensions from the same cell body (da Silva and Dotti, 2002). Yet, it appears that many of the same polarity regulators that obey singularity in other cell

types are similarly employed in these multipolar cells. It may be that a systems property of the polarization machinery fine-tunes the effectiveness of competition to allow the same molecular elements to promote or disregard singularity in different cell types.

5. Conclusions and future directions

5.1 Methods for investigating polarity establishment

The establishment of cell polarity is a fundamental process that has been extensively studied in many different organisms. Genetic techniques have been applied to understand polarity establishment, but fundamentally this is a spatial problem that is best studied with visual techniques. Live cell microscopy can provide valuable new insight into how cells polarize. However, microscopy in general can be damaging to cells and the G1 phase of the cell cycle in yeast appears to be particularity sensitive to illumination needed to follow fluorescently labeled proteins (Fig. 3.1). Arresting cells through the use of hydorxyurea prior to imaging is an effective means to circumvent the problems due to phototoxicity, however there are limitations to the utility of this method and the development of other means to film cells would be highly advantageous.

Although arresting cells with HU provides a valuable means to images cells during the G1 phase of the cell cycle, as a general protocol it is not without drawbacks. Arresting cells in HU results in changes to the cell morphology in yeast. Cells arrested in HU will continue to grow in a polarized manner during arrest (Jiang and Kang, 2003). This polarized growth is dependent on the bud site selection system (Kang and Jiang, 2005). In haploids, this growth is even more pronounced than in diploids due to the relatively small size and round morphology of haploid cells, and extended arrest in HU can result in cells that no longer bud according to the bud site selection system (i.e.

haploid cells that have been arrested in HU will bud from the distal tip of the daughter cell, rather than axially; data not shown).

With our current imaging technology arrest protocols will continue to be needed in the near future. As the results of Ozbudak demonstrate, cells can polarize in artifactual ways before going on to bud (Ozbudak et al., 2005). Developing additional arrest protocols to use in conjunction with HU arrest may provide useful secondary confirmation that any phenotypes observed are due to the physiology of the cell and not due to the arrest protocol. Arresting cells at mitotic exit through *cdc15* temperature sensitive mutants could provide another means of arresting cells at a different pointing the cell cycle. Isolating a synchronous population of early G1 cells through centrifugal elutriation, although potentially cumbersome for day to day experiments and somewhat perturbing itself, could also provide a synchronous population of cells without the attendant worries of cell cycle arrest.

G1 photosensitivity seems to be specific and may indicate involvement of a cell cycle regulator. Cells that have already formed a bud can often continue to grow under conditions that would block polarization and bud emergence, therefore G1 appears to be especially sensitive. An imaging-induced G1 arrest has been reported in mammalian tissue culture cells and may provide insight into our phototoxicity problem. Uetake et al. found that G1 was sensitive to the blue light needed to image GFP in human mammary epithelial cells, although to observe a cell cycle arrest the cells needed to experience a second perturbation (such as centriole ablation) (Uetake et al., 2007). In these cells, the

imaging-induced cell cycle arrest was dependent on p38, a component of the stress-response MAPK pathway (Uetake et al., 2007).

Yeast cells also have a stress-induced MAPK pathway, the "cell integrity" pathway (Levin, 2005). In yeast, these pathways are activated by stresses they might experience in the environment, such as osmotic, temperature, or ethanol shock. In response to stress, cells depolarize the actin cytoskeleton and continue to grow in an isotropic manner, presumably to help shore up the cell wall (Chowdhury et al., 1992; Kubota et al., 2004; Lillie and Brown, 1994). Imaging may be inducing a stress response, thus preventing cells from polarizing and budding even though the degree of light-induced damage might not be enough to kill the cells in a different part of the cell cycle. By blocking stress response through the deletion of *SLT2*, the MAP kinase, we may be able to render the cells insensitive to light in early G1, enabling us to film cells that had not been previously arrested.

Utilizing different technologies during image analysis could also aid our efforts. Currently, our image analysis has been on relatively raw images. By applying new analysis and processing techniques, we may be able to gain some new information. Deconvolving our images of yeast may improve our ability to detect polarization. By getting rid of some of the background fluorescence, we may uncover new information, especially about the early stages of polarity establishment. Additionally, increasing the signal to noise ration may allow us to decrease the exposure time needed to image cells, potentially increasing viability. Although increasing the amount of image processing may not be beneficial when first characterizing new protein dynamics, for comparing relative

protein polarization of pairs of red and green proteins, deconvolution may significantly increase our ability to determine relative timing of polarization.

5.2 Characterization of the polarization site

Through the use of the HU arrest protocol, we have begun to characterize the incipient bud site. We have been able to detect differences in protein polarization, both with respect to bud emergence and to other proteins. However, this analysis is still in an initial phase and can be expanded.

We have not yet imaged enough cells to have the statistical power to draw many conclusions about the relative polarization of proteins. Although we were able to image enough cells to determine that Bem1p-GFP polarized before Spa2p-GFP when they are both compared to bud emergence, the data concerning their polarization relative to one another were highly variable. By filming more cells we should be able to determine whether this variability is due to a small sample size or reflects true variability in polarity establishment. Although we do not yet have a "map" of polarization, we have been able to characterize polarization somewhat. For example, we know that Bem1p-GFP starts out as a broader area that then condenses down to a single spot, while Spa2p-GFP does not. Further filming should hopefully allow us to correlate these changes in polarization with other events, possible giving us mechanisms to test.

It would also be helpful to expand the set of fluorescent proteins we examine. A small group was chose for the initial stages as a proof of principle, but now that we have a means to film cells, the panel of proteins whose polarization is followed should be

expanded. Candidates for analysis by live-cell microscopy include the septins, the GEF Cdc24p, and the formin Bni1p. It would also be highly beneficial to develop a probe for actin cables. At the moment, we are only able to detect actin patches during timelapse analysis. Although actin patches polarize to sites of polarized growth, and there has not been a reported difference between polarization of cables and patches, we would like to be able to image both actin structures. As the tracks for polarized delivery of secretory vesicles, the actin cables are functionally distinct from actin patches and following their polarization would be informative. GFP-tagged actin, Act1p-GFP, is non-functional in yeast (Doyle and Botstein, 1996). Abp140p-GFP has been used successfully to label actin cables in yeast, however it is a very dim probe and not suitable for timelapse microscopy during G1 due to the amount of light needed to see the cables (Yang and Pon, 2002). Utilizing the actin-binding domain of an exongenous protein from another organism may enable us to visualize the process of actin cable polarization.

Our data concerning the timing of Bem1p polarization with respect to both bud emergence and actin patch polarization supports the model that the initial establishment of cell polarity occurs independent of the actin cytoskeleton. Given that several proteins in addition to Bem1p, such as the septins andCdc24p, are known to be able to polarize efficiently without a polymerized actin cytoskeleton (Ayscough et al., 1997), filming polarity establishment in the presence of the actin depolymerizing drug Lat A would allow us to determine whether the dynamics of polarity establishment are different from wild type polarization in the absence of an actin cytoskeleton. For example, would Bem1p-GFP still polarize to a broad crescent before condensing into a tighter patch? Are

the rates of exchange at the polarization site as determined by FRAP analysis the same in the absence of an actin cytoskeleton?

Imaging polarization in *rsr1Δ* cells yielded a highly unexpected result. Our analysis should be expanded to other polarization mutants. Live-cell microscopy may be particularly informative with regards to genes whose function in polarity establishment in unknown. For example, Boi1p and Boi2p appear to function in polarity establishment and deletion of both Bois results in bud emergence defects (Bender et al., 1996). However, it is till unclear what these proteins are contributing to polarity establishment. Following polarity establishment by live-cell microscopy in the absence of Boi1p and Boi2p may shed some light on their function in polarity establishment.

5.3 Bem1p-GFP oscillates in intensity in the absence of Rsr1p.

We were very surprised to see that in *rsr1Δ* cells, Bem1p-GFP is not consistently polarized at the incipient bud site, but instead appears to oscillate in intensity. The cause of these oscillations is unknown, however the fact that initial accumulation of Bem1p-GFP at the polarization site appeared unperturbed suggests that there may be a delayed negative feedback loop causing the Bem1p-GFP signal intensity to oscillate. There are two main candidates for the negative regulator of polarity establishment in this putative feedback loop, Cdc42p GAPs and the actin cytoskeleton.

In Chapter 2 we explored the negative impact actin-mediated endocytosis could have on Cdc42p polarity. Most importantly, it was maintenance of the polarized signal, not the initial establishment, which was hindered by endocytosis. Actin patches also

appeared to polarize after initial Bem1p-GFP polarity establishment (Fig. 4.4), placing at the bud site at the opportune time to disperse Bem1p polarization. Although the motile polarization site phenotype described may have been due to an artifact, the destabilization of the polarity patch in *rsr1Δ* cells reported by Ozbudak was at least in part due to the actin cytoskeleton (Ozbudak et al., 2005). Imaging *rsr1Δ* cells in the presence of Lat A should easily determine whether the actin cytoskeleton could be the source of the Bem1p-GFP oscillations. If actin appears to play a role in Bem1p-GFP oscillations, then actin patches and cables can be specifically targeted by mutations to determine their relative contributions.

Ozbudak and colleagues also suggested that Cdc42p GAPs could destabilize the polarization site in *rsr1Δ* cells (Ozbudak et al., 2005). Bem2p, Bem3p, Rga1p and Rga2p all localize to sites of polarized growth (Irazoqui and Lew, 2004), however the timing of their polarization relative to Cdc42p polarization is unknown. A reasonable hypothesis would be that GTP-Cdc42p recruits GAPs to the polarization site, however this recruitment could be delayed relative to GTP-Cdc42p polarization if levels of GTP-Cdc42p need to build up at the polarization site before recruiting the GAPs. Following Bem1p-GFP polarization in GAP deletion strains (both single deletions and in combination) could help determine which of the GAPs, if any, could contribute to Bem1p-GFP oscillations.

5.4 Actin-mediated polarity establishment

The proliferation of *BEM1-GFP-SNC2* cells demonstrated that actin-mediated polarity establishment could occur on a timescale relevant to budding. Forcing cells to rely on an actin-mediated mechanism to establish polarity also rendered them more susceptible to actin cytoskeletal perturbations. The model for actin-mediated symmetry breaking requires the protein being polarized to influence actin cable nucleation in its vicinity. Bnr1p-nucleated actin cables at the septin ring would not be sufficient to promote polarization as they are in wild type cells, because there would be no septin ring to localize Bnr1p. Indeed, we found that Bni1p was required for polarity establishment in *BEM1-GFP-SNC2* cells, even in the presence of Rsr1p (Table 1). This requirement for Bni1p gives us an artificial system in which to study the connection between Cdc42p and Bni1p. Studying the connection between Cdc42p and Bni1p in cells that can utilize the diffusional feedback loop is difficult due to the fact that Bni1p is not essential. Although we do not fully understand the regulation of Bni1p activity, the simplest model for localized activation of cable nucleation is that Cdc42p binds to the PBD domain in Bni1p, thereby recruiting and activating its nucleation activity to the polarization site. By testing a panel of Bni1p mutant constructs for their ability to rescue growth of *BEM1-GFP-SNC2 bni1Δ* cells, we can ask what portions of Bni1p are required for its localized nucleation activity.

5.5 Singularity in budding

Through a combination of mathematical modeling and synthetically re-wiring the yeast polarity machinery, our results support the model that singularity is inherent to the Cdc42p amplification mechanism. In addition to theoretically being able to guarantee singularity in *BEM1-GFP-SNC2* cells, it appears that it is competition between polarization sites that guarantees singularity in wild type cells polarizing through the GEF-PAK diffusional mechanism. What is the limiting factor for which polarization sites are competing? Goryachev and Pokhilko have suggested that complexes of Cdc24p and Bem1p are the limiting factor (Goryachev and Pokhilko, 2008). Bem1p-GFP overexpression was able to subvert singularity in *rsr1Δ* cells, suggesting that complexes containing Bem1p-GFP may be a limiting factor in polarity establishment. This result in is contrast to overexpression of Cdc42p-GFP, which blocked polarity establishment when expressed at high levels in the presence of Lat A (Altschuler et al., 2008). It would be interesting to test whether overexpression of Bem1p-GFP still leads to multiple polarization sites in the absence of an actin cytoskeleton, or whether it leads to a failure in polarity establishment, as in the case of Cdc42p-GFP. Titrating the amounts of various polarity regulators may help us to determine how cells are able to guarantee that they only form a single bud.

If yeast cells rely on efficient competition between polarization sites to generate, singularity, then decreasing competition efficiency may also yield a breakdown in singularity. Presumably, the efficiency of competition between multiple polarity sites in cells is in part due to the rapid turnover and diffusion of the components of the GEF-PAK

feedback loop at the polarity sites. Would slowing the movement of the GEF-PAK feedback loop components result in cells with two buds, or increase the incidence of multiple polarity sites? Cdc24p, Bem1p, and Cla4p are all peripheral membrane proteins whose association with the plasma membrane is mediated by lipid-binding domains (Fig.1.2). Would tethering these proteins to plasma membrane through lipid modification, for example the addition of a CAAX box for prenylation, slow competition in polarity establishment?

6. Materials and methods

6.1 Yeast strains and plasmids

Standard media were used for yeast growth (Guthrie and Fink, 1991). The yeast strains used are listed in Table 6.1. The *bem1::URA3* (Chenevert et al., 1992) and *rsr1::HIS3* (Schenkman et al., 2002) disruptions were as previously described. *bar1::URA3* was generated by the one-step PCR-based method (Baudin et al., 1993) using pRS306 (Sikorski and Hieter, 1989) as template. *rsr1::TRP1* was obtained from the John Pringle lab and was generated by the one-step PCR-based method (Baudin et al., 1993).

Strains expressing *BEM1-GFP* at the *BEM1* locus were created as previously described (Kozubowski et al., 2008). To generate strains expressing Bem1p-GFP-Snc2p (DLY8577), we targeted homologous recombination of a plasmid containing a C-terminal fragment of *BEM1* fused to GFP and *SNC2* (pDLB2823) at the wild-type *BEM1* locus. pDLB2823 contains the previously described C-terminal fragment of *BEM1*fused to a GFP, in which the stop codon of GFP was replaced by a linker containing a *Not*I site (Kozubowski et al., 2008). The entire *SNC2* ORF was inserted between the *Not*I site at the end of GFP and a *Sal*I site introduced before the stop codon and the *BEM1* 3' untranslated region. Integration was targeted to *BEM1* by cutting at the unique *Pst*I site, which results in the replacement of the endogenous *BEM1* with *BEM1-GFP-SNC2*, followed by an adjacent *LEU2* and promoterless C-terminal fragment of *BEM1* (designated as *BEM1-GFP-SNC2:LEU2*). Plasmid pDLB2920, for expression of Bem1p-

GFP-Snc2p^{V39A,M42A}, is identical to pDLB2823 except for the indicated mutations introduced by site-directed mutagenesis. Correct integration in one chromosome of a wild-type diploid was verified by PCR tests, and sporulation and dissection was used to derive the final strains.

For expression of Cdc3p-mCherry, pDLB3138 (YIp128-CDC3-mCherry, (Tong et al., 2007)) was cut at the unique *BglII* site to replace *CDC3* with *CDC3-mCherry*. pDLB3086 (YIp211-GIC2-PBD-RFP, (Tong et al., 2007)) was cut with *ApaI* to integrate *GIC2-PBD-RFP* at *URA3*. *SPA2-mCherry*, *ABP1-mCherry*, and *SPC42-mCherry* were generated by the PCR-based C-terminal tagging method (Longtine et al., 1998) using pDLB2865 (*pFA6a-mCherry-ADH1t-kanMX6*) as template. Strains expressing Bem1p-GFP from the *URA3* locus in addition to Bem1p-GFP-Snc2p were created by integrating pACB514 cut with *Stu*I (Butty et al., 2002).

To create strains in which P_{GAL}-dependent transcription of $SIC1^{\Delta 4p}$ was controlled by addition of β-estradiol, the synthetic transcription factor construct *GAL4DBD-hER-VP16* was targeted for integration at *URA3* by digestion of pPP1559 with *NdeI* (Takahashi and Pryciak, 2008). pDLB2738, a plasmid containing P_{GAL}-$SIC1^{\Delta 4p}$ (in which Sic1p residues T2, T5, T33, and S76 were mutated to alanine (Verma et al., 1997)) in pRS306 (Sikorski and Hieter, 1989) was digested at the unique *StuI* site to target integration at the *URA3* locus.

6.2 Live-cell microscopy

For live-cell imaging exponentially growing cells were mounted on a slide with a slab of synthetic medium solidified with 2% agarose (Denville Scientific, Inc., Metuchen, NJ). Images in Figures 4.1E and 4.2B were acquired using the AxioImager system described above. Images in Figures 4.4-6 and 4.8were acquired using an Axio Observer.A1 (Carl Zeiss, Inc., Thornwood, NY) with a 100x/1.4 Ph3 Plan Apochromat oil immersion objective controlled by MetaMorph software (Universal Imaging, Silver Spring, MD). Images were captured using a QuantEM backthinned EM-CCD camera (Photometrics, Ottobrunn, Germany). All timelapses consisted of DIC and fluorescent (GFP and, where indicated, RFP) images acquired over 11 z-planes with 0.5 μm steps.

***cdc24-1* arrest**

To film cells following *cdc24-1*-mediated arrest cells were grown overnight in syncthetic complete medium with 2% dextrose at 24°C. Exponentially growing cells were shifted to 37°C for 2.5 hrs and then mounted on a slide with a slab of synthetic medium solidified with 20% gelatin (Sigma-Aldrich) and sealed with valap (1:1:1 vaseline, lanolin, paraffin). A single GFP images was acquired every 10 s at room temperature (approximately 24°C) using a Zeiss Axioskop (Carl Zeiss, Inc., Thornwood, NY) with a 100x oil immersion objective. Images were captured using an ORCA cooled charge-coupled device camera (Hamamatsu Corp., Bridgewater, NJ), interfaced with MetaMorph software (Universal Imaging, Silver Spring, MD).

HU arrest

To film cells following arrest in hydroxyurea the cells of interest were grown overnight in synthetic complete medium with 2% dextrose at 30°C. Exponentially growing cells were arrested by addition of 200 mM hydroxyurea (Sigma-Aldrich, St. Louis, MO) to the culture medium for 2.5 hrs. Cells were washed once in fresh medium and then released in from synthetic complete medium at 30° for 1.25 hr at which point they were mounted for imaging. Cells were mounted on a slab of synthetic medium solidified with 2% agarose (Denville Scientific, Inc., Metuchen, NJ), sealed with Vaseline and imaged at room temperature (approximately 24°C). DIC and fluorescent (GFP and, where indicated, RFP) images acquired over 11 z-planes with 0.5 μm steps every 15 s (GFP and DIC) or every 20 s (GFP, RFP and DIC) using an Axio Observer.A1 (Carl Zeiss, Inc., Thornwood, NY) with a 100x/1.4 Ph3 Plan Apochromat oil immersion objective controlled by MetaMorph software (Universal Imaging, Silver Spring, MD). Images were captured using a QuantEM backthinned EM-CCD camera (Photometrics, Ottobrunn, Germany).

Photobleaching

Cells were mounted on 2% agarose slides and imaged on a SP5 confocal microscope (Leica Microsystems, Bannockburn, IL) using a 63x/1.20 water Plan Apochromat objective. Photobleaching experiments were done using the FRAPwizard in the Leica LAS AF software with 1 iteration of bleaching at 100% laser power and image acquisition at 4% power using an Argon/2 (488) laser. The data shown in Figure 1C were first normalized to pre-bleach signal intensity and then averaged over several

experiments. The recovery half-times were calculated from individual curve fits to the normalized data using Kaleidagraph (Synergy Software, Reading, PA).

6.3 Immunofluorescence and fixed-cell microscopy

Immunofluorescence

To visualize Cdc42p and Sec4p, cells were fixed for a total of 3 h in 3.6% formaldehyde, permeabilized with 0.5% SDS, and processed for immunofluorescence as previously described (Lehman et al., 1999; Redding et al., 1991). Anti-Cdc42p antibody (used at 1:200 dilution) and anti-Sec4p antibody (used at 1:100 dilution) were generously provided by Patrick Brennwald (UNC Chapel Hill). To visualize F-actin, cells were fixed as above, treated with acetone, and processed for staining with alexafluor488-phalloidin as previously described for rhodamine-phalloidin (Pruyne et al., 1998). Cells were examined using a Zeiss Axioskop (Carl Zeiss, Inc., Thornwood, NY) with a 100x oil immersion objective. Images were captured using an ORCA cooled charge-coupled device camera (Hamamatsu Corp., Bridgewater, NJ), interfaced with MetaMorph software (Universal Imaging, Silver Spring, MD). Images were processed for presentation using Photoshop (Adobe Systems, Inc., San Jose, CA). Individual cells or groups of cells in the correct focal plane were grouped together from one or more fields to assemble the figures.

Bud scar and birth scar staining

To visualize bud and births scars, cells were fixed in 3.7% formaldehyde for 1 h at room temperature, washed, and resuspended in immunofluorescence solution B (0.1 M

KPO_4, pH 7.5, and 1.2 M sorbitol). Birth scars were stained with 12.5 μg/ml Alexa 594–ConA (Invitrogen, Carlsbad, CA) in immunofluorescence solution B for 20 min at room temperature. Bud scars were stained with a solution of 0.05% Calcofluor (Sigma-Aldrich, St. Louis, MO) for 30 min at room temperature. Cells were examined using an AxioImager.A1 (Carl Zeiss, Inc., Thornwood, NY) with a 100x/1.4 Plan Apochromat oil immersion objective. Images were captured using an ORCA cooled charge-coupled device camera (Hamamatsu, Bridgewater, NJ) and interfaced with MetaMorph software (Universal Imaging, Silver Spring, MD). Images were processed for presentation using Photoshop (Adobe systems, San Jose, CA).

6.4 Other methods

Lat A and Lat B were purchased from Molecular Probes, Eugene, OR, and kept as 200x (Lat A) and 100x (Lat B) stocks in DMSO at –20°C.

Centrifugal elutriation

Enrichment of small daughter cells from exponentially growing cultures was achieved by centrifugal elutriation as described previously (Lew and Reed, 1993). After elutriation, cells were grown in rich medium YEPD at 37°C for 80 min or 180 min. Samples were fixed with 3.7% formaldehyde for 1 h at room temperature, washed once and resuspended in immunofluorescence solution B. Birth scars were stained as described above.

Analysis of growth rate and cell cycle distribution

For measurement of the population doubling time, cultures were diluted to 2 x 10^6 cells/mL in YEPD and grown at 30°C. 1 mL aliquots were fixed with 3.7% formaldehyde at 30 min intervals and sonicated. The absorbance was measured at 600 nm with a Beckman DU 640B Spectrophotometer (Beckman Coulter, Fullerton, CA).

FACS analysis was performed as previously described (Haase and Reed, 2002). Cells were fixed overnight in 70% ethanol, washed with H_2O, and incubated in 2 mg/ml RNaseA (Sigma-Aldrich, St. Louis, MO) in 50 mM Tris-HCl (pH 8.0) overnight at 37°C. Following treatment with 5 mg/ml pepsin (Sigma-Aldrich, St. Louis, MO) in 0.45% HCl (vol/vol) for 15 min, DNA was stained with Sytox Green (Invitrogen, Carlsbad, CA) in 50 mM Tris-HCl (pH 7.5). DNA content of 10,000 cells was measured with a Becton Dickinson FACScan and analyzed with CellQuest software (Becton Dickinson Biosciences, San Jose, CA).

Immunoblotting

Lysis of yeast, SDS-PAGE, and immunoblotting were performed as described previously (Keaton et al., 2008). The mouse monoclonal anti-GFP antibody (Roche Diagnostics, Indianapolis, IN) was used at a 1:1000 dilution. The anti-Cdc11 polyclonal antibody (Santa Cruz Biotechnology, Santa Cruz, CA) was used at a 1:10000 dilution.

Table 2 Yeast strains used in this study

Strain	Relevant genotype	Source
ABY551	**a**/α *MYO2::HIS3/MYO2::HIS3*	(Schott et al., 1999)
ABY553	**a**/α *myo2-16::HIS3/myo2-16::HIS3*	(Schott et al., 1999)
ABY971	**a**/α *tpm1-2::LEU2/tpm1-2::LEU2 tpm2Δ::HIS3/tpm2Δ::HIS3*	(Pruyne et al., 1998)
ABY973	**a**/α *tpm2::HIS3/tpm2::HIS3*	(Pruyne et al., 1998)
DDY342	α *act1-113::HIS3*	(Ayscough et al., 1997)
DDY345	α *act1-117::HIS3*	(Ayscough et al., 1997)
DDY354	**a** *ACT1::HIS3*	(Ayscough et al., 1997)
DDY595	**a** *bar1 sla2-41*	(Wesp et al., 1997)
DLY5[1]	**a**/α *bar1/BAR1*	(Lew and Reed, 1993)
DLY3644[1]	**a** *his3 HIS2 GAL1p-SWE1::LEU2*	(Irazoqui et al., 2005)
DLY5029	**a**/α *rsr1::HIS3/ rsr1::HIS3 bem1::URA3/BEM1*	(Kozubowski et al., 2008)
DLY7543[2]	**a**/α *MYO2::HIS3/MYO2::HIS3 GAL1p-SWE1myc::URA3*	(Irazoqui et al., 2005)
DLY7544[3]	**a**/α *myo2-16::HIS3/myo2-16::HIS3 GAL1p-SWE1-myc::URA3*	(Irazoqui et al., 2005)
DLY7595[4]	**a**/α *SPA2-GFP:URA3/SPA2-GFP:URA3*	This study
DLY8017[4]	**a**/α *SPA2-GFP:URA3/SPA2-GFP:URA3 rsr1::TRP1/rsr1::TRP1*	This study
DLY8246[4]	α *cdc24-1 BEM1-GFP:URA3*	This study
DLY8388[4]	**a**/α *SEC4-GFP:URA3/SEC4*	This study
DLY8454[4]	α *cdc24-1 SPA2-GFP:URA3*	This study
DLY8500[4]	α *cdc24-2 SEC4-GFP:URA3*	This study
DLY8577[4]	**a**/α *BEM1-GFP-SNC2:LEU2/BEM1*	This study
DLY8601[4]	**a** *BEM1-GFP-SNC2:LEU2*	This study
DLY8666[4]	**a** *BEM1-GFP-SNC2:LEU2 rsr1::TRP1*	This study
DLY8990[4]	**a** *BEM1-GFP:LEU2 rsr1::TRP1*	This study
DLY8997[1]	**a**/α *BEM1-GFP-SNC2:LEU2/BEM1 sac6::URA3/SAC6*	This study

Table 2 continued

DLY9002[1]	**a**/α *BEM1-GFP(AAAKKS):LEU2/BEM1 sac6::URA3/SAC6*	This study
DLY9008	**a**/α *BEM1-GFP-SNC2:LEU2/BEM1 tpm2::HIS3*	This study
DLY9010	**a**/α *BEM1-GFP(AAAKKS):LEU2/BEM1 tpm2::HIS3/TPM2*	This study
DLY9016[4]	**a**/α *BEM1-GFP-SNC2:LEU2/BEM1 rsr1::TRP1/RSR1 pea2::HIS3/PEA2*	This study
DLY9022[4]	**a**/α *BEM1-GFP-SNC2:LEU2/BEM1 bud6::HIS3/BUD6*	This study
DLY9024[4]	**a**/α *BEM1-GFP(AAAKKS):LEU2/BEM1 bud6::HIS3/BUD6*	This study
DLY9032[4]	**a**/α *BEM1-GFP:LEU2/BEM1*	This study
DLY9044[4]	**a**/α *BEM1-GFP-SNC2:LEU2/BEM1 bni1::HIS3/BNI1 rsr1::TRP1/RSR1*	This study
DLY9056[4]	**a**/α *BEM1-GFP(AAAKKS):LEU2/BEM1 rsr1::TRP1/RSR1 bni1::HIS3/BNI1*	This study
DLY9069[4]	**a** *BEM1-GFP:LEU2*	This study
DLY9122[4]	**a**/α *BEM1-GFP-SNC2:LEU2/ BEM1-GFP-SNC2:LEU2*	This study
DLY9123[4]	**a**/α *BEM1-GFP-SNC2:LEU2/BEM1 rsr1::TRP1/ rsr1::TRP1*	This study
DLY9124[4]	**a**/α *BEM1-GFP-SNC2:LEU2/ BEM1-GFP-SNC2:LEU2 rsr1::TRP1/ rsr1::TRP1*	This study
DLY9133[4]	**a**/α *BEM1-GFP-SNC2:LEU2/BEM1 spa2::HIS3/SPA2*	This study
DLY9198[4]	**a**/α *BEM1-GFP:LEU2/BEM1 rsr1::TRP1/ rsr1::TRP1*	This study
DLY9200[4]	**a**/α *BEM1-GFP:LEU2/ BEM1-GFP:LEU2 rsr1::TRP1/ rsr1::TRP1*	This study
DLY9207[4]	**a**/α *BEM1-GFP:LEU2/BEM1 pea2::HIS3/pea2::HIS3*	This study
DLY9224[4]	**a**/α *BEM1-GFP-SNC2:LEU2/BEM1 tpm1::URA3/tpm1::URA3*	This study
DLY9251[1]	**a**/α *BEM1-GFP:LEU2/BEM1 tpm1::URA3/tpm1::URA2*	This study
DLY9257[4]	**a**/α *BEM1-GFP:LEU2/BEM1 spa2::HIS3/spa2::HIS3*	This study
DLY9343[1]	**a**/α *BEM1-GFP-SNC2:LEU2/BEM1 cap2::URA3/cap2::URA3*	This study
DLY9344[1]	**a**/α *BEM1-GFP:LEU2/BEM1 cap2::URA3/cap2::URA3*	This study
DLY9432[4]	α *BEM1-GFP-SNC2:LEU2 SPA2-mCherry:kan^R rsr1::TRP1*	This study
DLY9439[4]	**a** *BEM1-GFP:LEU2 SPA2-mCherry:kan^R rsr1::TRP1*	This study
DLY9641[4]	**a**/α *BEM1-GFP-SNC2(V39A,M42A):LEU2/BEM1 rsr1::TRP1/ rsr1::TRP1*	This study
DLY9826[4]	α *BEM1-GFP-SNC2:LEU2 GIC2-PBD-RFP:URA3 rsr1::TRP1*	This study

Table 2 continued

DLY9831[4]	*α BEM1-GFP:LEU2 GIC2-PBD-RFP:URA3 rsr1::TRP1*	This study
DLY9921[4]	**a**/*α SPA2-mCherry:Kan^R/ SPA2-mCherry:Kan^R BEM1-GFP:LEU2/BEM1-GFP/LEU2*	This study
DLY9927[4]	**a**/*α SPA2-mCherry:Kan^R/ SPA2-mCherry:Kan^R SEC4-GFP:URA3/SEC4-GFP:URA3*	This study
DLY9985[4]	**a**/*α BEM1-GFP:LEU2/BEM1 ABP1-mCherry:Kan^R/ABP1 rsr1::TRP1/RSR1*	This study
DLY10092[4]	*α BEM1-GFP-SNC2:LEU2 CDC3-mCherry:LEU2 rsr1::TRP1*	This study
DLY10096[4]	*α BEM1-GFP:LEU2 CDC3-mCherry:LEU2 rsr1::TRP1*	This study
DLY11123[4]	**a**/*α BEM1-GFP-SNC2:LEU2/ BEM1-GFP-SNC2:LEU2 rsr1::TRP1/ rsr1::TRP1 SPC42-mCherry:kan^R/SPC42*	This study
DLY11227[4]	**a**/*α BEM1-GFP-SNC2:LEU2/BEM1-GFP-SNC2:LEU2 GIC2-PBD-RFP:URA3/GIC2-PBD-RFP:URA3 rsr1::TRP1/rsr1::TRP1*	This study
DLY11229[4]	**a**/*α BEM1-GFP-SNC2:LEU2/ BEM1-GFP-SNC2:LEU2 CDC3-mCherry:LEU2/CDC3-mCherry:LEU2 rsr1::TRP1/ rsr1::TRP1*	This study
DLY11230[4]	**a**/*α BEM1-GFP-SNC2:LEU2/ BEM1-GFP-SNC2:LEU2 SPA2-mCherry:kan^R/ SPA2-mCherry:kan^R rsr1::TRP1/ rsr1::TRP1 bar1::URA3/BAR1*	This study
DLY11231[5]	**a**/*α BEM1-GFP-SNC2:LEU2/BEM1-GFP-SNC2:LEU2 rsr1::TRP1/rsr1::TRP1 pRS426-BEM1-GFP*	This study
DLY11242[4]	**a**/*α BEM1-GFP-SNC2:LEU2/ BEM1-GFP-SNC2:LEU2 ABP1-mCherry:kan^R/ABP1-mCherry:kan^R rsr1::TRP1/ rsr1::TRP1*	This study
DLY11264[4]	**a**/*α BEM1-GFP-SNC2:LEU2/ BEM1-GFP-SNC2:LEU2 rsr1::TRP1/ rsr1::TRP1 BEM1-GFP:URA3/URA3*	This study
DLY11266[4]	**a**/*α BEM1-GFP:LEU2/ BEM1-GFP:LEU2 rsr1::TRP1/ rsr1::TRP1 BEM1-GFP:URA3/URA3*	This study
DLY11309[4]	**a**/*α BEM1-GFP-SNC2(V39A,M42A):LEU2/BEM1 rsr1::TRP1/ rsr1::TRP1 GIC2-PBD-RFP:URA3/URA3*	This study
DLY11320[4]	**a**/*α BEM1-GFP:LEU2/ BEM1-GFP:LEU2 ABP1-mCherry:kan^R/ABP1-mCherry:kan^R rsr1::TRP1/ rsr1::TRP1*	This study
DLY11321[4]	**a**/*α BEM1-GFP-SNC2:LEU2/BEM1 rsr1::TRP1/ rsr1::TRP1 GIC2-PBD-RFP:URA3/URA3*	This study
DLY11322[4]	**a**/*α BEM1-GFP-SNC2:LEU2/ BEM1-GFP-SNC2:LEU2 rsr1::TRP1/ rsr1::TRP1 P_{GAL1}-SIC1$^{\Delta 4P}$:URA3/P_{ADH1}-GAL4DBD-hER-VP16:URA3*	This study

Table 2 continued

DLY11323[4]	**a**/α *BEM1-GFP:LEU2/ BEM1-GFP:LEU2 rsr1::TRP1/ rsr1::TRP1* P_{GAL1}*-SIC1*$^{\Delta 4P}$*:URA3/*P_{ADH1}*-GAL4DBD-hER-VP16:URA3*	This study
GPY10[1]	**a** *bar1 rdi1::URA3*	David Stone
RH1800	**a** *bar1*	(Friant et al., 2000)
RH3809	**a** *bar1 lcb1-100*	(Friant et al., 2000)

[1] Strains in the BF264-15Du background (*ura3*Δ*ns leu2-3,112 trp1-1a ade1 his2*).
[2] Generated by transforming ABY551 with pRS306-GAL1-SWE1myc (McMillan et al., 1998).
[3] Generated by transforming ABY553 with pRS306-GAL1-SWE1myc (McMillan et al., 1998).
[4] Strains in the YEF473 background (*his3-*Δ*200 leu2-*Δ*1 lys2-801 trp1-*Δ*63 ura3-52)*
[5] Generated by transforming DLY9200 with DLB3191.

7. Simple competition models for Bem1p-GFP-Snc2p foci

We imagine that Bem1p-GFP-Snc2p molecules can be in one of four compartments: in one of two foci on the plasma membrane (amounts denoted by h_1 and h_2), in the plasma membrane but not in either focus (amount denoted by h_m), or in an internal pool (amount denoted by h_i). We assume that Bem1p-GFP-Snc2p synthesis and degradation are balanced, so the total amount, H_o, of Bem1p-FP-Snc2p is conserved, and we have

$$h_1 + h_2 + h_m + h_i = H_o. \tag{1}$$

We assume that Bem1p-GFP-Snc2p is delivered from the internal pool to the two foci via action cables, with total flux αh_i split between the two foci in a manner proportional to the amounts already in the foci. Bem1p-GFP-Snc2p is removed from both of the foci as well as the general membrane and delivered to the internal pool by endocytosis, at rates proportional to the amounts in the compartments. To accommodate the likelihood (based on actin patch clustering) that endocytosis at foci (γh_1 and γh_2) is more active than endocytosis in the general membrane (δh_m), we use different rate constants. Finally, Bem1p-GFP-Snc2p escapes from the foci to the general membrane compartment by diffusion. Here we are interested in contrasting two different scenarios. Either diffusional loss is proportional to the amounts $h1$ and $h2$ (this will be called the proportional model) or diffusional loss is proportional to $(h_1)^\eta$ and $(h_2)^\eta$ where η is a power satisfying $0 < \eta < 1$ (this will be called the non-proportional model). Biologically, we believe that $0.5 < \eta < 1$.

7.1 Analysis of the proportional model

The differential equations of the proportional model are as follows:

$$\frac{dh_1}{dt} = \alpha \frac{h_1(t)}{h_1(t) + h_2(t)} h_i(t) - \beta h_1(t) - \gamma h_1(t) \tag{2}$$

$$\frac{dh_m}{dt} = \beta h_1(t) + \beta h_2(t) - \delta h_m(t) \tag{3}$$

$$\frac{dh_2}{dt} = \alpha \frac{h_2(t)}{h_1(t) + h_2(t)} h_i(t) - \beta h_2(t) - \gamma h_2(t) \tag{4}$$

$$\frac{dh_i}{dt} = \gamma h_1(t) + \gamma h_2(t) - \delta h_m(t) - \alpha h_i(t). \tag{5}$$

Here α, β, γ, and δ are positive constants; their values do not affect the calculations or the conclusions. If ($\bar{h}_1, \bar{h}_2, \bar{h}_m, \bar{h}_i$) is an equilibrium point, then

$$\beta(\bar{h}_1 + \bar{h}_2) = \delta \bar{h}_m, \tag{6}$$

and

$$\gamma(\bar{h}_1 + \bar{h}_2) + \delta \bar{h}_m = \alpha h_i, \tag{7}$$

so it follows from (1) that

$$\bar{h}_1 + \bar{h}_2 = \frac{H_o}{1 + \frac{\beta}{\delta} + \frac{\gamma+\beta}{\alpha}}. \tag{8}$$

Conversely, if we choose any non-negative $\bar{h}_1$ and $\bar{h}_2$ that satisfy (8) and define $\bar{h}_m$ and $\bar{h}_i$ by (6) and (7), then ($\bar{h}_1$, $\bar{h}_2$, $\bar{h}_m$, $\bar{h}_i$) is an equilibrium point. Thus, for each H_o, the set of equilibrium points in the positive orthant is the line segment given by (6), (7) and (8).

If we use (1) to substitute for $h_1 + h_2$ in (3) and (5), we find that h_m and h_i satisfy a pair of linear equations:

$$\begin{pmatrix} h_m \\ h_i \end{pmatrix}' = H_o \begin{pmatrix} \gamma \\ \beta \end{pmatrix} - A \begin{pmatrix} h_m \\ h_i \end{pmatrix}, \qquad A = \begin{pmatrix} (\gamma+\alpha) & (\gamma-\delta) \\ \beta & (\beta+\delta) \end{pmatrix}.$$

For all positive choices for the constants $\alpha, \beta, \gamma, \delta$, the eigenvalues of A have strictly positive real parts. Thus given H_o, and any initial conditions, the solutions $h_m(t)$ and $h_i(t)$ converge to $\bar{h}_m = \alpha\beta H_o/\det(A)$ and $\bar{h}_i = \delta(\gamma+\beta)H_o/\det(A)$. By adding equations (2) and (4) we see that $h_1(t) + h_2(t)$ satisfies

$$(h_1(t) + h_2(t))' = \alpha h_i(t) - (\gamma+\beta)(h_1(t) + h_2(t)),$$

from which it follows that $h_1(t) + h_2(t)$ converges to the value given by (8) independent of the initial conditions.

Finally, by dividing (2) by (4) we see that $\frac{h_1'}{h_2'} = \frac{h_1}{h_2}$, so

$$\left(\frac{h_1}{h_2}\right)' = \frac{h_1' h_2 - h_1 h_2'}{h_2^2} = 0.$$

Thus the ratio $h_1(t)/h_2(t)$ remains constant and the limit point on the line given by (8) is determined by the initial ratio of h_1 and h_2.

We remark that if the total amount of Bem1p-GFP-Snc2p, namely H_o, is kept fixed and noise is added, the system will drift randomly along the line of equilibria given by (8).

7.2 Analysis of the non-proportional model

For the non-proportional model the differential equations are

$$\frac{dh_1}{dt} = \alpha \frac{h_1(t)}{h_1(t)+h_2(t)} h_i(t) - \beta h_1(t)^\eta - \gamma h_1(t) \tag{9}$$

$$\frac{dh_m}{dt} = \beta h_1(t)^\eta + \beta h_2(t)^\eta - \delta h_m(t) \tag{10}$$

$$\frac{dh_2}{dt} = \alpha \frac{h_2(t)}{h_1(t)+h_2(t)} h_i(t) - \beta h_2(t)^\eta - \gamma h_2(t) \tag{11}$$

$$\frac{dh_i}{dt} = \gamma h_1(t) + \gamma h_2(t) + \delta h_m(t) - \alpha h_i(t). \tag{12}$$

where $0 < \eta < 1$. As before, the total amount of Bem1p-GFP-Snc2p is conserved so (1) holds. To investigate equilibria, we set the right hand sides to zero finding:

$$\beta \bar{h}_1^\eta + \beta \bar{h}_2^\eta = \delta \bar{h}_m \tag{13}$$

$$\delta \bar{h}_m + \gamma(\bar{h}_1 + \bar{h}_2) = \alpha \bar{h}_i \tag{14}$$

$$\left(1+\frac{\gamma}{\alpha}\right)(\bar{h}_1 + \bar{h}_2) + \beta\left(\frac{1}{\delta}+\frac{1}{\alpha}\right)(\bar{h}_1^\eta + \bar{h}_2^\eta) = H_o \tag{15}$$

Let h_o and h_{oo} denote the two unique positive numbers such that:

$$\left(1+\frac{\gamma}{\alpha}\right)(2h_o) + \beta\left(\frac{1}{\delta}+\frac{1}{\alpha}\right)(2h_o^\eta) = H_o \tag{16}$$

$$\left(1+\frac{\gamma}{\alpha}\right)(2h_{oo}) + \beta\left(\frac{1}{\delta}+\frac{1}{\alpha}\right)(2h_{oo}^\eta) = H_{oo} \tag{17}$$

Then, (h_o, h_o, $\frac{\beta}{\delta}2h_o^\eta$, $\frac{\gamma}{\alpha}2h_o + \frac{\beta}{\alpha}2h_o^\eta$) is an equilibrium with equal amounts of Bem1p-GFPSnc2p in each spot on the membrane. A short argument, which uses the

assumption that $\eta \neq 1$, shows that this is the only equilibrium for which both $\bar{h}_1$ and $\bar{h}_2$ are strictly positive. However, (h_{oo}, 0, $\frac{\beta}{\delta}h_{oo}^{\eta}$, $\frac{\gamma}{\alpha}h_{oo}+\frac{\beta}{\alpha}h_{oo}^{\eta}$) and (0, h_{oo}, $\frac{\beta}{\delta}h_{oo}^{\eta}$, $\frac{\gamma}{\alpha}h_{oo}+\frac{\beta}{\alpha}h_{oo}^{\eta}$) are equilibria with nothing in spot two and nothing in spot one, respectively.

We consider the dynamics of $h_1(t)$ and $h_2(t)$ first. Rearranging equations (9) and (11) and then dividing (9) by (11) gives

$$\frac{h_1' + \beta h_1(t)^{\eta} + \gamma h_1(t)}{h_2' + \beta h_2(t)^{\eta} + \gamma h_2(t)} = \frac{h_1(t)}{h_2(t)},$$

or,

$$h_2(t)h_1'(t) - h_1(t)h_2'(t) = \beta(h_2(t)^{\eta} h_1(t) - h_1(t)^{\eta} h_2(t)) \tag{18}$$

Differentiating $\frac{h_1(t)}{h_2(t)}$ as above and substituting (18) and rearranging, we find that the ratio $\frac{h_1(t)}{h_2(t)}$ satisfies the differential equation:

$$\left(\frac{h_1}{h_2}\right)' = \beta h_2^{\eta-1}\left(\left(\frac{h_1}{h_2}\right) - \left(\frac{h_1}{h_2}\right)^{\eta}\right). \tag{19}$$

Therefore, if $\frac{h_1(0)}{h_2(0)} = 1$ we conclude $\frac{h_1(t)}{h_2(t)} = 1$ for all $t \geq 0$, i.e the amount in spot one always equals the amount in spot two. On the other hand, if $\frac{h_1(0)}{h_2(0)} < 1$, then the right hand side of (19) is strictly negative at $t = 0$ so the ratio will decrease. Since $\eta < 1$ and h_2 must be bounded above by H_o, the coefficient $h_2^{\eta-1}$ can not become arbitrarily small. It follows that $h_1(t) \to 0$ at some finite time. Similarly, if $\frac{h_1(0)}{h_2(0)} > 1$, then the right hand side of (19) is positive so the ratio will increase. By considering the differential equation for $\frac{h_2(t)}{h_1(t)}$, one sees, by the argument used above, that $h_2(t) \to 0$ at a finite time.

These calculations show that if the two spots start with equal amounts of Bem1p-GFP-Snc2p then the two spots will always have equal amounts. However, if one spot starts with a larger amount than the other spot, the smaller spot will vanish in finite time. A complete analytical proof of the behavior of all orbits of the system (9) - (12) is beyond the scope of this short supplement. Machine computations show that for all positive choices of the constants $\alpha, \beta, \gamma, \delta$, any $0 < \eta < 1$, and any initial condition whose components are strictly positive, the behavior is as follows:

(a) If $h_1(0) = h_2(0) > 0$, then the orbit approaches $(h_o, h_o, \frac{\beta}{\delta}2h_o^{\eta}, \frac{\gamma}{\alpha}2h_o + \frac{\beta}{\alpha}2h_o^{\eta})$

(b) If $h_1(0) > h_2(0) > 0$, then the orbit approaches $(h_{oo}, 0, \frac{\beta}{\delta}h_{oo}^{\eta}, \frac{\gamma}{\alpha}h_{oo} + \frac{\beta}{\alpha}h_{oo}^{\eta})$

(c) If $0 < h_1(0) < h_2(0)$, then the orbit approaches $(0, h_{oo}, \frac{\beta}{\delta}h_{oo}^{\eta}, \frac{\gamma}{\alpha}h_{oo} + \frac{\beta}{\alpha}h_{oo}^{\eta})$

7.3 Parameter estimation

We used five experimental observations to derive rough estimates for the model parameters, assuming that single-focus polarized cells reflect the final model steady state.

First, Western blotting (Fig 4.2C) suggests that Bem1p-GFP-Snc2p is about half as abundant as Bem1p, which is estimated to be present at about 6000 copies/cell (Ghaemmaghami et al., 2003). Thus, we estimate $H_o = 3000$.

Second, about 30% of the total v-SNARE pools are estimated to be internal (Galan et al., 2001). With similar estimates for Bem1p-GFP-Snc2p, we get $h_i = 900$, $h_1 + h_m = 2100$.

Third, examination of confocal slices suggests that Bem1p-GFP-Snc2p is about 5

times more concentrated in the focus than it is in the general cell membrane (Fig. 7.1). The area of a focus with radius $0.5\mu m$ is 1% of the total surface area of a yeast cell with radius $2.5\mu m$. Thus, $h_1 = 100$ and $h_m = 2000$ at steady state.

Fourth, we can estimate the rate of Bem1p-GFP-Snc2p delivery to a focus from internal pools from the 35 s half-time of fluorescence recovery in the FRAP data of Fig 4.1D, as $0.5h_1 \times 35 = \alpha h_i$. Thus, we get $\alpha = 0.0016s^{-1}$. Finally, endocytosis is much more active in the focus than in the general membrane, as revealed by the concentration of actin patches at the focus. The ratio of endocytosis within versus outside the focus was estimated at 40:1 (Marco et al., 2007), so we set $\gamma = 40\delta$.

Substituting the steady-state values into (13) and (14), and assuming $\eta = 0.5$, we get:

$\alpha = 0.0016$

$\beta = 0.048$

$\gamma = 0.0095$

$\delta = 0.00024$

Similar parameter estimates were generated for other values of η. Machine computation of the evolution of h_1, h_2, h_m, and h_i from given starting conditions was performed using MatLab. We note that the model is only designed for the situation when the concentration of Bem1p-GFP-Snc2p in the two foci is higher than that in the general

membrane: it is intended to model competition between established foci but not initial establishment of the foci.

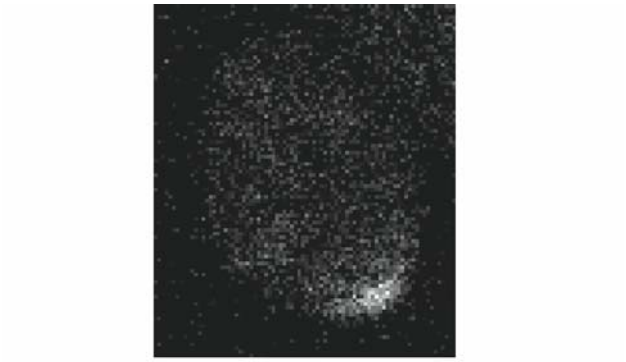

Figure 7.1 Estimating the amount of protein in the polarized spot

A sample image used to estimate the relative amount of Bem1p-GFP-Snc2p that localizes to the polarization site. Live *BEM1-GFP-SNC2* diploid cells mounted on a 2% agarose slab were imaged using a SP5 confocal microscope (Leica Microsystems, Bannockburn, IL) with a 63x/1.20 water Plan Apochromat objective. The amount of protein at the polarized spot relative to the non-polarized membrane in the cell was estimated from the relative signal intensities of confocal images through the middle cells.

References

Adamo, J.E., J.J. Moskow, A.S. Gladfelter, D. Viterbo, D.J. Lew, and P.J. Brennwald. 2001. Yeast Cdc42 functions at a late step in exocytosis, specifically during polarized growth of the emerging bud. *J Cell Biol*. 155:581-92.

Adams, A.E.M., D. Botstein, and D.G. Drubin. 1991. Requirement of yeast fimbrin for actin organization and morphogenesis *in vivo*. *Nature*. 354:404-408.

Adams, A.E.M., D.I. Johnson, R.M. Longnecker, B.F. Sloat, and J.R. Pringle. 1990. *CDC42* and *CDC43*, two additional genes involved in budding and the establishment of cell polarity in the yeast *Saccharomyces cerevisiae*. *J. Cell Biol.* 111:131-142.

Adams, A.E.M., and J.R. Pringle. 1984. Relationship of actin and tubulin distribution to bud growth in wild-type and morphogenetic-mutant *Saccharomyces cerevisiae*. *J. Cell Biol.* 98:934-945.

Alberts, A.S. 2001. Identification of a carboxyl-terminal diaphanous-related formin homology protein autoregulatory domain. *J Biol Chem*. 276:2824-30.

Altschuler, S.J., S.B. Angenent, Y. Wang, and L.F. Wu. 2008. On the spontaneous emergence of cell polarity. *Nature*. 454:886-9.

Amatruda, J.F., J.F. Cannon, K. Tatchell, C. Hug, and J.A. Cooper. 1990. Disruption of the actin cytoskeleton in yeast capping protein mutants. *Nature*. 344:352-354.

Amberg, D.C., E. Basart, and D. Botstein. 1995. Defining protein interactions with yeast actin in vivo. *Nat Struct Biol*. 2:28-35.

Assemat, E., E. Bazellieres, E. Pallesi-Pocachard, A. Le Bivic, and D. Massey-Harroche. 2008. Polarity complex proteins. *Biochim Biophys Acta*. 1778:614-30.

Ayscough, K.R., J. Stryker, N. Pokala, M. Sanders, P. Crews, and D.G. Drubin. 1997. High rates of actin filament turnover in budding yeast and roles for actin in establishment and maintenance of cell polarity revealed using the actin inhibitor latrunculin-A. *J. Cell Biol.* 137:399-416.

Barral, Y., V. Mermall, M.S. Mooseker, and M. Snyder. 2000. Compartmentalization of the cell cortex by septins is required for maintenance of cell polarity in yeast. *Mol. Cell*. 5:841-851.

Baudin, A., O. Ozier-Kalogeropoulos, A. Denouel, F. Lacroute, and C. Cullin. 1993. A simple and efficient method for direct gene deletion in *Saccharomyces cerevisiae*. *Nucleic Acids Res.* 21:3329-3330.

Bender, A. 1993. Genetic evidence for the roles of the bud-site-selection genes BUD5 and BUD2 in control of the Rsr1p (Bud1p) GTPase in yeast. *Proc Natl Acad Sci U S A*. 90:9926-9.

Bender, A., and J.R. Pringle. 1989. Multicopy suppression of the cdc24 budding defect in yeast by CDC42 and three newly identified genes including the ras-related gene RSR1. *Proc. Natl. Acad. Sci. U.S.A.* 86:9976-9980.

Bender, A., and J.R. Pringle. 1991. Use of a screen for synthetic lethal and multicopy suppressee mutants to identify two new genes involved in morphogenesis in *Saccharomyces cerevisiae*. *Mol. Cell. Biol.* 11:1295-1305.

Bender, L., H. Shuen Lo, H. Lee, V. Kokojan, J. Peterson, and A. Bender. 1996. Associations among PH and SH3 domain-containing proteins and Rho-type GTPases in yeast. *J. Cell Biol.* 133:879-894.

Boldogh, I.R., S.L. Ramcharan, H.C. Yang, and L.A. Pon. 2004. A type V myosin (Myo2p) and a Rab-like G-protein (Ypt11p) are required for retention of newly inherited mitochondria in yeast cells during cell division. *Mol Biol Cell*. 15:3994-4002.

Booher, R.N., R.J. Deshaies, and M.W. Kirschner. 1993. Properties of Saccharomyces cerevisiae wee1 and its differential regulation of p34CDC28 in response to G1 and G2 cyclins. *EMBO J.* 12:3417-3426.

Bose, I., J.E. Irazoqui, J.J. Moskow, E.S. Bardes, T.R. Zyla, and D.J. Lew. 2001. Assembly of scaffold-mediated complexes containing Cdc42p, the exchange factor Cdc24p, and the effector Cla4p required for cell cycle-regulated phosphorylation of Cdc24p. *J Biol Chem*. 276:7176-86.

Branzei, D., and M. Foiani. 2006. The Rad53 signal transduction pathway: Replication fork stabilization, DNA repair, and adaptation. *Exp Cell Res*. 312:2654-9.

Brown, J.L., M. Jaquenoud, M.P. Gulli, J. Chant, and M. Peter. 1997. Novel Cdc42-binding proteins Gic1 and Gic2 control cell polarity in yeast. *Genes Dev*. 11:2972-82.

Buttery, S.M., S. Yoshida, and D. Pellman. 2007. Yeast formins Bni1 and Bnr1 utilize different modes of cortical interaction during the assembly of actin cables. *Mol Biol Cell*. 18:1826-38.

Butty, A.C., N. Perrinjaquet, A. Petit, M. Jaquenoud, J.E. Segall, K. Hofmann, C. Zwahlen, and M. Peter. 2002. A positive feedback loop stabilizes the guanine-nucleotide exchange factor Cdc24 at sites of polarization. *Embo J*. 21:1565-1576.

Butty, A.C., P.M. Pryciak, L.S. Huang, I. Herskowitz, and M. Peter. 1998. The role of Far1p in linking the heterotrimeric G protein to polarity establishment proteins during yeast mating. *Science*. 282:1511-6.

Cabib, E., and B. Bowers. 1975. Timing and function of chitin synthesis in yeast. *J Bacteriol*. 124:1586-93.

Castellano, F., P. Montcourrier, J.C. Guillemot, E. Gouin, L. Machesky, P. Cossart, and P. Chavrier. 1999. Inducible recruitment of Cdc42 or WASP to a cell-surface receptor triggers actin polymerization and filopodium formation. *Curr Biol*. 9:351-60.

Caviston, J.P., S.E. Tcheperegine, and E. Bi. 2002. Singularity in budding: a role for the evolutionarily conserved small GTPase Cdc42p. *Proc Natl Acad Sci U S A*. 99:12185-90.

Chant, J. 1999. Cell polarity in yeast. *Annu. Rev. Cell Dev. Biol*. 15:365-391.

Chant, J., K. Corrado, J.R. Pringle, and I. Herskowitz. 1991. Yeast BUD5, encoding a putative GDP-GTP exchange factor, is necessary for bud site selection and interacts with bud formation gene BEM1. *Cell*. 65:1213-1224.

Chant, J., and I. Herskowitz. 1991. Genetic control of bud site selection in yeast by a set of gene products that constitute a morphogenetic pathway. *Cell*. 65:1203-1212.

Chant, J., and J.R. Pringle. 1995. Patterns of bud-site selection in the yeast *Saccharomyces cerevisiae*. *J. Cell Biol.* 129:751-765.

Chen, G.C., Y.J. Kim, and C.S. Chan. 1997. The Cdc42 GTPase-associated proteins Gic1 and Gic2 are required for polarized cell growth in Saccharomyces cerevisiae. *Genes Dev*. 11:2958-71.

Chen, G.C., L. Zheng, and C.S. Chan. 1996. The LIM domain-containing Dbm1 GTPase-activating protein is required for normal cellular morphogenesis in Saccharomyces cerevisiae. *Mol Cell Biol*. 16:1376-90.

Chenevert, J., K. Corrado, A. Bender, J. Pringle, and I. Herskowitz. 1992. A yeast gene (*BEM1*) necessary for cell polarization whose product contains two SH3 domains. *Nature*. 356:77-79.

Chowdhury, S., K.W. Smith, and M.C. Gustin. 1992. Osmotic stress and the yeast cytoskeleton: phenotype-specific suppression of an actin mutation. *J. Cell Biol.* 118:561-571.

Cvrckova, F., C. De Virgilio, E. Manser, J.R. Pringle, and K. Nasmyth. 1995. Ste20-like protein kinases are required for normal localization of cell growth and for cytokinesis in budding yeast. *Genes Dev.* 9:1817-1830.

da Silva, J.S., and C.G. Dotti. 2002. Breaking the neuronal sphere: regulation of the actin cytoskeleton in neuritogenesis. *Nat Rev Neurosci*. 3:694-704.

Delley, P.A., and M.N. Hall. 1999. Cell wall stress depolarizes cell growth via hyperactivation of RHO1. *J. Cell Biol.* 147:163-174.

Devreotes, P.N., and S.H. Zigmond. 1988. Chemotaxis in eukaryotic cells: a focus on leukocytes and Dictyostelium. *Annu Rev Cell Biol*. 4:649-86.

Dobbelaere, J., M.S. Gentry, R.L. Hallberg, and Y. Barral. 2003. Phosphorylation-Dependent Regulation of Septin Dynamics during the Cell Cycle. *Dev Cell*. 4:345-57.

Dohlman, H.G., and J.W. Thorner. 2001. Regulation of G protein-initiated signal transduction in yeast: paradigms and principles. *Annu Rev Biochem*. 70:703-54.

Doyle, T., and D. Botstein. 1996. Movement of yeast cortical actin cytoskeleton visualized in vivo. *Proc Natl Acad Sci U S A*. 93:3886-91.

Drees, B., C. Brown, B.G. Barrell, and A. Bretscher. 1995. Tropomyosin is essential in yeast, yet the TPM1 and TPM2 products perform distinct functions. *J Cell Biol*. 128:383-92.

Drubin, D.G., J. Mulholland, Z. Zhu, and D. Botstein. 1990. Homology of yeast actin-binding protein to signal transduction proteins and myosin-I. 343:288-290.

Elledge, S.J., Z. Zhou, J.B. Allen, and T.A. Navas. 1993. DNA damage and cell cycle regulation of ribonucleotide reductase. [Review]. *Bioessays*. 15:333-9.

Etienne-Manneville, S. 2004. Cdc42 - the centre of polarity. *J Cell Sci*. 117:1291-300.

Etienne-Manneville, S., and A. Hall. 2003. Cell polarity: Par6, aPKC and cytoskeletal crosstalk. *Curr Opin Cell Biol*. 15:67-72.

Evangelista, M., K. Blundell, M.S. Longtine, C.J. Chow, N. Adames, J.R. Pringle, M. Peter, and C. Boone. 1997. Bni1p, a yeast formin linking Cdc42p and the actin cytoskeleton during polarized morphogenesis. *Science*. 276:118-122.

Evangelista, M., D. Pruyne, D.C. Amberg, C. Boone, and A. Bretscher. 2002. Formins direct Arp2/3-independent actin filament assembly to polarize cell growth in yeast. *Nat Cell Biol*. 4:260-9.

Ford, S.K., and J.R. Pringle. 1991. Cellular morphogenesis in the *Saccharomyces cerevisiae* cell cycle: localization of the *CDC11* gene product and the timing of events at the budding site. *Dev. Genet.* 12:281-292.

Friant, S., B. Zanolari, and H. Riezman. 2000. Increased protein kinase or decreased PP2A activity bypasses sphingoid base requirement in endocytosis. *Embo J*. 19:2834-44.

Galan, J.M., A. Wiederkehr, J.H. Seol, R. Haguenauer-Tsapis, R.J. Deshaies, H. Riezman, and M. Peter. 2001. Skp1p and the F-box protein Rcy1p form a non-SCF complex involved in recycling of the SNARE Snc1p in yeast. *Mol Cell Biol*. 21:3105-17.

Garrard, S.M., C.T. Capaldo, L. Gao, M.K. Rosen, I.G. Macara, and D.R. Tomchick. 2003. Structure of Cdc42 in a complex with the GTPase-binding domain of the cell polarity protein, Par6. *Embo J*. 22:1125-33.

Ghaemmaghami, S., W.K. Huh, K. Bower, R.W. Howson, A. Belle, N. Dephoure, E.K. O'Shea, and J.S. Weissman. 2003. Global analysis of protein expression in yeast. *Nature*. 425:737-41.

Gierer, A., and H. Meinhardt. 1972. A theory of biological pattern formation. *Kybernetik*. 12:30-9.

Gladfelter, A.S., J.R. Pringle, and D.J. Lew. 2001. The septin cortex at the yeast mother-bud neck. *Curr. Opin. Microbiol.* 4:681-689.

Goehring, A.S., D.A. Mitchell, A.H. Tong, M.E. Keniry, C. Boone, and G.F. Sprague, Jr. 2003. Synthetic Lethal Analysis Implicates Ste20p, a p21-activated Protein Kinase, in Polarisome Activation. *Mol Biol Cell*. 14:1501-16.

Goryachev, A.B., and A.V. Pokhilko. 2008. Dynamics of Cdc42 network embodies a Turing-type mechanism of yeast cell polarity. *FEBS Lett*. 582:1437-1443.

Gotta, M., M.C. Abraham, and J. Ahringer. 2001. CDC-42 controls early cell polarity and spindle orientation in C. elegans. *Curr Biol*. 11:482-8.

Goud, B., A. Salminen, N.C. Walworth, and P.J. Novick. 1988. A GTP-binding protein required for secretion rapidly associates with secretory vesicles and the plasma membrane in yeast. *Cell*. 53:753-68.

Grill, S.W., P. Gonczy, E.H. Stelzer, and A.A. Hyman. 2001. Polarity controls forces governing asymmetric spindle positioning in the Caenorhabditis elegans embryo. *Nature*. 409:630-3.

Grote, E., G. Vlacich, M. Pypaert, and P.J. Novick. 2000. A snc1 endocytosis mutant: phenotypic analysis and suppression by overproduction of dihydrosphingosine phosphate lyase. *Mol Biol Cell*. 11:4051-65.

Guthrie, C., and G.R. Fink. 1991. Guide to yeast genetics and molecular biology. *In* Methods Enzymol. Vol. 194. 1-933.

Haase, S.B., and S.I. Reed. 2002. Improved flow cytometric analysis of the budding yeast cell cycle. *Cell Cycle*. 1:132-6.

Halme, A., M. Michelitch, E.L. Mitchell, and J. Chant. 1996. Bud10p directs axial cell polarization in budding yeast and resembles a transmembrane receptor. *Curr. Biol*. 6:570-579.

Harkins, H.A., N. Page, L.R. Schenkman, C. De Virgilio, S. Shaw, H. Bussey, and J.R. Pringle. 2001. Bud8p and Bud9p, proteins that may mark the sites for bipolar budding in yeast. *Mol Biol Cell*. 12:2497-518.

Harris, S.D. 2008. Branching of fungal hyphae: regulation, mechanisms and comparison with other branching systems. *Mycologia*. 100:823-32.

Henry, K.R., K. D'Hondt, J. Chang, T. Newpher, K. Huang, R.T. Hudson, H. Riezman, and S.K. Lemmon. 2002. Scd5p and clathrin function are important for cortical actin organization, endocytosis, and localization of sla2p in yeast. *Mol Biol Cell*. 13:2607-25.

Herskowitz, I. 1988. Life cycle of the budding yeast *Saccharomyces cerevisiae. Microbiol. Rev.* 52:536-553.

Ho, J., and A. Bretscher. 2001. Ras regulates the polarity of the yeast actin cytoskeleton through the stress response pathway. *Mol Biol Cell*. 12:1541-55.

Holly, S.P., and K.J. Blumer. 1999. PAK-Family Kinases Regulate Cell and Actin Polarization throughout the Cell Cycle of Saccharomyces cerevisiae. *J Cell Biol*. 147:845-856.

Hung, T.J., and K.J. Kemphues. 1999. PAR-6 is a conserved PDZ domain-containing protein that colocalizes with PAR-3 in Caenorhabditis elegans embryos. *Development*. 126:127-35.

Iglesias, P.A., and P.N. Devreotes. 2008. Navigating through models of chemotaxis. *Curr Opin Cell Biol*. 20:35-40.

Imamura, H., K. Tanaka, T. Hihara, M. Umikawa, T. Kamei, K. Takahashi, T. Sasaki, and Y. Takai. 1997. Bni1p and Bnr1p: downstream targets of the Rho family small G-proteins which interact with profilin and regulate actin cytoskeleton in Saccharomyces cerevisiae. *Embo J*. 16:2745-55.

Irazoqui, J.E., A.S. Gladfelter, and D.J. Lew. 2003. Scaffold-mediated symmetry breaking by Cdc42p. *Nat Cell Biol*. 5:1062-70.

Irazoqui, J.E., A.S. Howell, C.L. Theesfeld, and D.J. Lew. 2005. Opposing roles for actin in Cdc42p polarization. *Mol Biol Cell*. 16:1296-304.

Irazoqui, J.E., and D.J. Lew. 2004. Polarity establishment in yeast. *J Cell Sci*. 117:2169-71.

Ito, T., Y. Matsui, T. Ago, K. Ota, and H. Sumimoto. 2001. Novel modular domain PB1 recognizes PC motif to mediate functional protein-protein interactions. *Embo J*. 20:3938-46.

Iwase, M., J. Luo, S. Nagaraj, M. Longtine, H.B. Kim, B.K. Haarer, C. Caruso, Z. Tong, J.R. Pringle, and E. Bi. 2006. Role of a Cdc42p effector pathway in recruitment of the yeast septins to the presumptive bud site. *Mol Biol Cell*. 17:1110-25.

Jaffe, L.A. 1976. Fast block to polyspermy in sea urchin eggs is electrically mediated. *Nature*. 261:68-71.

Jaquenoud, M., and M. Peter. 2000. Gic2p may link activated Cdc42p to components involved in actin polarization, including Bni1p and Bud6p (Aip3p). *Mol Cell Biol*. 20:6244-58.

Jiang, Y.W., and C.M. Kang. 2003. Induction of S. cerevisiae filamentous differentiation by slowed DNA synthesis involves Mec1, Rad53 and Swe1 checkpoint proteins. *Mol Biol Cell*. 14:5116-24.

Kaksonen, M., Y. Sun, and D.G. Drubin. 2003. A pathway for association of receptors, adaptors, and actin during endocytic internalization. *Cell*. 115:475-87.

Kang, C.M., and Y.W. Jiang. 2005. Genome-wide survey of non-essential genes required for slowed DNA synthesis-induced filamentous growth in yeast. *Yeast*. 22:79-90.

Kang, P.J., E. Angerman, K. Nakashima, J.R. Pringle, and H.O. Park. 2004a. Interactions among Rax1p, Rax2p, Bud8p, and Bud9p in marking cortical sites for bipolar bud-site selection in yeast. *Mol Biol Cell*. 15:5145-57.

Kang, P.J., B. Lee, and H.O. Park. 2004b. Specific residues of the GDP/GTP exchange factor Bud5p are involved in establishment of the cell type-specific budding pattern in yeast. *J Biol Chem*. 279:27980-5.

Kang, P.J., A. Sanson, B. Lee, and H.O. Park. 2001. A GDP/GTP exchange factor involved in linking a spatial landmark to cell polarity. *Science*. 292:1376-1378.

Karpova, T.S., S.L. Reck-Peterson, N.B. Elkind, M.S. Mooseker, P.J. Novick, and J.A. Cooper. 2000. Role of actin and Myo2p in polarized secretion and growth of Saccharomyces cerevisiae. *Mol Biol Cell*. 11:1727-37.

Keaton, M.A., L. Szkotnicki, A.R. Marquitz, J. Harrison, T.R. Zyla, and D.J. Lew. 2008. Nucleocytoplasmic trafficking of G2/M regulators in yeast. *Mol Biol Cell*. 19:4006-18.

Kemphues, K. 2000. PARsing embryonic polarity. *Cell*. 101:345-8.

Kim, H.B., B.K. Haarer, and J.R. Pringle. 1991. Cellular morphogenesis in the *Saccharomyces cerevisiae* cell cycle: localization of the *CDC3* gene product and the timing of events at the budding site. *J. Cell Biol.* 112:535-544.

Klis, F.M., A. Boorsma, and P.W. De Groot. 2006. Cell wall construction in Saccharomyces cerevisiae. *Yeast*. 23:185-202.

Knaus, M., M.P. Pelli-Gulli, F. van Drogen, S. Springer, M. Jaquenoud, and M. Peter. 2007. Phosphorylation of Bem2p and Bem3p may contribute to local activation of Cdc42p at bud emergence. *EMBO J*. 26:4501-13.

Koch, G., K. Tanaka, T. Masuda, W. Yamochi, H. Nonaka, and Y. Takai. 1997. Association of the Rho family small GTP-binding proteins with Rho GDP dissociation inhibitor (Rho GDI) in Saccharomyces cerevisiae. *Oncogene*. 15:417-22.

Kozubowski, L., K. Saito, J.M. Johnson, A.S. Howell, T.R. Zyla, and D.J. Lew. 2008. Symmetry-Breaking Polarization Driven by a Cdc42p GEF-PAK Complex. *Curr Biol*. 18:1719-26.

Kubota, S., I. Takeo, K. Kume, M. Kanai, A. Shitamukai, M. Mizunuma, T. Miyakawa, H. Shimoi, H. Iefuji, and D. Hirata. 2004. Effect of ethanol on cell growth of budding yeast: genes that are important for cell growth in the presence of ethanol. *Biosci Biotechnol Biochem*. 68:968-72.

Leberer, E., D. Dignard, D. Harcus, D.Y. Thomas, and M. Whiteway. 1992. The protein kinase homologue Ste20p is required to link the yeast pheromone response G-protein bg subunits to downstream signaling components. *EMBO J.* 11:4815-4824.

Leberer, E., C. Wu, T. Leeuw, A. Fourest-Lieuvin, J.E. Segall, and D.Y. Thomas. 1997. Functional characterization of the Cdc42p binding domain of yeast Ste20p protein kinase. *EMBO J.* 16:83-97.

Leeuw, T., A. Fourest-Lieuvin, C. Wu, J. Chenevert, K. Clark, M. Whiteway, D.Y. Thomas, and E. Leberer. 1995. Pheromone response in yeast: association of Bem1p with proteins of the MAP kinase cascade and actin. *Science*. 270:1210-1213.

Lehman, K., G. Rossi, J.E. Adamo, and P. Brennwald. 1999. Yeast homologues of tomosyn and lethal giant larvae function in exocytosis and are associated with the plasma membrane SNARE, Sec9. *J Cell Biol*. 146:125-40.

Levchenko, A., and P.A. Iglesias. 2002. Models of eukaryotic gradient sensing: application to chemotaxis of amoebae and neutrophils. *Biophys J*. 82:50-63.

Levin, D.E. 2005. Cell wall integrity signaling in Saccharomyces cerevisiae. *Microbiol Mol Biol Rev*. 69:262-91.

Lew, D.J., and S.I. Reed. 1993. Morphogenesis in the yeast cell cycle: regulation by Cdc28 and cyclins. *J. Cell Biol.* 120:1305-1320.

Lew, D.J., and S.I. Reed. 1995. A cell cycle checkpoint monitors cell morphogenesis in budding yeast. *J. Cell Biol.* 129:739-749.

Lewis, M.J., B.J. Nichols, C. Prescianotto-Baschong, H. Riezman, and H.R. Pelham. 2000. Specific retrieval of the exocytic SNARE Snc1p from early yeast endosomes. *Mol Biol Cell*. 11:23-38.

Li, F., and H.N. Higgs. 2003. The mouse Formin mDia1 is a potent actin nucleation factor regulated by autoinhibition. *Curr Biol*. 13:1335-40.

Lillie, S.H., and S.S. Brown. 1994. Immunofluorescence localization of the unconventional myosin, Myo2p, and the putative kinesin-related protein, Smy1p, to the same regions of polarized growth in *Saccharomyces cerevisiae*. *J. Cell Biol.* 125:825-842.

Longtine, M.S., A. McKenzie III, D.J. DeMarini, N.G. Shah, A. Wach, A. Brachat, P. Philippsen, and J.R. Pringle. 1998. Additional modules for versatile and economical PCR-based gene deletion and modification in *Saccharomyces cerevisiae*. *Yeast*. 14:953-961.

Madden, K., and M. Snyder. 1992. Specification of sites for polarized growth in Saccharomyces cerevisiae and the influence of external factors on site selection. *Mol Biol Cell*. 3:1025-35.

Marco, E., R. Wedlich-Soldner, R. Li, S.J. Altschuler, and L.F. Wu. 2007. Endocytosis optimizes the dynamic localization of membrane proteins that regulate cortical polarity. *Cell*. 129:411-22.

Marquitz, A.R., J.C. Harrison, I. Bose, T.R. Zyla, J.N. McMillan, and D.J. Lew. 2002. The Rho-GAP Bem2p plays a GAP-independent role in the morphogenesis checkpoint. *Embo J*. 21:4012-25.

Masuda, T., K. Tanaka, H. Nonaka, W. Yamochi, A. Maeda, and Y. Takai. 1994. Molecular cloning and characterization of yeast rho GDP dissociation inhibitor. *J Biol Chem*. 269:19713-8.

Matsui, Y., R. Matsui, R. Akada, and A. Toh-e. 1996. Yeast src homology region 3 domain-binding proteins involved in bud formation. *J Cell Biol*. 133:865-78.

McMillan, J.N., R.A.L. Sia, E.S.G. Bardes, and D.J. Lew. 1999. Phosphorylation-independent inhibition of Cdc28p by the tyrosine kinase Swe1p in the morphogenesis checkpoint. *Mol. Cell. Biol.* 19:5981-5990.

McMillan, J.N., R.A.L. Sia, and D.J. Lew. 1998. A morphogenesis checkpoint monitors the actin cytoskeleton in yeast. *J. Cell Biol.* 142:1487-1499.

Moseley, J.B., and B.L. Goode. 2006. The yeast actin cytoskeleton: from cellular function to biochemical mechanism. *Microbiol Mol Biol Rev*. 70:605-45.

Moseley, J.B., I. Sagot, A.L. Manning, Y. Xu, M.J. Eck, D. Pellman, and B.L. Goode. 2004. A Conserved Mechanism for Bni1- and mDia1-induced Actin Assembly and Dual Regulation of Bni1 by Bud6 and Profilin. *Mol Biol Cell*. 15:896-907.

Munemitsu, S., M.A. Innis, R. Clark, F. McCormick, A. Ullrich, and P. Polakis. 1990. Molecular cloning and expression of a G25K cDNA, the human homolog of the yeast cell cycle gene CDC42. *Mol Cell Biol*. 10:5977-82.

Nern, A., and R.A. Arkowitz. 1999. A Cdc24p-Far1p-Gbetagamma protein complex required for yeast orientation during mating. *J Cell Biol*. 144:1187-202.

Onsum, M.D., and C.V. Rao. 2009. Calling heads from tails: the role of mathematical modeling in understanding cell polarization. *Curr Opin Cell Biol*. 21:74-81.

Ozaki-Kuroda, K., Y. Yamamoto, H. Nohara, M. Kinoshita, T. Fujiwara, K. Irie, and Y. Takai. 2001. Dynamic localization and function of Bni1p at the sites of directed growth in Saccharomyces cerevisiae. *Mol Cell Biol*. 21:827-39.

Ozbudak, E.M., A. Becskei, and A. van Oudenaarden. 2005. A System of Counteracting Feedback Loops Regulates Cdc42p Activity during Spontaneous Cell Polarization. *Dev Cell*. 9:565-71.

Parent, C.A., and P.N. Devreotes. 1999. A cell's sense of direction. *Science*. 284:765-70.

Park, H.O., and E. Bi. 2007. Central roles of small GTPases in the development of cell polarity in yeast and beyond. *Microbiol Mol Biol Rev*. 71:48-96.

Park, H.O., E. Bi, J.R. Pringle, and I. Herskowitz. 1997. Two active states of the Ras-related Bud1/Rsr1 protein bind to different effectors to determine yeast cell polarity. *Proc Natl Acad Sci U S A*. 94:4463-8.

Park, H.O., J. Chant, and I. Herskowitz. 1993. BUD2 encodes a GTPase-activating protein for Bud1/Rsr1 necessary for proper bud-site selection in yeast. *Nature*. 365:269-74.

Peter, M., A.M. Neiman, H.-O. Park, M. van Lohuizen, and I. Herskowitz. 1996. Functional analysis of the interaction between the small GTP binding protein Cdc42 and the Ste20 protein kinase in yeast. *EMBO J.* 15:7046-7059.

Peterson, J., Y. Zheng, L. Bender, A. Myers, R. Cerione, and A. Bender. 1994. Interactions between the bud emergence proteins Bem1p and Bem2p and Rho- type GTPases in yeast. *J Cell Biol*. 127:1395-406.

Preuss, D., J. Mulholland, A. Franzusoff, N. Segev, and D. Botstein. 1992. Characterization of the Saccharomyces Golgi complex through the cell cycle by immunoelectron microscopy. *Mol Biol Cell*. 3:789-803.

Pringle, J.R. 1991. Staining of bud scars and other cell wall chitin with Calcofluor. *Methods Enzymol.* 194:732-735.

Pringle, J.R., E. Bi, H.A. Harkins, J.E. Zahner, C. De Virgilio, J. Chant, K. Corrado, and H. Fares. 1995. Establishment of cell polarity in yeast. *Cold Spring Harbor Symp. Quant. Biol.* 60:729-744.

Pruyne, D., and A. Bretscher. 2000a. Polarization of cell growth in yeast. *J. Cell Sci.* 113:571-585.

Pruyne, D., and A. Bretscher. 2000b. Polarization of cell growth in yeast. I. Establishment and maintenance of polarity states. *J Cell Sci*. 113 (Pt 3):365-75.

Pruyne, D., L. Gao, E. Bi, and A. Bretscher. 2004. Stable and dynamic axes of polarity use distinct formin isoforms in budding yeast. *Mol Biol Cell*. 15:4971-89.

Pruyne, D.W., D.H. Schott, and A. Bretscher. 1998. Tropomyosin-containing actin cables direct the Myo2p-dependent polarized delivery of secretory vesicles in budding yeast [In Process Citation]. *J Cell Biol*. 143:1931-45.

Raths, S., J. Rohrer, F. Crausaz, and H. Riezman. 1993. end3 and end4: two mutants defective in receptor-mediated and fluid-phase endocytosis in Saccharomyces cerevisiae. *J Cell Biol*. 120:55-65.

Redding, K., C. Holcomb, and R.S. Fuller. 1991. Immunolocalization of Kex2 protease identifies a putative late Golgi compartment in the yeast Saccharomyces cerevisiae. *J Cell Biol*. 113:527-38.

Richman, T.J., M.M. Sawyer, and D.I. Johnson. 2002. Saccharomyces cerevisiae Cdc42p localizes to cellular membranes and clusters at sites of polarized growth. *Eukaryot Cell*. 1:458-68.

Roemer, T., K. Madden, J. Chang, and M. Snyder. 1996. Selection of axial growth sites in yeast requires Axl2p, a novel plasma membrane glycoprotein. *Genes Dev*. 10:777-793.

Roumanie, O., C. Weinachter, I. Larrieu, M. Crouzet, and F. Doignon. 2001. Functional characterization of the Bag7, Lrg1 and Rgd2 RhoGAP proteins from Saccharomyces cerevisiae. *FEBS Lett*. 506:149-56.

Sagot, I., S.K. Klee, and D. Pellman. 2002. Yeast formins regulate cell polarity by controlling the assembly of actin cables. *Nat Cell Biol*. 4:42-50.

Schenkman, L.R., C. Caruso, N. Page, and J.R. Pringle. 2002. The role of cell cycle-regulated expression in the localization of spatial landmark proteins in yeast. *J Cell Biol*. 156:829-41.

Schott, D., J. Ho, D. Pruyne, and A. Bretscher. 1999. The COOH-Terminal Domain of Myo2p, a Yeast Myosin V, Has a Direct Role in Secretory Vesicle Targeting. *J Cell Biol*. 147:791-808.

Schott, D., T. Huffaker, and A. Bretscher. 2002. Microfilaments and microtubules: the news from yeast. *Curr Opin Microbiol*. 5:564-74.

Segal, M., and K. Bloom. 2001. Control of spindle polarity and orientation in Saccharomyces cerevisiae. *Trends Cell Biol*. 11:160-6.

Segall, J.E. 1993. Polarization of yeast cells in spatial gradients of alpha mating factor. *Proc Natl Acad Sci U S A*. 90:8332-6.

Sheu, Y.J., B. Santos, N. Fortin, C. Costigan, and M. Snyder. 1998. Spa2p interacts with cell polarity proteins and signaling components involved in yeast cell morphogenesis. *Mol Cell Biol*. 18:4053-69.

Shinjo, K., J.G. Koland, M.J. Hart, V. Narasimhan, D.I. Johnson, T. Evans, and R.A. Cerione. 1990. Molecular cloning of the gene for the human placental GTP-binding protein Gp (G25K): identification of this GTP-binding protein as the human homolog of the yeast cell-division-cycle protein CDC42. *Proc Natl Acad Sci U S A*. 87:9853-7.

Sikorski, R.S., and P. Hieter. 1989. A system of shuttle vectors and yeast host strains designed for efficient manipulation of DNA in *Saccharomyces cerevisiae*. *Genetics*. 122:19-27.

Simon, M.N., C. De Virgilio, B. Souza, J.R. Pringle, A. Abo, and S.I. Reed. 1995. Role for the Rho-family GTPase Cdc42 in yeast mating-pheromone signal pathway. *Nature*. 376:702-705.

Slater, M.L. 1973. Effect of reversible inhibition of deoxyribonucleic acid synthesis on the yeast cell cycle. *J. Bacteriol.* 113:263-270.

Sloat, B.F., A.E.M. Adams, and J.R. Pringle. 1981. Roles of the *CDC24* gene product in cellular morphogenesis during the *Saccharomyces cerevisiae* cell cycle. *J. Cell Biol.* 89:395-405.

Sloat, B.F., and J.R. Pringle. 1978. A mutant of yeast defective in cellular morphogenesis. *Science*. 200:1171-3.

Smith, G.R., S.A. Givan, P. Cullen, and G.F. Sprague, Jr. 2002. GTPase-activating proteins for Cdc42. *Eukaryot Cell*. 1:469-80.

Snyder, M., S. Gehrung, and B.D. Page. 1991. Studies concerning the temporal and genetic control of cell polarity in *Saccharomyces cerevisiae*. *J. Cell Biol.* 114:515-532.

Sopko, R., D. Huang, J.C. Smith, D. Figeys, and B.J. Andrews. 2007. Activation of the Cdc42p GTPase by cyclin-dependent protein kinases in budding yeast. *EMBO J*. 26:4487-500.

Spector, I., N.R. Shochet, Y. Kashman, and A. Groweiss. 1983. Latrunculins: novel marine toxins that disrupt microfilament organization in cultured cells. *Science*. 219:493-5.

Stevenson, B.J., B. Ferguson, C. De Virgilio, E. Bi, J.R. Pringle, G. Ammerer, and G.F. Sprague, Jr. 1995. Mutation of *RGA1*, which encodes a putative GTPase-activating protein for the polarity-establishment protein Cdc42p, activates the pheromone- response pathway in the yeast *Saccharomyces cerevisiae*. *Genes Dev.* 9:2949-2963.

Takahashi, S., and P.M. Pryciak. 2008. Membrane localization of scaffold proteins promotes graded signaling in the yeast MAP kinase cascade. *Curr Biol*. 18:1184-91.

Takizawa, P.A., J.L. DeRisi, J.E. Wilhelm, and R.D. Vale. 2000. Plasma membrane compartmentalization in yeast by messenger RNA transport and a septin diffusion barrier. *Science*. 290:341-344.

Tkacz, J.S., and J.O. Lampen. 1972. Wall replication in *Saccharomyces* species: use of fluorescein-conjugated concanavalin A to reveal the site of mannan insertion. *J. Gen. Microbiol.* 72:243-247.

Tong, Z., X.D. Gao, A.S. Howell, I. Bose, D.J. Lew, and E. Bi. 2007. Adjacent positioning of cellular structures enabled by a Cdc42 GTPase-activating protein-mediated zone of inhibition. *J Cell Biol*. 179:1375-84.

Turing, A. 1952. The Chemical Basis of Morphogenesis. *Philos Trans R Soc Lond B Biol Sci*. 237:37-72.

Uetake, Y., J. Loncarek, J.J. Nordberg, C.N. English, S. La Terra, A. Khodjakov, and G. Sluder. 2007. Cell cycle progression and de novo centriole assembly after centrosomal removal in untransformed human cells. *J Cell Biol*. 176:173-82.

Valdez-Taubas, J., and H.R. Pelham. 2003. Slow diffusion of proteins in the yeast plasma membrane allows polarity to be maintained by endocytic cycling. *Curr Biol*. 13:1636-40.

Verma, R., R.S. Annan, M.J. Huddleston, S.A. Carr, G. Reynard, and R.J. Deshaies. 1997. Phosphorylation of Sic1p by G1 Cdk required for its degradation and entry into S phase. *Science*. 278:455-60.

Versele, M., and J. Thorner. 2004. Septin collar formation in budding yeast requires GTP binding and direct phosphorylation by the PAK, Cla4. *J Cell Biol*. 164:701-15.

Watanabe, N., T. Kato, A. Fujita, T. Ishizaki, and S. Narumiya. 1999. Cooperation between mDia1 and ROCK in Rho-induced actin reorganization. *Nat Cell Biol*. 1:136-43.

Wedlich-Soldner, R., S. Altschuler, L. Wu, and R. Li. 2003. Spontaneous cell polarization through actomyosin-based delivery of the Cdc42 GTPase. *Science*. 299:1231-5.

Wedlich-Soldner, R., and R. Li. 2003. Spontaneous cell polarization: undermining determinism. *Nat Cell Biol*. 5:267-70.

Wedlich-Soldner, R., S.C. Wai, T. Schmidt, and R. Li. 2004. Robust cell polarity is a dynamic state established by coupling transport and GTPase signaling. *J Cell Biol*. 166:889-900.

Weiss, E.L., A.C. Bishop, K.M. Shokat, and D.G. Drubin. 2000. Chemical genetic analysis of the budding-yeast p21-activated kinase Cla4p. *Nat. Cell Biol*. 2:677-685.

Wesp, A., L. Hicke, J. Palecek, R. Lombardi, T. Aust, A.L. Munn, and H. Riezman. 1997. End4p/Sla2p interacts with actin-associated proteins for endocytosis in Saccharomyces cerevisiae. *Mol Biol Cell*. 8:2291-306.

Winters, M.J., and P.M. Pryciak. 2005. Interaction with the SH3 domain protein Bem1 regulates signaling by the Saccharomyces cerevisiae p21-activated kinase Ste20. *Mol Cell Biol*. 25:2177-90.

Wu, J.Q., J.R. Kuhn, D.R. Kovar, and T.D. Pollard. 2003. Spatial and temporal pathway for assembly and constriction of the contractile ring in fission yeast cytokinesis. *Dev Cell*. 5:723-34.

Yamaguchi, Y., K. Ota, and T. Ito. 2007. A novel Cdc42-interacting domain of the yeast polarity establishment protein Bem1. Implications for modulation of mating pheromone signaling. *J Biol Chem*. 282:29-38.

Yang, H.C., and L.A. Pon. 2002. Actin cable dynamics in budding yeast. *Proc Natl Acad Sci U S A*. 99:751-6.

Yang, S., M.J. Cope, and D.G. Drubin. 1999. Sla2p is associated with the yeast cortical actin cytoskeleton via redundant localization signals. *Mol Biol Cell*. 10:2265-83.

Zahner, J.E., H.A. Harkins, and J.R. Pringle. 1996. Genetic analysis of the bipolar pattern of bud site selection in the yeast Saccharomyces cerevisiae. *Mol Cell Biol*. 16:1857-70.

Zhao, Z.S., T. Leung, E. Manser, and L. Lim. 1995. Pheromone signalling in *Saccharomyces cerevisiae* requires the small GTP-binding protein Cdc42p and its activator Cdc24p. *Mol. Cell. Biol.* 15:5246-5257.

Zheng, Y., R. Cerione, and A. Bender. 1994. Control of the yeast bud-site assembly GTPase Cdc42. Catalysis of guanine nucleotide exchange by Cdc24 and stimulation of GTPase activity by Bem3. *J Biol Chem*. 269:2369-72.

Ziman, M., D. Preuss, J. Mulholland, J.M. O'Brien, D. Botstein, and D.I. Johnson. 1993. Subcellular localization of Cdc42p, a *Saccharomyces cerevisiae* GTP- binding protein involved in the control of cell polarity. *Mol Biol Cell*. 4:1307-16.

Biography

Audrey Sinclair Howell
Born October 3rd, 1980 in Birmingham, AL

Education:
Ph.D. Genetics and Genomics, Duke University, 2009
Sc.B. Biology, Brown University, 2003

Honors:
Graduate Research Fellowship, National Science Foundation, 2005-2008

Publications:
Kozubowski, L., K. Saito, J.M. Johnson, **A.S. Howell**, and D.J. Lew. 2009. Response: GEF localization, not just activation, is needed for yeast polarity establishment. *Curr Biol*. 19:R195.

Kozubowski, L., K. Saito, J.M. Johnson, **A.S. Howell**, T.R. Zyla, and D.J. Lew. 2008. Symmetry-Breaking Polarization Driven by a Cdc42p GEF-PAK Complex. *Curr Biol*. 18:1719-26.

Tong, Z., X.D. Gao, **A.S. Howell**, I. Bose, D.J. Lew, and E. Bi. 2007. Adjacent positioning of cellular structures enabled by a Cdc42 GTPase-activating protein-mediated zone of inhibition. *J Cell Biol*. 179:1375-84.

Hodge, L.K., M.P. Klassen, B.X. Han, G. Yiu, J. Hurrell, **A. Howell**, G. Rousseau, F. Lemaigre, M. Tessier-Lavigne, and F. Wang. 2007. Retrograde BMP signaling regulates trigeminal sensory neuron identities and the formation of precise face maps. *Neuron*. 55:572-86.

Irazoqui*, J.E., **A.S. Howell***, C.L. Theesfeld, and D.J. Lew. 2005. Opposing roles for actin in Cdc42p polarization. *Mol Biol Cell*. 16:1296-304. *co-first authors

Thacker, E., B. Kearns, C. Chapman, J. Hammond, **A. Howell**, and A. Theibert. 2004. The arf6 GAP centaurin alpha-1 is a neuronal actin-binding protein which also functions via GAP-independent activity to regulate the actin cytoskeleton. *Eur J Cell Biol*. 83:541-54.